THE JOURNAL OF APPLIED CHEMISTRY OF THE USSR

Vol. 24 1951

FEB

IN ENGLISH TRANSLATION

CONSULTANTS BUREAU
152 WEST 42ND ST. NEW YORK 18, N. Y.

—An agency for the interpretation of international knowledge—

TABLE OF CONTENTS

		page	Russ. page
1.	Academician Nikolai Dmitrevich Zelinsky. M. B. Turova-Polyak	133	117
2.	Some Problems of the Theory of the Formation of Porcelain Body. P. P. Budnikov and Kh. P. Gevorkyan	141	125
3.	The Thermochemical Conversion of Ferrous Sulfate. M.E.Pozin and A.M.Ginstling	151	134
4.	The Nature of the Reaction of Chrome Coordination Compounds with the Principal Groups in Protein. I. P. Strakhov	159	142
5.	The Specific Gravities of Molten Salts in Systems of Congruently Fusing Compounds. L. P. Vereshchetina and N. P. Luzhnaya	165	148
6.	The Effect of the Geometrical Parameters of the Electrolyzer upon the Distribution of Electric Energy Within it. V.P.Mashovets, N.V.Pomotskaya, N.L.Komarov et al.	169	154
7.	An Investigation of the Cathodic Process in Solutions of Nitric Acid and in the HNO_3-H_2SO_4-H_2O System. I. Oknin	181	167
8.	A Photocolorimetric Method of Determining Small Quantities of Milk Sugar. M. N. Tulchinsky	193	179
	BRIEF COMMUNICATIONS		
9.	The Solubility of Sodium Nitrite and Nitrate in Water when Soda is Present. I. N. Kuzminykh and E. I. Yakhontova	199	185
10.	The Solubility of Naphthalene in Coal-Tar Oils. M. M. Potashnikov	203	189
11.	The Saturation Vapor Pressures of β-Picoline, γ-Picoline, and 2,6-Lutidine. L. L. Liplavk and E. P. Boliter	207	191
12.	The Effect of the Concentration of Acids upon their Attacking Carbon Steels. S. A. Balezin and T. I. Krasovitskaya	213	197
13.	Double Substitutions of Methyl Ketones in Furfurylidene Ketones. V. I. Tikhonova	219	202
14.	A Compound Helix as a Catalyst Carrier. N. Z. Kotelkov	223	205
15.	Protecting Iron Against Corrosion under Atmospheric Conditions by Coatings of Oil. A. Ya. Drinberg and M. G. Rokhlin	227	210
16.	Protecting Iron Against Corrosion by Coatings of Oil and Changes in the Latter's Physical Properties as the Result of Aging. A. Ya. Drinberg and M. G. Rokhlin	233	215
17.	Changes in the Elementary Composition of Oil Films during Various Aging Procedures. A. Ya. Drinberg and M. G. Rokhlin	239	220
18.	Letters to the Editor. V. Zhuravlev and M. Sychev	243	223
	Plate	245	

THE JOURNAL OF APPLIED CHEMISTRY OF THE U.S.S.R.

Volume XXIV
February 1951

IN ENGLISH TRANSLATION

Copyright, 1951

CONSULTANTS BUREAU
152 West 42 Street
New York 18, N.Y.

Printed in France

Annual subscription $80.00, Single issue $12.00

ACADEMICIAN NIKOLAI DMITREVICH ZELINSKY

(On his 90th Birthday)

This February the scientific world and the public opinion of the Soviet Union will mark the ninetieth birthday and nearly the seventieth anniversary of the scientific, pedagogical, and civic activity of Academician Nikolai Dmitrevich Zelinsky, Hero of Socialist Labor and Professor of Moscow University.

Nikolai Dmitrevich Zelinsky's name is indissolubly bound up with the development of organic chemistry, chiefly with the development of petroleum chemistry and organic analysis and with research on the structure of proteins.

Nikolai Dmitrevich was born in the city of Tiraspol in 1861. After completing the Tiraspol District School, and then the Odessa gymnasium, he entered Novorossisk University (in Odessa), from which he was graduated in 1884. While still a student, Nikolai Dmitrevich became interested in organic chemistry and completed his first scientific paper "On the Product of Adding Methylamine to Methylglycidic Acid" under the guidance of Prof. Melikova (Melikashvili), which was printed in 1884 in the Journal of the Russian Physico-Chemical Society.

After graduation, Nikolai Dmitrevich went abroad on a faculty scholarship to specialize in organic chemistry under Profs. J. Wislicenus (Leipzig) and W.Meyer (Goettingen). While working in Prof. Meyer's laboratory, Zelinsky synthesized β,β'-dichlorodiethyl sulfide for the first time; this was later called "yperite" (during the First World War), and Zelinsky himself suffered severe burns during its synthesis.

Upon his return from abroad, in 1889, Zelinsky defended his master's thesis entitled "The Problem of Isomerism in the Thiophene Series." In this original work, devoted to compounds that were but little known at the time (thiophene had been discovered in 1883), Nikolai Dmitrevich Zelinsky pointed out the analogies between the properties of benzene and thiophene. This thesis was the foundation stone for the subsequent evolution of the chemistry of heterocyclic compounds.

Soon after defending his master's thesis, Nikolai Dmitrevich, still a young scientist, began work in a new field - the stereoisomerism of organic acids. At that time stereochemistry was a new and promising branch of organic chemistry. Some scientists accepted the concepts of stereochemistry with difficulty and reluctantly, at times even with hostility. Despite this, Nikolai Dmitrevich Zelinsky started upon this new road and in 1891 submitted his doctoral dissertation, "Researches on the Phenomena of Stereoisomerism in Unsaturated Carbon Compounds." In this dissertation Zelinsky reached the conclusion that "the composition, structure, mass, crystalline form, and spatial arrangement of the atoms and atom groups... are the foundation for the development of one of the most interesting branches of chemical mechanics," which "opens up wide horizons for deeper understanding of our notions of the chemical particle and its dynamics, while the statistical concepts of the theory of structure will be provided with real dynamic meaning."

Working under the conditions of that time, Zelinsky was able to complete this dissertation only thanks to his great experimental skill. His conclusions were entirely new and original and promoted the spread of stereochemical concepts here at home.

His ability to investigate theoretical problems profoundly, to generalize from scientific facts, and to foresee the paths along which the science would develop, together with his brilliance as an experimenter, all favored the young scientist's career. Talented young men began to flock about him, aiding him in his research. Among his students during this initial period of his scientific career were A.M. Bezredka, A.A.Bychikhin, A.G.Doroshevsky, and S.G.Krapivin.

At the same time as he began his brilliant scientific career, Zelinsky began his activity as a teacher. In 1888, he was appointed a lecturer at Novorossisk University, and in 1893 he was appointed adjunct professor of Moscow University, at the recommendation of Prof. N.A.Menshutkin, and moved from Odessa to Moscow.

As Nikolai Dmitrevich recalls, the students and laboratory assistants of the chairs of organic and analytical chemistry at Moscow University gave him a cordial welcome. He was very glad to see students coming to him presently with the request for permission to work under his guidance. These students included N.A.Shilov, L.A.Chugaev, F.A.Korbe, and others. They were talented youngsters, according to Nikolai Dmitrevich, who felt a powerful attraction toward theoretical and experimental work. The number of students desiring to work under Nikolai Dmitrevich Zelinsky grew rapidly.

This marked the beginning of the intensive and manysided scientific and teaching careers of Nikolai Dmitrevich, who staked out for himself a whole field in the development of organic chemistry. Zelinsky's lectures on organic chemistry were simple in form, but full of extensive and profound knowledge. They were always illustrated by a wealth of preparations and accompanied by interesting demonstrations. During his lectures he always reported on the latest scientific achievements, thus awakening interest in his subject among his youthful auditors. Nikolai Dmitrevich Zelinsky devoted much attention to the practical laboratory work of his students. He was the first professor in the University of Moscow to place laboratory work on an adequately high level: the students prepared 25-30 organic preparations, then studied organic analysis, and only after this had been completed did the proffessor assign them the themes of their diploma theses. The procedure established by Zelinsky for laboratory exercises in organic chemistry in the University of Moscow is still in use today.

It was not without apprehension that students approached Nikolai Dmitrevich Zelinsky for the themes of their diploma theses. But after the very first days spent in the laboratory this feeling would vanish, never to return. Zelinsky's naturalness and attentiveness, his endeavors to explain and inculcate the habits and methods necessary for a young researcher made them grow to like scientific work.

Though demanding and implacably severe, especially when the clarity of an experiment was involved, Nikolai Dmitrevich Zelinsky had a remarkable ability to guide youngsters along the path of their own creative initiative, untiringly following the development of the work done by each of his young assistants. His example inspired all of those who worked with him. Nikolai Dmitrevich was severe and demanding in all matters connected with scientific work. But at the same time he entered into the personal problems of his pupils with attentiveness, solicitude, and warm participation.

The scientific activity of Nikolai Dmitrevich Zelinsky is too extensive, varied, and manysided to be comprehensively described within the confines of a brief survey. Zelinsky has published more than 500 research papers. This enormous number of papers is characterized by the variety of topics dealt with, on the one hand, and by their theoretical and practical timeliness on the other.

The first Mowcow period of Nikolai Dmitrevich Zelinsky's career lasted eighteen

years (1893-1911). Organic synthesis and the chemistry of petroleum were his principal fields of interest at the time.

An outstanding pupil of Zelinsky's at the time was S.S.Nametkin, an eminent researcher in the chemistry of petroleum and terpenes, who has since been elected to the Academy of Sciences. Nikolai Dmitrevich and Nametkin have been warm friends ever since.

In order to shed light upon the nature of the (primarily cyclic) hydrocarbons in our Caucasus petroleums, Nikolai Dmitrevich Zelinsky synthesized standard samples of numerous hydrocarbons, mainly cyclopentanes and cyclohexanes, so that their properties could be compared with those of the hydrocarbons in the petroleums in question.

Nikolai Dmitrevich employed varied methods to synthesize the hydrocarbons, some of them proposed for the first time. His fundamental work on the synthesis of the naphthenes has been one of the principal steps in the development of our knowledge of the composition of petroleum. His work on the ketonization of the naphthenes and the conversion of naphthenes into alcohols and acids comes under this same heading.

In his researches on the chemistry of petroleum Zelinsky has continued the glorious traditions of Russian organic chemists. But it was only after the great socialist revolution of October, 1917 that these researches were fully developed and applied.

In addition to his synthetic researches, in 1911 Nikolai Dmitrevich resumed the research project he had started in 1898 on the catalytic properties of palladium. In that year, the Journal of the Russian Chemical Society published a paper, "Dehydrogenation by Catalysis," in which Zelinsky reported on this major discovery - the dehydrogenation of hexahydro aromatic hydrocarbons with palladium and platinum. Recollecting that period, Nikolai Dmitrevich recounts that he set aside all other work and concentrated on that problem; he had to do so, as this was the time (1911) when he had to leave the laboratory he had established in the University of Moscow.

This was the era of periodic reactionary attacks against Moscow University. The entire administration of the university was dismissed by order of the Minister of Education.

In protest, the leading professors and instructors resigned. One of them was Nikolai Dmitrevich Zelinsky.

Zelinsky moved to St. Petersburg, where he lived from 1912 to 1917. There he held a post as director of the Central Laboratory of the Ministry of Finances, at the same time holding the modest chair of staple commodities in the Economics Faculty of the Polytechnic Institute. This is the period in which he did his research on the nature of petroleum, with the objective of preparing aromatic compounds, and on the hydrolysis of proteins, in which he discovered activated charcoal and investigated its properties, and in which he began his research on the condensation of acetylene with activated charcoal, which was later completed in Moscow.

During the imperialist war, in 1915, when poison gas had to be dealt with, Nikolai Dmitrevich set about making a universal gas mask that would protect the wearer from any poison gas then known, no matter what its composition.

Zelinsky made his first report on charcoal as a universal agent to counter the effects of poison gas in August, 1915. This was followed by persistent, unremitting labor to find ways and means of increasing the absorptive properties of charcoal and ways of activating it. The famous Zelinsky gas mask was the result of this self-denying labor, in which S.S.Stepanov, Zelinsky's laboratory assistant for many years, participated.

In February, 1916 this gas mask was adopted as part of the equipment of the Russian Army, and from the time the army was actually supplied with gas masks, Nikolai Dmitrevich received many touching expressions of gratitude from men who had had occasion to test the remarkable action of the new gas mask in battle. The Zelinsky gas mask saved hundreds of thousands of lives.

The activated charcoal discovered by Zelinsky has also been widely employed in industry as an excellent absorbent and catalyst.

In 1917, Nikolai Dmitrevich Zelinsky, like so many of his associates who had left Moscow University in 1911, was able to return to his former professorship. He was a representative of those prominent members of the Russian intelligentsia who supported the October Revolution from the very first days without hesitation and contributed to the advancement of Soviet science and the nation's economy.

The Soviet period – the even more fruitful period – of Nikolai Dmitrevich Zelinsky's career began with his return to Moscow. Together with his associates, he set about fulfilling various commissions of a technical and industrial nature, arising from Socialist construction.

Thus, at the beginning of the Civil War (1918), Nikolai Dmitrevich Zelinsky undertook a comprehensive research project, at the request of the People's Commissar of War and the Navy, on the production of synthetic gasoline. After considering the destructive cracking of high-molecular petroleum residues, Zelinsky came to the conviction that solar oil, fuel oil, and other high-molecular compounds could be broken down into simpler ones by the action of aluminum chloride and relatively low temperatures. The reaction product proved to be a mixture of volatile hydrocarbons, boiling in the 25-180° range, their yield being some 63%. Thus, during the Civil War, with the country's economy in collapse, when the oil fields were cut off from the center of the country, Nikolai Dmitrevich was the first to point out a new method for producing gasoline, which proved its worth under industrial conditions and ensured a supply of synthetic fuel for the Soviet Air Force.

Researches on the chemistry of shale oil, especially, its desulfurization, researches on the aromatization of petroleum and its individual fractions by means of catalytic dehydrogenation (at the request of Soyuzneft), the synthesis of dimethylindigo from xylene, the contact oxidation of naphthalene by atmospheric oxygen into phthalic anhydride (at the request of the Aniline Trust), and many other projects were completed in this field.

The second Moscow period of Nikolai Dmitrevich Zelinsky's career was marked by the development and application of catalysis in organic chemistry. Here we have, mainly, Zelinsky's researches on catalytic hydrogenation and dehydrogenation, as well as his discovery of "irreversible catalysis".

All of Zelinsky's work on catalysis is permeated by the concept of the existence of a link between the form of a molecule and its catalytic conversions. He regards a change in the molecule's form as the reason for catalysis. These ideas of Zelinsky's on the cause of contact catalytic action approximate the views of D.I.Mendeleev on the subject.

Nikolai Dmitrevich Zelinsky's pupils and associates had the good fortune to observe the gradual establishment and development of the field of organic catalysis and to work under the guidance of so remarkable a chemist and a man as Nikolai Dmitrevich Zelinsky.

Nikolai Dmitrevich pointed out a long time ago that the best catalysts for hydrogenation in the gas phase were platinum and palladium. A large number of carbocyclic and heterocyclic compounds has been hydrogenated with these catalysts. Subsequently Zelinsky proposed a new osmium catalyst, which possesses extremely pronounced hydrogenating properties. This catalyst can be used to hydrogenate many

compounds in the cold, to hydrogenate some heterocyclic compounds that are hard to hydrogenate without rupturing their rings (sylvan and tetrahydrosylvan), and to perform other hydrogenations.

A large amount of experimental data on catalytic hydrogenation enabled Zelinsky to arrive at an interesting conclusion regarding the opening of rings during this reaction. He found that the ease with which rings are opened diminishes successively as we pass from three-membered to four-membered, five-membered, and six-membered rings.

The hydrogenation of cyclopentane and its derivatives, which involves the rupturing of the cycle and the formation of paraffin hydrocarbons, deserves special attention. This reaction may be employed to improve automotive gasolines.

Nikolai Dmitrevich Zelinsky's researches on the catalytic dehydrogenation of numerous derivatives of cyclohexane and of bi- and tricyclic hydrocarbons containing a hydroaromatic ring, as well as the dehydrogenation of heterocyclic compounds with five-membered and six-membered rings, constitute a major contribution to organic catalysis. The dehydrogenation experiments were performed with platinum, palladium and nickel on alumina. N.D.Zelinsky was the first to suggest the use of the latter, which has proved its value in catalytic hydrogenation and dehydrogenation.

In view of its great importance the dehydrogenation reaction has been studied, both qualitatively and quantitatively, in many individual hydrocarbons.

In addition to their theoretical significance in shedding light upon the mechanism of catalytic reactions, these researches on catalytic dehydrogenation have been put to practical use. They are employed to ascertain the chemical nature of petroleums, especially the petroleums of new oil fields, as well as to ensure the correct utilization of petroleum hydrocarbons (catalytic aromatization). These researches on the dehydrogenation of petroleum crudes provided an inexhaustible source for the production of aromatic hydrocarbons used, as we know, in the aniline-dye industry, and in the manufacture of pharmaceutical preparations, explosives, many types of plastics, etc.

The singular reaction involving the simultaneous hydrogenation and dehydrogenation of incompletely saturated derivatives of cyclohexane, which N.D.Zelinsky has called "irreversible catalysis", sheds light upon the role of the catalyst in these proceses as well as upon the features of the hydrocarbons in this group.

In his study of the properties of various catalysts and of the effect of the methods used for their preparation upon their activity, Zelinsky showed that so-called catalyst fatigue is a regular phenomenon, taking place as a result of the deformation of the carbon molecules, the fragments of which cover the surface of the catalyst with a carbonaceous film. In 1925, he was the first to suggest a way of combatting this phenomenon by burning such films away. This method is widely used at the present time in industry to regenerate catalysts.

Moreover, catalysis is closely bound up with organic synthesis for Nikolai Dmitrevich: he synthesizes substances in order to carry out various catalytic reactions with them, on the one hand, and on the other, he solves major synthesis problems by means of catalysis.

Several other reactions come under the heading of organic catalysis: the contact condensation of acetylene with aromatic hydrocarbons in the presence of activated charcoal; the reduction of organic compounds containing oxygen with the same contact agent; the isomerization of various ring hydrocarbons into compounds with six-membered rings by halogen salts of aluminum; the cleavage of organic compounds by aluminum chloride, etc.

Nikolai Dmitrevich isolated hydrocarbon fractions that greatly resembled petroleum by reacting aluminum chloride with cholesterol, phytosterol, rubber, resin

acids, and other compounds. In all of these cases, optically active initial materials yielded optically active petroleum. All this compelled Zelinsky to abandon the inorganic theory of the origin of petroleum and become a supporter of the organic theory.

The catalytic reactions investigated by N.D.Zelinsky also include the catalytic desulfurization of high-sulfur oils. This method involves catalytic hydrogenation at atmospheric pressure and relatively low temperatures. This method is of tremendous practical importance. It opens the way for the wide employment of high-sulfur crudes in internal-combustion engines.

Thus the phenomena of catalysis and the study and development of petroleum chemistry have been favorite research subjects throughout N.D.Zelinsky's lifetime. These two fields of work are closely interwoven in his activity, constituting a single subject in essence. Zelinsky's researches have enriched the fields of organic catalysis and petroleum chemistry with a vast quantity of theoretical and practical material and have made him one of the founders of these important branches of chemistry.

All the topics of N.D.Zelinsky's researches discussed up to now have dealt, in the main, with the chemistry of hydrocarbons, chiefly those of cyclic structure.

The breadth of Zelinsky's scientific interests includes a region, however, that seems to be far removed from his usual fields of interest - the protein compounds, and he has been able to make important contributions in this field. The so-called autoclave hydrolysis of proteins bears his name, taking place in the presence of dilute acids at somewhat higher pressure and at temperatures of the order of 180°. Under these conditions proteins break down into amino acids and diketopiperazines. Nikolai Dmitrevich Zelinsky was the first to advance the notion that these compounds, like the peptides, are constituents of the complicated protein molecule. These researches have opened a new chapter in the study of the structure of the protein molecule.

The problem of synthetic rubber is an extremely acute one in the Soviet Union, and it was natural that Zelinsky could not fail to take part in solving it. He established a laboratory in which methods of preparing various kinds of synthetic rubber were elaborated. Research on the production of the raw materials for the synthesis of rubber from non-foodstuffs is now under way in Zelinsky's laboratory, with his immediate participation.

In addition to the major lines of endeavor listed above, Nikolai Dmitrevich has participated in the solution of other new and interesting problems, such as: the organization of research on the Raman spectra of individual hydrocarbons; research at ultrahigh pressures, which opens up new possibilities in organic synthesis; and other problems.

This far from complete survey of the career of Nikolai Dmitrevich Zelinsky demonstrates that he has been able to channel the most profound theoretical investigations into their practical application, making them available to industry.

It is appropriate at this point to quote the words addressed by Zelinsky to youth on the occasion of his eightieth birthday: "Chemistry has often conferred upon me the very great delight of understanding hitherto unexplored secrets of nature. It has enabled me to be of service to people, to make their labor easier, to deliver them from some suffering, occasionally from disaster. It has enabled me to become a man who has not been of no use to my fatherland; it has marked out the road along which I have been able to make some useful contribution to socialist construction and to the defense of the land of the Soviets."

Though engaged for nearly seventy years in scientific work, Nikolai Dmitrevich Zelinsky has always been a highly successful teacher. As we have already said, his principal pedagogical activity has had Moscow University as its scene. This is

what he says about this aspect of his work: "I retain many happy, bright memories of the Moscow laboratory where I have worked all my life. All these memories are linked to my scientific and pedagogical activity in this laboratory, among my cherished pupils and associates. Scientific intercourse and friendly collective work with my senior and junior associates have been the enduring foundation upon which the Moscow school of chemists has been established, on a par with the contemporary status of chemical science and endeavoring to aid in the cause of establishing a state upon new, just, socialist foundations."

Notwithstanding his heavy schedule, Nikolai Dmitrevich has always found time for additional pedagogical and organizational activity. The Courses of Higher Education for Women were founded in Moscow at the end of the nineties (converted into the Second Moscow University in 1917). Nikolai Dmitrevich Zelinsky organized the chair of organic chemistry in this institution and was the first to hold the chair. Later he took an active part in organizing the Shanyavsky People's University, and participated in the organization of many chemical laboratories.

It is not surprising, therefore, that Nikolai Dmitrevich Zelinsky, with this comprehensive and manysided scientific and teaching basis, has nutured a whole galaxy of Soviet organic chemists, who possess in their teacher a model of unbounded devotion to science. The number of pupils who have come forth from Zelinsky's laboratory is extraordinarily great. It is, of course, impossible to list them here by name. Many of them are today academicians, corresponding members of the Academy, doctors of science, and professors in institutions of higher learning.

Nikolai Dmitrevich is very active in civic affairs: he is one of the organizers and an honorary member of the D.I.Mendeleev All-Union Chemical Society; he takes a very active part in the work of the oldest society of naturalists in our country - the Moscow Society of Naturalists, whose president he has been since 1935.

Nikolai Dmitrevich Zelinsky's career is a living example of what a leading Soviet scientist should be: a learned humanist, and an advocate of truth and social justice. In reply to the instigators of an imperialist war, Nikolai Dmitrevich recently made the following statement to the press:

"I cannot remain silent in this time of tension, when every day brings us new evidence of the growing danger of war. I should like to add my voice to the voices of hundreds of millions of honest people on our planet. But it is hardly enough merely to wish for peace - one must actively and passionately fight for peace. I shall soon be ninety years old, I have given two-thirds of a century to science, and that entitles me to demand of my professional colleagues - Soviet and foreign - that they hearken to the voice of an old scientist who well knows the price of peace and war."

Nikolai Dmitrevich Zelinsky's scientific achievements have received wide recognition. The Soviet government has taken cognizance of them more than once. Nikolai Dmitrevich is a Hero of Socialist Labor (1945), a triple Stalin Prize winner (1942, 1946, 1948), and an Honored Worker in Science (1926). He has been decorated with three Orders of Lenin and two Orders of the Red Banner of Labor.

The Zelinsky school is proud of its teacher, honored and beloved by all, always responsive to his pupils and associates, the founder of major branches of organic chemistry, and a true son of his fatherland.

This has been the glorious life of Academician Nikolai Dmitrevich Zelinsky - a non-party Bolshevik, a leading citizen.

We wish him good cheer and strength for the welfare and prosperity of our great fatherland.

M.B. Turova-Polyak

SOME PROBLEMS OF THE THEORY OF THE FORMATION OF PORCELAIN BODY

P. P. Budnikov and Kh. O. Gevorkyan

In the porcelain industry, firing is the principal stage of the technological process. During firing, high temperature produces a product as the result of certain physical and chemical processes. The course of these processes is governed by their thermodynamic conditions. In an industrial kiln these processes are controlled by changing the thermodynamic conditions, finally resulting in the formation of a ceramic product that possesses valuable technical properties (mechanical strength, electrical insulation properties, use as refractories, impermeability to water, and thermal stability).

For this reason improving the production of ceramic ware requires, first of all, the correct control of the industrial firing process, which in turn involves the possession of clear notions of the nature of the physical and chemical changes that take place in ceramic materials at high temperatures.

Study of these processes of ceramic firing and, particularly, of the firing of porcelain, has been the objective of numerous investigations by Soviet scientists. The manysided researches of Baikov, Vernadsky, Belyankin, Zemyatchensky, Ponomarev, Lapin, Sokolov, and others, have resulted in the accumulation of extensive experimental material during the past decade, shedding light upon the problem of the formation of porcelain body.

The principal tools in these investigations have been the polarizing microscope and X rays. Efforts have been made during recent years to employ a new instrument – the electron microscope – in this research.

Furthermore, considerable success has been had during the past few years with the investigation of the formation of porcelain by means of microscopic examination by reflected light. It should be noted that 26 years ago a reflected-light microscope was first used by Zemyatchensky to study the microstructure of porcelain [1].

In many cases studying porcelain in reflected light proves to be more effective than studying it with the micropolariscope.

As for the micropolariscope and X rays, despite all their merits, they often prove inadequate for the solution of certain problems. This is sometimes due to the high dispersion of the mineral particles comprising the masses under examination, and in other instances to the formation of amorphous sheaths around the crystalline substance during firing, which are detected neither by a microscope nor by X rays.

Notwithstanding all this, we now have enough information on the microstructure to be able to throw some light upon the complicated physical and chemical phenomena involved in the firing of porcelain and faience.

Constitution of the vitreous phase. When porcelain pastes, prepared from various mixtures of the three basic constituents – kaolin, feldspar, and quartz – are fired, the constituents react with one another: at first in solid-state reactions, in the low-temperature region, and then in the liquid phase as well, at temperatures above 1000°.

These processes are essentially this:

At comparatively low temperatures the minerals of the crude mix decompose, steam and other gaseous products being evolved. This stage of firing also involves intramolecular changes in the kaolinite and polymorphic transformations of the silica and the China clay.

In the light of modern notions of the chemical reactions occurring in the solid state we may assert that certain reactions take place among the kaolinite residue, the quartz, and the feldspar long before the liquid phase is reached.

Nevertheless, it has been proved experimentally that the major processes involved in the making of porcelain take place at higher temperatures, when a liquid phase has made its appearance in the paste being fired. The constitution of a liquid phase in the porcelain paste is due to the fusion of the feldspar. At a temperature of about 1170° the potash feldspar fuses incongruently, giving rise to crystalline leucite and glass. The fusion of the potash feldspar results in an increase in its volume. Some of the melt, though only a small part of it, is formed below the melting point of feldspar owing to the fusion of minor mineral impurities in the paste, which constitute low-fusing eutectics.

The liquid phase causes the particles of quartz and of the kaolinite residue to adhere together, this phenomenon being due, in the initial stage of fusion of the feldspar, to adhesion interaction at the surfaces of contact between the liquid and crystalline phases; this adherence is an effect of surface forces.

As for the more thoroughgoing reaction of the molten feldspar with the high-melting crystalline particles, these processes are insignificant during this introductory period.

As the temperature is raised, the viscosity of the molten feldspar drops, and the effect of the surface forces acting at the interphase boundaries becomes more pronounced. The crystalline particles come closer together, the paste grows denser, and its porosity diminishes. This corresponds to the well-known phenomenon of shrinkage of the body.

The porcelain body is not deformed during this stage of high-temperature firing, notwithstanding the increase in the volume of the molten feldspar. This extremely valuable property of porcelain paste is due to the following factors: a) the slowness with which the feldspar melts; the temperature range within which potash feldspar melts (from the beginning of fusion to complete melting) is some 250 to 300°; and b) the high viscosity of molten feldspar (the feldspar particles are frequently vitrified while preserving their original shape).

Raising the temperature lowers the viscosity of the melt, and hence increases the mobility and reactivity of the feldspar particles. Under these conditions there sets in an intensive physical and chemical interaction between the molten feldspar and the crystalline particles. As a result of this interaction, the kaolinite residue and the quartz begin to dissolve in the molten feldspar. The rate at which this dissolution takes place depends upon the chemical composition and the physical state of the paste, as well as upon the firing temperature.

It is obvious that the dissolution of the high-melting crystalline particles must cause a corresponding change in the liquid phase. Moreover, as considerable experimental data have shown, prolonging the firing causes an increase in the amount of the liquid phase: in isothermal heating, the change in the volume of the liquid phase is a logarithmic function of the duration of heating.

After the firing, when the kiln cools down, the molten feldspar does not crystallize because of its high viscosity, but hardens in a vitreous state. A vitreous phase is constituted in the porcelain body, producing its translucency and other properties of the body.

The proportion of the vitreous phase in the microstructure of the porcelain body depends upon the percentage of feldspar in the paste and the firing temperature. That is precisely why many authors have found in their microscopic investigations that the percentage of glass in porcelain body fluctuates within very wide limits - from 35 to 60% (most often 40-50%).

The vitreous phase of porcelain body is quite heterogeneous. It is evident that either particles of quartz or of the kaolinite residue are in contact with the molten feldspar: accordingly, the molten feldspar surrounding the quartz grains will be enriched with silica, while the molten feldspar surrounding the kaolinite grains will be enriched with the substance of the kaolinite residue.

Thus, after the porcelain body has cooled, it contains, besides the basic feldspar glass, with a refractive index of 1.49, glass surrounding the contours of the residual quartz, with a refractive index of 1.46, and glass within the range of the particles of the kaolinite residue, with a refractive index of 1.55. Some authors call the latter "argillaceous" or "kaolinitic" glass.

As for the "siliceous" glass, its nature has been more or less clearly established: it is fused feldspar, enriched with a siliceous substance due to the peripheral dissolution of the quartz grains.

As for the "kaolinitic" glass, it must be said that we have no definite explanation of its constitution. Inasmuch as the formation of "kaolinitic" glass is the result of the dissolution of the kaolinite residue in the molten feldspar, an interpretation of the nature of "kaolinitic" glass requires first of all an explanation of the nature of the kaolinite residue. The problem of what the kaolinite residue consists of can be considered only in connection with the problem of mullitization during the formation of porcelain.

Mullitization of the body. The processes mentioned above, which take place in the firing of porcelain and involve the liquid phase, are closely linked to the mullitization of the body, which is of considerable importance in ceramic technology. Investigations of mullitization very often arrive at results that do not agree with each other.

In the past, the question: "Mullite or sillimanite?" was discussed in the literature. The principal source of dispute in the years of scientific polemics on this problem was the close mineralogical resemblance between the crystals of mullite and sillimanite, which made it impossible for microscopic and X-ray examination to settle this question for many years.

By now, numerous contemporary researches, the data on the phase equilibria in the Al_2O_3 - SiO_2 system, in particular, have established the fact that the only one of these two oxides that is stable in the temperature and concentration range we are interested in is mullite. Nevertheless the term "sillimanite" is still encountered in many recent descriptions of the microstructure of porcelain body. It is worthy of note in this connection that as far back as 60 years ago the noted Russian scientist Vernadsky [2], who was one of the first to describe the microstructure of porcelain body, stated on the basis of his analyses of the new crystalline formations he had observed in porcelain body that the chemical composition of these new formations differed from that of sillimanite. This fact is all the more noteworthy because methods of scientific experimentation were still quite imperfect at the end of the past century, when Vernadsky's paper was published.

In connection with the assertions that mullite and sillimanite are identical and the assumptions that crystalline formations of the solid solution type are present, we might say that the data of chemical analysis refute the possibility of any such supposition and support the chemical and mineralogical individuality of mullite.

After the problem of "mullite or sillimanite" had been solved, the most recent papers on mullitization pose two new questions, to which different authors give differing answers: 1) what is mullite formed from; and 2) what is the nature of the quantitative changes produced in mullite by heating the body to high temperatures.

The answer to be expected to the first question is that the formation of mullite is due either to changes in the kaolinite or to crystallization of a saturated melted alumino-silicate.

Numerous reports on the microstructure of porcelain body have established the fact that the principal source of mullite is the decomposition product of kaolinite; but when no liquid phase is present, the minute mullite crystals formed as the result of intramolecular processes are in an embryonic stage, and their linear dimensions are so small that they are extremely hard to detect by the usual methods of studying microstructure. The appearance of the liquid phase promotes the growth of the crystals.

There is another interpretation of this problem, however: some authors, for example, believe that mullite is not formed from the kaolinite residue alone. They assume that mullite crystals can crystallize out of molten feldspar. To be sure, if we have a melt containing Al_2O_3 and SiO_2, why shouldn't crystals of mullite crystallize out of such a melt when it cools? Even the equilibrium diagram indicates that at a certain temperature and a certain ratio of these two oxides, the products of crystallization of the alumino-silicate melt ought to contain mullite.

In this connection, we must first underline the thermodynamic nature of the equilibrium diagrams. These diagrams have one defect: they consider the process without allowing for the time factor - a most important factor in crystallization processes, both in industrial kilns as well as in nature.

When we also bear in mind that in the temperature range we have been considering for the firing of porcelain, the feldspar is not entirely melted, but is in an extremely viscous "semimelted" state, the metastability of the porcelain body while firing and the absence of mullite crystals in the products of the fused feldspar after cooling become obvious.

Evidently, full light can be shed upon this problem by a study of the cooled melt of pure feldspar; as the result of such study many authors have established that mullite is not formed under these conditions.

The question then arises: what can the basis of the opposing viewpoint be? It seems to us that the sole reason for its appearance is the fact that mullite crystals are found within the confines of the feldspar grain. This latter fact, which has been established in many descriptions of the microstructure of porcelain body, must be interpreted differently, namely: the presence of mullite within the confines of the feldspar grain is most likely due to the diffusion of particles of the kaolinite residue into the fused feldspar.

Summing up the principal facts concerning the problem of what is the source of mullitization in porcelain body, we must state that the major arguments in support of the formation of mullite from the products of intramolecular transformation of the kaolinite are as follows:

1) Mullite is formed only in those porcelain bodies whose pastes contain kaolinite.

2) The product formed by cooling a melt of pure feldspar contains no mullite.

3) The manifest crystallization of mullite within the confines of the feldspar grain cannot be due to the latter, inasmuch as the percentage of silica in the fused feldspar is obviously insufficient for the formation of mullite.

We have the following contradictory conclusions regarding the second problem: the nature of the quantitative mullite changes occurring during high-temperature firing:

a) According to some research workers, the amount of mullite in the body rises constantly as the temperature is raised and the firing time is prolonged, the linear dimensions of the mullite crystals growing at the same time.

b) According to other researchers, during firing the amount of mullite increases up to a certain temperature, any further rise in temperature causing a drop in the percentage of mullite, owing to its dissolution in the liquid phase.

The principal reason for the manifestation of such widely divergent interpretations of "mullitization" changes is the lack of an accurate method for making an analytical determination of the percentage of mullite in ceramic products. Development of an accurate method of determining the percentage of mullite is one of the most pressing tasks now facing us; a positive solution of this problem will be of great importance in deepening our knowledge of the processes involved in the firing of ceramics.

Notwithstanding this, so much experimental material on the problem of mullitization has been accumulated during the past few decades that it seems feasible to examine this problem in the light of the available data and to arrive at some very clear conclusions.

The problem of the mullitization of porcelain body can be regarded solely in close relationship to the data on the thermal analysis of kaolinite. In our literature there are numerous references to three joulean effects observed on the heating curve of kaolinite, which are the result of definite intramolecular changes that kaolinite undergoes when heated. These three effects have been interpreted very divergently during the past 60 years, there being no generally accepted opinions on the subject at the present time.

In our paper [3] on the nature of the joulean effects in kaolinite, reporting the results of thermodynamic and X-ray investigations, we found that:

1) The product of the endothermal joulean effect (in the temperature range of 500-550°) is metakaolin, which is formed as the result of the dehydration of kaolinite, in accordance with the following equation:

$$Al_2O_3 \cdot 2SiO_2 \cdot 2H_2O \rightarrow Al_2O_3 \cdot 2SiO_2 + 2H_2O;$$

2) The exothermal joulean effect in the 900-1100° range corresponds to the breakdown of the metakaolin:

$$Al_2O_3 \cdot 2SiO_2 \rightarrow \gamma\text{-}Al_2O_3 + 2SiO_2;$$

3) The second exothermal effect observed in the 1200-1300° range is due to the chemical interaction of the free oxides, resulting in the formation of mullite, according to the following equation:

$$3Al_2O_3 + 6SiO_2 \rightarrow 3Al_2O_3 \cdot 2SiO_2 + 4SiO_2.$$

The last equation indicates that there is some excess silica left over after the mullite is formed. This fact is in good agreement with the data of Belyankin and Feodotyev [4], who showed that amorphous silica is crystallized in the temperature range of the second exothermal effect. These authors quite convincingly and clearly cite in support of their opinion the fact that the second exothermal effect on the kaolinite heating curve coincides with the corresponding effect shown in the heating curve of silica gel.

Several papers have been published in recent years on the quantitative study of the mullitization process. Generalizing the results of these researches enables us

to use them in further support of the foregoing interpretation of the second exothermal effect as the result of chemical reaction between the oxides, giving rise to mullite.

When we examine the work of Budnikov and Shmukler [5], Freberg [6], Goncharov [7], and other authors, we see that most of the mullite is formed in a rather narrow temperature band, 1150-1250°, during the process of firing.

We must stress the point that this temp. range of intensive mullitization (1150-1250°) coincides with the temperature range for the second exothermal effect observed when pure kaolinite is fired.

This extremely interesting circumstance enables us to relate the mullitization process of porcelain to the physical and chemical changes of pure kaolinite, due to the second exothermal effect. The establishment of this link between the two phenomena enables us to reach the following conclusions.

1. The data on the quantitative measurements of the mullite yield confirm that the second exothermal effect on the kaolinite heating curve corresponds to a chemical reaction involving the formation of mullite from the oxides:

$$3Al_2O_3 + 2SiO_2 \rightarrow 3Al_2O_3 \cdot 2SiO_2.$$

2. There are numerous experimental data indicating that the reaction involved in the formation of mullite does not take place in every medium that consists of the two oxides Al_2O_3 and SiO_2.

We may point to the cooling of a feldspar melt without any mullite being formed.

The most favorable conditions for the formation of mullite are the presence of the constituent oxides Al_2O_3 and SiO_2, formed after the kaolinite crystal lattice has been ruptured (which takes place when the kaolinite products have been heated above 1000°).

We think this fact can be explained as follows: the free particles of Al_2O_3 and SiO_2 are in a state of maximum chemical activity immediately after the decomposition of the kaolinite, when there are no chemical bonds between them. When in this state, the chemical reaction involved in the formation of mullite takes place with high speed, owing to the high reactivity of the constituents (Al_2O_3 and SiO_2).

3. As for the fact that there is no appreciable amount of mullite in the products obtained by firing an argillaceous substance at lower temperatures (below 1150°); though there are qualitative indications of the appearance of mullite below the temperature of the second exothermal effect, this proves that mullite is formed at a low rate at such low temperatures.

Hence, the presence of mullite lines in X-ray photos of kaolinite taken at temperatures much below 1150° may be explained as due to the absence of sharp temperature boundaries in kaolinite reactions, which may also take place at lower temperature, though at a lower reaction rate and with a lower yield of the reaction product (in this instance, mullite).

Therefore, the fact that mullite is found below 1150° cannot serve as a basis for explaining the first exothermal effect as due to the formation of mullite.

4. The foregoing conclusion regarding the "active" state of the firing products immediately after the rupturing of the kaolinite lattice in the temperature range of the second exothermal effect enables us to make the following assertion, which is of value in the management of the industrial firing of porcelain materials: It is advisable to slow down the temperature rise or even to "hold" it in the temperature range of 1100-1250°, at which the fired materials are in a disordered state and consist of the oxides Al_2O_3 and SiO_2 with increased reactivity; this ought to increase the rate at which the body is mullitized.

Consideration of the process of mullitization of the body and of the related second exothermal effect in the kaolinite heating curve enables us to clear up the meaning of the term "kaolinitic glass."

It is quite impossible to agree with the view that there is such a thing as "argillaceous" glass in porcelain, since there cannot be any kaolinitic substance in the paste of the ware being fired as soon as the feldspar begins to melt. What has been said about the nature of the second exothermic effect in the kaolinite heating curve shows that at that temperature the kaolinite has been replaced by mullite and amorphous silica. For the same reason we cannot accept the assertions concerning the dissolution of silica (the oxide) in the molten feldspar.

The nature of the so-called "kaolinitic" glass may be explained as follows: inasmuch as the decomposition products of the kaolinitic substance are crystals of mullite and excess amorphous silica, the latter (which is fairly soluble) readily enters the molten feldspar, enriching it with siliceous substance and forming a silica-feldspar glass, which is interpenetrated by the minute acicular crystals of mullite.

Thus the "siliceous" and "kaolinitic" glasses in the microstructure of porcelain differ but little in their chemical composition: in both cases the glass is formed chiefly as the result of the dissolution of the silica in the molten feldspar. The glass formed by the dissolution of the kaolinite residue differs from the "siliceous" glass in that it contains minute crystals of mullite.

Thus three kinds of glass are to be distinguished in the microstructure of porcelain body:

1) Feldspar glass.

2) Silica-feldspar glass, without mullite, enveloping the residual grains of quartz.

3) Silica-feldspar glass with inclusions of mullite within the confines of the products of the change in the kaolinite residue.

Diagram of the formation of porcelain body. Despite the contradictions in the results of some chemical and structural investigations of the structure of porcelain body, a very extensive body of experimental material has been accumulated during the past half-century, dealing with the processes involved in the firing of porcelain.

A comprehensive examination of these data has served as the basis for a diagram we have developed for the formation of porcelain body, generalizing the results of numerous X-ray, microscopic, and chemical investigations.

This diagram covers the principal stages of firing and the sequence in which the physical and chemical processes occur that result in the formation of the porcelain body. Since the latter take place chiefly at high temperatures with the liquid phase playing a part, we have concentrated upon the processes occurring in the second stage of firing. The low-temperature processes, which involve various changes in the solid phase, especially changes in the kaolinite and the quartz, are described in very great detail in the literature: there is very little difference between the nature of these processes in the first stage of firing porcelain and the similar processes involved in the firing of other ceramic materials.

That is why, in this diagram, all these extremely complicated physical and chemical changes in the low-temperature firing stage, up to the beginning of the formation of the liquid phase, have been combined into one group under the heading of "processes in the solid phase."

Moreover, we have been guided by the following propositions in our consideration

Diagram of the Formation of Porcelain Body

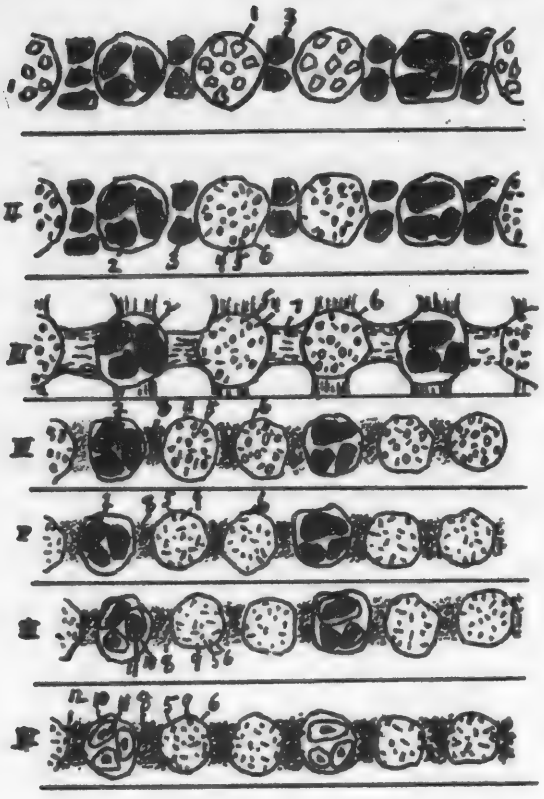

1 - Kaolinite; 2 - quartz; 3 - feldspar; 4 - SiO_2; 5 - primary mullite in the kaolinite residue; 6 - boundary of the kaolinite's reaction with the feldspar; 7 - molten feldspar; 8 - feldspar melt; 9 - silica - molten feldspar within the confines of the kaolinite residue; 10 - fused edge of quartz; 11 - residual quartz; 12 - mullite within the confines of the feldspar melt (diffusion).

I - Composition of the raw porcelain paste (kaolinite + quartz + feldspar).

II - Initial firing period: "processes in the solid phase." Products: quartz + feldspar + kaolinite residue with mullite inclusions + silica.

III - Second firing period: fusion of the feldspar. Drops of the melt cement the solid particles; increase in mechanical strength as a result of liquid adhesion phenomena.

IV - Third firing period: lowering of the viscosity of the liquid phase as a result of the rise in temperature. Heightened effect of the surface forces acting at the interphase boundaries; shrinkage of the body.

V - Fourth firing period: period of the reaction of the molten feldspar with SiO_2. Reaction with the amorphous SiO_2 arising from the product of the kaolinite residue, giving rise to silica - molten feldspar, with the interspaces filled with minute mullite crystals.

VI - Fourth firing period: period of the reaction of the molten feldspar with the quartz grains; a fringe of the liquid phase constituting silica - molten feldspar, is formed at the boundaries of the quartz grains.

VII - Fifth firing period: period of the crystallization of mullite within the molten feldspar as the result of the diffusion of the substance of the kaolinite residue. Appreciable decrease in the dimensions of the residual quartz, owing to the continuing fusion.

---

of the process of porcelain formation in its most general aspect:

1) The initial mixture of porcelain paste consists of three minerals; kaolinite, quartz, and feldspar.

2) Fully "ripened" porcelain body contains: a) residual quartz; b) fused quartz; c) feldspar glass; d) feldspar glass with silica dissolved in it - the product of the decomposition of the kaolinite; e) mullite in the glass, formed from the silica coming from the kaolinite residue; and f) mullite within the fused feldspar.

It should be noted that there are references in the literature to some other elements in the microstructure of porcelain body, observed by various authors. We did not include these atypical, accidental crystalline substances in our list of the component parts of the microstructure of porcelain. An example of this is cristobalite, which many authors believe is present in the microstructure of porcelain body, though most of the research papers on this topic deny the degeneration of quartz into cristobalite.

We have chosen as characteristic of porcelain only those constituents that have been found in nearly every research paper describing the microstructure of porcelain and about whose existence there is no doubt whatsoever.

In our diagram, the process of the formation of porcelain body is divided into five major periods (see the diagram on p. 148).

SUMMARY

1. Quantitative data on the process of mullitization prove that the period of intensive mullite formation coincides with that of the second exothermal effect in the heating curve of kaolinite.

2. The cited data are further confirmation of the interpretation of the second exothermic effect as the result of the chemical reaction between the free oxides Al_2O_3 and SiO_2, giving rise to mullite.

3. After the first exothermal effect, above 1000° and up to 1250°, the oxides Al_2O_3 and SiO_2 in the decomposition products of kaolinite are in an "active" state.

The heightened reactivity of the oxides at these temperatures is responsible for intense mullitization.

4. In view of the high chemical activity of the decomposition products of kaolinite after the completion of the first exothermal effect, it is advisable in industrial firing of porcelain to slow down the rate at which the temperature is raised and even to hold it constant in this temperature range, as this ought to promote the intensive mullitization of the body.

5. The vitreous phase in porcelain body comprises: a) feldspar glass; b) silica - feldspar glass (without mullite), enveloping the quartz grains; and c) silica - feldspar glass, containing mullite, within the confines of the particles of the kaolinite residue.

6. A diagram is set forth for the formation of porcelain body, covering the successive steps in the principal processes of firing and the formation of the principal structural elements of porcelain.

LITERATURE CITED

[1] P.A.Zemyatchensky. Material for a study of the Natural Productive Forces of Russia. 46 (1924).

[2] V.I.Vernadsky, Bull. soc. franc. mineral-., 13 (1890).

[3] B.S.Shvetsov and Kh.O.Gevorkyan, J.Appl. Chem., XV, 5 (1942).

[4] D.S.Belyankin and K.M.Feodotyev, Proc. Acad. Sci. USSR, 15, 3 (1949).

[5] P.P.Budnikov and K.M.Shmukler, J. Appl. Chem. 19, 10-11 (1946).

[6] A.K.Freberg, Collected Dissertations of the Leningrad Institute of Chemical Technology (1940).

[7] V.V.Goncharov and A.T.Kleinberg, Refractories, 4, 1192 (1938).

Received May 3, 1950.

THE THERMOCHEMICAL CONVERSION OF FERROUS SULFATE*

M. E. Pozin and A. M. Ginstling

The literature contains no references to the problem of the mechanism involved in the thermochemical conversion of ferrous sulfate when mixed with reducing agents. And yet knowledge of this is required for an understanding and practical utilization of the influence of the underlying conditions of this process upon its course and rate, besides being important for the light it throws upon the theory of a large group of processes resembling the one in question.

The present paper represents a theoretical and experimental investigation of the mechanism involved in this process.

The following are the principal topics dealt with: 1) the principal and intermediate reactions in the process; 2) the feasibility and the mechanism of the reaction of ferrous sulfate with carbon without direct contact between them; 3) the part played by an inert solid in the process; 4) the limiting stage of the process; 5) the mechanism of the effect of reducing agents upon the process; 6) the mechanism involved in the effect of a gas upon its composition; and 7) the significance of the granulometric composition of the particles of sulfate and carbon.

The thermochemical conversion of ferrous sulfate when mixed with reducing agents may be represented as follows:

When $FeSO_4$ is heated to above 550-580°, these reactions occur:

$$2FeSO_4 \rightleftarrows 2FeO + 2SO_3, \qquad (1)$$

$$SO_3 \rightleftarrows SO_2 + \tfrac{1}{2}O_2, \qquad (2)$$

$$2FeO + \tfrac{1}{2}O_2 \rightleftarrows Fe_2O_3, \qquad (3)$$

constituting a process described by the customary overall equation:

$$2FeSO_4 \rightleftarrows Fe_2O_3 + SO_2 + SO_3. \qquad (4)$$

The presence of sulfur trioxide and ferric oxide in the system as the result of Reaction (4) causes the following equilibrium to be set up:

$$Fe_2O_3 + 3SO_3 \rightleftarrows Fe_2(SO_4)_3. \qquad (5)$$

Hence, the process involved in the decomposition of ferrous sulfate may also be represented by this equation:

$$6FeSO_4 \rightleftarrows 3SO_2 + 2Fe_2O_3 + Fe_2(SO_4)_3. \qquad (6)$$

When reducing agents are present, the oxygen liberated in Reaction (2) is bound into an oxide. Reacting with the carbon or sulfur in the reducing agent, it forms CO, CO_2 or a mixture of the two, respectively, in accordance with the following reactions:

$$C + O_2 \longrightarrow CO_2, \qquad (7)$$

$$2C + O_2 \longrightarrow 2CO, \qquad (8)$$

$$2CO + O_2 \longrightarrow 2CO_2, \qquad (9)$$

---

*Report III of a series on this topic.

or sulfur dioxide, in accordance with this reaction:

$$S + O_2 \longrightarrow SO_2. \qquad (10)$$

The sulfur dioxide and trioxide liberated by the dissociation of the sulfates in accordance with the reactions (4) and (5) diffuse from the solid particles into the gas phase through the diffusion layer of ferric oxide, which grows in size throughout the process. The carbon monoxide evolved by the incomplete oxidation of the carbon diffuses to the sulfate particles through the same layer, being oxidized there to CO_2 by the oxygen liberated in Reaction (2). The carbon dioxide is diffused in conterflow to the carbon monoxide.

On the whole, therefore, the thermochemical conversion of the ferrous sulfate - reducing agent mixture takes place without direct chemical interaction between the solid substances and without any participation of the liquid phases. It occurs in the gas phase.

This outline of the process is based upon the following considerations:

1. The reality of each of the reactions (1) – (10) in the temperature range 580-700° has been proved repeatedly by experiment and is beyond question.

2. The dissociation pressure of ferrous sulfate in Reaction (4) is much higher than the dissociation pressure of ferric sulfate in Reaction (5). We know, for instance, that the dissociation pressure of $FeSO_4$ at 614, 634, and 650° is 254, 328, and 600 mm Hg, respectively [1], while that of $Fe_2(SO_4)_3$ is 70, 113, and 149 mm Hg [2]. This indicates that Reaction (5) is the limiting reaction in the conversion of ferrous sulfate into ferric sulfate.

3. In general, the side reactions that may occur when CO, C, SO_2, and S are present in the system, involving the formation of sulfur, carbon oxysulfide, and carbon disulfide:

$$2C + SO_2 \rightleftarrows CO + COS, \qquad (11)$$

$$4CO + 2SO_2 \rightleftarrows 4CO_2 + S_2, \qquad (12)$$

$$2CO + S_2 \rightleftarrows 2COS, \qquad (13)$$

$$2COS \rightleftarrows CO_2 + CS_2, \qquad (14)$$

cannot play any essential role in this process. When oxygen is present, whether entering from the outside or evolved in accordance with Reaction (2), the carbon, sulfur, and carbon monoxide will, of course, be converted in accordance with Reactions (7) – (10), rather than (11) – (14), since their equilibrium and velocity constants are incomparably smaller under the process conditions.

4. The probability of direct reaction between the ferrous sulfate and the carbon in the coal is very small in view of the negligibly small actual surface of contact between them and the presence of a diffusion layer of solid products.

5. It is impossible for a liquid phase to appear in the system, since the melting points of the initial, intermediate, and end products, and of any possible eutectic mixtures, are much higher than the maximum temperature of the process.

Some of the propositions underlying the suggested flow sheet required experimental verification.

EXPERIMENTAL

We first tested the feasibility of reacting ferrous sulfate with carbon without their being in direct contact. This was done by heating layers of the sulfate and of carbonaceous materials, which were carefully isolated from each other by porcelain or quartz, in a furnace in a current of nitrogen.

These tests were run with coke in order to eliminate the influence of volatile constituents in the coal.

The results of the test series, reproduced in part in Table 1 and Fig. 1, clearly indicate the existence of interaction between the sulfate and the carbon when they are isolated from each other, or, in other words, the reality of their interaction via the gas phase.

TABLE 1

Thermochemical Conversion of Ferrous Sulfate by an Isolated Reducing Agent in a Current of Nitrogen at 650° *

With no reducing agent present		With coke		With coal	
τ	x	τ	x	τ	x
10	34.4	9	30.8	6	26.1
30	48.3	26	48.2	13	49.4
60	60.1	40	60.9	40	68.5
–	–	60	75.3	60	76.8

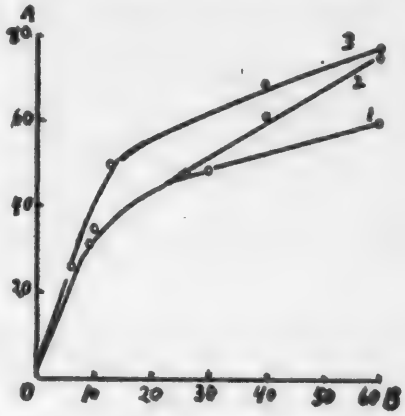

Fig. 1. Conversion of ferrous sulfate by an isolated reducing agent in nitrogen at 650°.

A-% sulfatic sulfur, in terms of SO_2; B-Elapsed time from start of run, min.; 1-Without a reducing agent; 2-coke; 3-coal.

The influence of an inert solid introduced in the original mixture may serve as an indication of how the process takes place either by direct contact and direct interaction of the solid particles of the initial reagents, or in some other way.

The inert solid should retard the process, depending upon the reagent surface it occupies, provided the process takes place via the direct interaction of the solid particles, while it ought not to cause any appreciable slowing up of the process if the latter involves the reaction of a gas or a liquid with the solid. In the latter case, the gaseous or liquid reagent can gain access to the surface of the solid reagent when a certain quantity of inert is present almost as if the latter were not present.

We employed this circumstance to ascertain the actual course of the process by testing the thermochemical conversion of a sulfate-coal mixture with and without a finely crystalline inert solid (silica). The carbon-sulfate ratio in the mixture was kept constant. The tests were run at 650° in nitrogen.

The results of these tests, reproduced in Table 2 and Fig. 2, indicate that an inert solid causes practically no slowing down of the process when a fairly large amount of it is added to the mixture. These results thus also show that the process takes place in the gas phase.

Our experiments have shown that the reducing agent (coal, pyrites) intensifies the process under consideration [3].

To evaluate the results of experiments using a sulfur reducing agent correctly, we had to know whether the pyrites placed in the initial mixture simply serve as an additional source of sulfur, which is transferred to the gas phase during the decomposition of the mixture, the observed intensification of the process thus being apparent rather than real.

A series of tests were run to shed light on this problem. The results were as follows.

When the pyrites were kept at 650° in a current of nitrogen, flowing in the

* In all the tables, τ is the time elapsed from the beginning of a test (in min.), and x is the percentage of sulfatic sulfur, in terms of SO_2.

TABLE 2

Conversion of Ferrous Sulfate Mixed with Coal in a Current of Nitrogen at 650° (Composition of the Mixture: 90% $FeSO_4 \cdot H_2O$ + 10% C)
Process Rate with and without an Inert Solid Present

Without an inert		With 25% SiO_2	
5	93.3	3	77.6
20	97.3	20	96.0
42	97.7	40	97.1
60	98.3	60	98.5

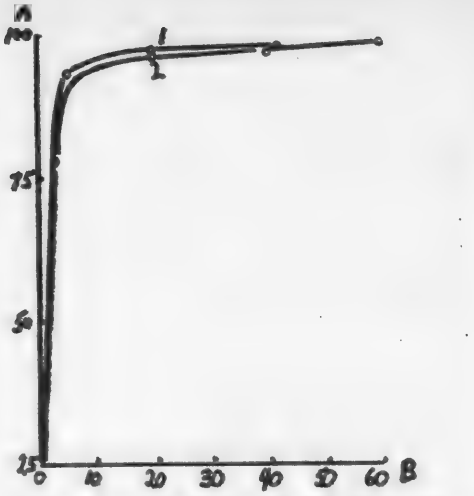

Fig. 2. Conversion of ferrous sulfate mixed with coal in a current of nitrogen at 650°. Process rate with and without an inert solid present.

A-Degree of sulfate conversion,%. B-Elapsed time from start of run, min. 1-Without a reducing agent; 2-25% SiO_2.

gas phase at the rate of 3 liters per hour, for 23 minutes, about 25% of the total pyritic sulfur was extracted.

Under these conditions the thermal dissociation of the sulfate totaled about 43%.

Thus, if the pyrites added to the sulfate had acted merely as a supplementary source of sulfur, and if the pyrites and the sulfate had behaved wholly independently of each other when heated together, with a mixture containing 84.3% $FeSO_4$ and 15.7% FeS_2, about:

$$43 \cdot 0.843 + 25 \cdot 0.157 = 40.2\%$$

of the total sulfur in the mixture would have been converted into the gas phase.

In actuality, however, the decomposition of this pyrites-sulfate mixture for 23 minutes under the conditions specified above caused the extraction of nearly 96% of the sulfur into the gas phase as SO_2 and SO_3. This shows that pyrites added to the charge cause a marked intensification of the process of decomposing the sulfate.

This process outline fully explains the mechanism involved in the intensifiying action of the reducing agent upon the process.

It is evident that the proceeding of Reaction (5) from right to left at constant temperature depends wholly upon the partial pressure of SO_3 in the gas phase above the $Fe_2(SO_4)_3$. The reduction of the partial pressure of SO_3, required for intensifying Reaction (5), is effected by Reaction (2), it being known from the expression for the latter's equilibrium constant:

$$K_p = \frac{p_{SO_3}}{p_{SO_2} \cdot p_{O_2}^{0.5}}, \qquad (15)$$

that when the SO_2 concentration is constant, reducing the partial pressure of the oxygen results in lowering the partial pressure of the sulfur trioxide.

It is therefore natural that the presence of carbon or pyrites in the initial mixture, which brings about the reactions (7) – (10) or the reaction involving the combustion of FeS_2 and thus causing a diminution in the concentration of oxygen in the reaction zone, speeds up the process of converting the ferrous sulfate.

This makes it evident that increasing the concentration of oxygen in the reaction zone by adding it from without, shifting the equilibrium of Reaction (2) to

the left and Reaction (5) to the right, must slow down the thermal decomposition of ferrous sulfate.

This is fully borne out by the experimental data we have secured on the rate of dissociation of $FeSO_4$ in an atmosphere of an inert gas containing various percentages of oxygen [4].

When the initial mixture contains reducing agents that can be oxidized by the added oxygen, it is natural to expect a different variation of the process rate with the percentage of oxygen in the original gaseous mixture. We know that the combustion rate increases with a rising percentage of oxygen in the reaction zone, all other conditions remaining the same. Hence, when a sulfur reducing agent is employed, the higher the oxygen concentration in the gas phase, the more sulfur is released per unit time in the form of SO_2 and SO_3.

What is more important, however, is that the combustion of the reducing agent results in raising the temperature of the entire charge.

In the case in question, the temperature of the charge will rise at a rate that depends upon the percentage of oxygen in the gas, and, inasmuch as the rate at which the sulfate is decomposed increases as the temperature rises, this decomposition will be correspondingly more intensive.

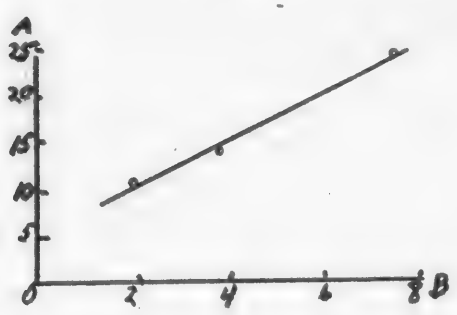

Fig. 3. Conversion of sulfate mixed with coal in a current of nitrogen at 600°. Extent of conversion after 5 minutes as a function of the surface of the coal grains.

A-% conversion of the sulfate; B-Mean surface of the coal grains, cm^2.

TABLE 3

Conversion of Ferrous Sulfate Mixed with Coal in a Current of Nitrogen at 600°

Extent of conversion after 5 minutes for various surfaces of the coal particles.

Wt. of coal, g	Initial radius of coal particles, mm	Surface of coal particles cm^2			Per cent conversion of sulfate
		Initial	After 5 minutes	Average	
0.025	0.232	2.0	1.89	1.94	10.5
0.025	0.133	3.51	3.14	3.32	14.05
0.025	0.071	6.6	5.52	6.06	24.2

It is evident that accelerating or slowing down the process by means of oxygen must be governed by the ratio between the sulfate and the reducing agent in the initial mixture. In particular, the percentage of oxygen in the gas phase must exert a positive effect upon the process rate as long as there is enough of the reducing agent in the mixture.

Such a mechanism of the influence of oxygen upon the process rate fully explains the test results obtained in the conversion of the sulfate charge in an oxygen-nitrogen atmosphere of varying composition [4].

At a given degree of conversion, the larger the initial particles of sulfate, the thicker will be the diffusion layer of ferric sulfate on the surface of the sulfate particles.

Hence, if the kinetics of the process are governed by the diffusion of the substances through this layer, formed on the sulfate particles, the diameter of the

latter must have a decisive effect upon the process rate. On the other hand, the size of the particles of the reducing agent governs the velocity of Reactions (7) – (10) and, hence, of Reactions (2) and (5).

Therefore, if all other conditions remain the same, the process rate will be practically independent of the size of the sulfate particles, so long as the diffusion layer is relatively thin. At the very start of the process it should be proportional to the surface of the particles of the reducing agent.

Moreover, during a certain intermediate period, the process rate depends upon the size of the particles of reducing agent and sulfate. And, finally, when we shift to the diffusion region, in which the limiting stage of the process is the diffusion of the reagents through the layer of ferric oxide, the process rate, all other conditions being equal, will be practically governed by the size of the sulfate particles.

It is a matter of course that the smaller the ratio between the dimensions of the sulfate and coal particles, the more marked will be the first period (with the process rate governed by the size of the coal particles), while the larger this ratio, the more important will be the last period (with the diffusion kinetics governed by the size of the sulfate particles).

It is precisely this variation of the process rate with the grain size of the components of the initial mixture that has been established during our investigations.

When the coal particles are larger than 0.05 mm in diameter, the process rate at the very start is proportional to the surface of the coal particles. This is seen from the figures in Table 3 and the graph in Fig. 3. As the process progresses, this proportionality vanishes to such an extent that diminishing the diameter of the coal particles 600% increases the extent of sulfate conversion after 60 minutes only 25%.

It is obvious that in this case the process rate is governed by the dimensions of the particles of ferrous sulfate. In fact, dividing their mean diameter by a factor of 1.7 increases the conversion of the sulfate after 60 minutes under the same conditions by a factor of 1.5 [3].

The variation of the process rate, which is limited by diffusion into spherical particles, with the size of the latter, is given, in general, by the following equation [5]:

$$I = 1 - \frac{2}{3} G - (1 - G)^{2/3} = K \cdot \frac{1}{R^2} \cdot \tau , \qquad (16)$$

where $G = x/100$ is the fraction of the substance converted; R is the initial radius of the particles of this substance; τ is the time; and K is a coefficient indicating the physical properties of the reacting substances and products under the process conditions.

TABLE 4

Comparison of Experimental Data with Equation (17)

R_1	R_2	$\left(\frac{R_1}{R_2}\right)^2$	τ	G_1	G_2	I_1	I_2	$\frac{I_2}{I_1}$
0.073	0.124	0.35	40	0.791	0.537	0.1215	0.0248	0.35
0.073	0.124	0.35	60	0.849	0.581	0.1505	0.0531	0.35

It follows from Equation (16) that if I_1 and I_2 are the values of the function I corresponding to the conversions G_1 and G_2 of a sulfate whose particles have the radii R_1 and R_2, respectively, then:

$$\frac{I_2}{I_1} = \left(\frac{R_1}{R_2}\right)^2 . \qquad (17)$$

Table 4, in which the value of I_2/I_1 has been computed from the data on the conversion of a sulfate whose particles have a mean radius of 0.073 and 0.124 mm, respectively, enables us to compare the experimental data with the values computed from Equation (17). The tabular data are for the conversion of a sulfate mixed with coal in a current of nitrogen at 600°.

The agreement of the values of I_2/I_1 with those of $\left(\frac{R_1}{R_2}\right)^2$ indicate that the process rate is actually limited ultimately by the diffusion of the substances through the layer of ferric oxide.

SUMMARY

1. The thermochemical conversion of ferrous sulfate involves a series of intermediate reactions, the slowest of which is the reaction

$$Fe_2(SO_4)_3 \rightleftarrows Fe_2O_3 + 3SO_3,$$

the rate of which is governed by the partial pressure of the sulfur trioxide in the reaction zone.

2. The reaction of ferrous sulfate with coal and pyrites takes place via the gas phase and is practically independent of the actual surface of contact between the particles of the solid reducing agent and the sulfate.

3. At the beginning, the process rate is limited by the excess of free oxygen in the reaction zone and by the intensity of its combustion, which shifts the equilibrium of the dissociation of the ferrous sulfate and the sulfur trioxide toward the formation of the end products of the process – SO_2 and Fe_2O_3. Accordingly, introducing the reducing agent in the initial mixture and diminishing the percentage of oxygen in the initial gas intensifies the process considerably.

4. As the diffusion layer of the solid reaction product – ferric oxide – grows thicker, the part played by diffusion in this process increases, so that after a certain time the process rate is governed entirely by the rate of diffusion.

5. The variation of the process rate with the size of the particles of the initial substances (all other conditions remaining the same) entails a gradual shift of the former from the region of chemical kinetics via an intermediate region to the region of diffusion kinetics: at the beginning of the process, its velocity is proportional to the surface of the reducing agent particles; during the intermediate period it is a function of the particle size of both constituents of the mixture; and in the final period it is practically determined by the size of the ferrous sulfate particles alone.

LITERATURE CITED

[1] E. Greulich, Z. anorg. Chem., 168, 201 (1927).

[2] L. Wohler et al., Ber., 41, 707 (1908).

[3] M.E.Pozin and A.M.Ginstling, J. Appl. Chem. 23, 11 (1950).

[4] M.E.Pozin and A.M.Ginstling, J. Appl. Chem. 23, 12, 1245 (1950).

[5] A.M.Ginstling and B.I.Brounshtein, J. Appl. Chem. 23, 12, 1249 (1950).

Received March 17, 1950.

THE NATURE OF THE REACTION OF CHROME COORDINATION COMPOUNDS WITH THE PRINCIPAL GROUPS IN PROTEIN

I. P. Strakhov

Many researchers [1,2] class the reaction of chrome coordination compounds with collagen during the tanning process as a so-called "suturing" reaction. They assume that polychromic oxo compounds enter into the reaction, forming compounds of the complex inner salt type with the carboxyl and amino groups of the collagen, with bridges between adjacent polypeptide chains of the macromolecule. The reaction may involve the coordination of a carboxyl group of one polypeptide chain with an amino group of another by the chromium atom.

Splicing of this sort, which takes place during the tanning process, provides an explanation of such phenomena as the temperature rise when tanned leathers are welded together, the loss of the ability to swell up in acids and alkalies, and their not being hydrolyzed by ferments.

But these phenomena are merely indirect corroboration that the reaction of chrome coordination compounds with the active groups in protein is of this type. Numerous investigations of the effect of deamination of collagen upon the fixation of chrome compounds have failed to provide us with entirely clear understanding of the nature of the reaction of chrome coordination compounds with the active groups in collagen.

Study of the shift of the isoelectric point of collagen when it is reacted with tanning substances [3] has led to the conclusion that the addition of chrome coordination compounds to protein involves the formation of covalent and coordination bonds.

Recent researches [4,5] on the effect of the deamination and esterification of collagen upon the fixation of the chromecompounds likewise provide no clear answer concerning the nature of their interaction. Though in esterification the reaction may involve not only the hydrogen of the carboxyl group, the authors were unsuccessful in their employment of a chrome compound, which may contain positively and negatively charged complex chromium ions. All this made it impossible to establish the nature of the reaction of chrome compounds with collagen.

Settling this question is of importance in practice in establishing the correct operational procedure for chrome tanning. Another feature of the research is that chrome compounds of different composition and charge are employed in tanning.

The present paper has as its objective determining the nature of the interaction of various chrome coordination compounds with active protein groups by making a study of this interaction in different proteins and high-polymer nonprotein compounds that possess some common active groups.

With this in view, we chrome-tanned unchanged collagen, collagen with blocked amino groups, silk fibroin, and fiber polyamides.

EXPERIMENTAL

To increase the reliability of the results obtained in this study of the nature of the interaction with proteins, we used rather elementary chrome compounds for tanning, the charges on which were different. The compounds were prepared from (chemically pure) chromic hydrochloride and chromic sulfate by increasing the basicity with a caustic alkali; and from $Cr(OH)_3$ by reacting it with concentrated sulfuric acid at high temperature, followed by increasing the basicity with an alkali.

The resulting chrome compounds had the following characteristics (Table 1).

TABLE 1

Nature of the chrome compound in solution	Per cent basicity	Direction of migration
Chromic hydrochloride + NaOH	33.78	Toward the cathode
Chromic sulfate + NaOH	36.12	Toward the cathode
Chromic hydroxide + H_2SO_4 + NaOH	32.5	Toward the anode

The derma of cowhide was used as the collagen. The preliminary operations to isolate the derma were performed as in the leather industry. After the derma had been softened and washed with cold water, it was dehydrated with alcohol. The composition of the dehydrated derma is given by the following analytical figures for the absolutely anhydrous substance:

Mineral substances 0.32%,
Fatty substances 6.37%,
Protein substance 92.31%,
pH of a potassium chloride extract.. 5.75 .

The silk fibroin was obtained from raw silk by removing the sericin with olein soap.

In practice the silk was degummed in three baths at a temperature of 93-94°C, spending 1.5 hours in each bath. The concentration of olein soap in the first bath was 20 g per liter, with 10 g per liter in the second bath and 15 g per liter in the third. Twenty-five times the weight of solution was used. After the third bath, the silk was washed with boiling water, the temperature being gradually reduced to 36°C, until all the alkali was removed. This was checked by using phenolphthalein with the wash water, until no coloring was produced.

The polyamide used was a fiber produced by polymerizing ε-caprolactam. The structure of the polymerized caprolactam may be represented schematically as follows:

$$\ldots\text{-NH-}(CH_2)_5\text{-CO·NH-}(CH_2)_5\text{-CO·NH-}(CH_2)_5\text{-CO-}\ldots \quad [8]$$

The macromolecule of the polyamide has a linear threadlike structure, without any side groups. The resemblance between the polyamide macromolecule and that of proteins is due to the presence of amide (peptide) connecting groups -CONH- in the polyamide. The chrome tanning of the polyamide fibers aimed at shedding light upon the part played by peptide groups in binding tanning compounds.

The samples of collagen, silk fibroin, and polyamide fibers were soaked with water before tanning. They were soaked in 20 times their weight of distilled water for 14 hours. The soaked samples were tanned with the chrome compounds mentioned above. Tanning lasted 96 hours without turning.

The composition of the tanning baths was as follows: 10 times the volume of liquid; solution temperature 27°; Cr_2O_3 concentration - 20 g/liter. The bath was stirred once a day during the tanning process.

After tanning was complete, the spent liquor was poured off, and the samples were allowed to lie at room temperature for 18 hours. This was followed by washing with distilled water until all the uncombined chrome compounds had been washed out.

During the washing process, we found that the polyamide samples resumed their original color, i.e., the color they had before tanning. This indicated that the chrome compounds were either not fixed at all in these fibers or were fixed to a negligible extent. No chromium was found when the chrome-tanned polyamide samples were analyzed. The results of analysis of the chrome-tanned samples of collagen and silk fibroin are given in Table 2.

TABLE 2

Cr_2O_3 concentration in tanning liquor, g/liter	pH of initial solution	Collagen		Silk fibroin	
		Per cent Cr_2O_3 in samples			
		Of absolutely dry weight	Of 100 parts of protein	Of absolutely dry weight	Of 100 parts of protein
		Basic chromic chloride 33.78% basicity (cathodic)			
20	2.8	5.3	6.45	1.5	1.5
		Basic chromic sulfate 36.12% basicity (cathodic)			
20	2.85	8.7	12.0	1.6	1.62
		Basic chromic sulfate 32.5% basicity (anodic)			
20	3.05	7.1	9.27	1.3	1.34

The data in Table 2 indicate that the binding of chrome compounds by collagen and silk fibroin depends upon the nature of the chrome coordination compound. About 1.7 times less basic chromic chloride than basic cathodic chromic sulfate is fixed by collagen, while 1.4 and 1.5 times less of it is fixed than the basic anodic chromic sulfate.

The results listed in this table indicate the sharp difference between collagen and silk fibroin in their fixation of chrome compounds. In the samples tanned with basic chromic chloride, 4 to 5 times as much of the chrome compounds were fixed by the collagen as by the fibroin, and in tanning with basic chromic sulfate, 5 to 6 times as much of the chrome compounds were fixed by the collagen as by the fibroin. It should be noted that most of the chrome compound is fixed in the samples tanned with the basic cathodic chromic sulfate.

The absence of any fixation of chrome compounds by the polyamide fibers might be attributed, at first sight, to the fact that under ordinary conditions the polyamides are highly condensed because of the energy of intermolecular interaction, whereas normal tanning processes require that available surfaces be rendered accessible to the tanning particles, i.e., that the substance be swelled somewhat. Peptization of the polyamide fibers ruptures the intermolecular interaction forces, including the hydrogen bonds. To effect this, the polyamide fiber was treated with phenol, after which the latter was washed out by intensive washing. If the tanning substances react with the hydrogen bonds, no matter what the nature of the substances, a polyamide treated in such a manner ought to fix some quantity of tanning compounds.

The polyamide fibers were treated with solutions containing 25 and 50 grams

of phenol per liter. The solution used was 25 times the weight of the fiber, the temperature was 18.5°C, and the treatment lasted 6.5 hours. The polyamide fibers that were treated with a solution containing 50 g of phenol per liter swelled up appreciably. The swelling was less noticeable in the solution containing 25 grams of phenol per liter. The phenol-treated fibers were washed with distilled water until the ferric-chloride test was negative. The fibers were tanned with the specified chrome compounds immediately after washing was complete. After tanning, the samples were washed with distilled water; the color of the fibers was the same as in their original state.

Analysis of the chrome-tanned fibers indicated that chrome compounds do not react with the peptide groups of a polyamide, no matter what their composition or charge.

Other tests were run to explore the effect of a preliminary treatment of the collagen with formaldehyde upon the fixing of the chrome compounds listed above. Formaldehyde treatment diminishes the number of active basic groups in the collagen, the number of carboxyl groups remaining the same; this ought to affect the fixation of different chrome compounds differently.

To make sure that all the reactive groups had entered into the reaction, the formaldehyde treatment lasted 100 days, the formaldehyde concentration being 50 grams per liter, and the solution pH being kept at 9.4-9.6. To prevent the accumulation of salts in the solution as a result of the neutralization of the formic acid by the caustic alkali, the formaldehyde solution was changed whenever its pH dropped. The formaldehyde-treated collagen was washed with distilled water to get rid of the unreacted formaldehyde. The extent to which the unreacted formaldehyde had been eliminated was determined by a qualitative reaction of the wash water with resorcinol. Then the samples were tanned in the same way as the collagen that had not been treated with formaldehyde.

TABLE 3

Cr_2O_3 concentration in the tanning solution, g/liter	Per cent Cr_2O_3 (per 100 parts of protein substance)	
	Untreated collagen	Collagen treated with formaldehyde
Basic chromic chloride 33.8% basicity (cathodic)		
20	6.45	6.36
Basic chromic sulfate 36.1% basicity (cathodic)		
20	12.0	8.15
Basic chromic sulfate 33% basicity (anodic)		
20	9.27	6.8

The results of the fixing of chrome compounds by treated and untreated collagen are listed in Table 3.

The data in Table 3 show that chrome-tanning a formaldehyde-treated collagen with cationic chromic chloride compounds produces no change in the amount of fixed chrome compounds, compared with collagen that has not been treated with formaldehyde.

But when formaldehyde-treated collagen is chrome-tanned with basic chromic sulfate, the fixation averages 25% less of both the cationic and the anionic chrome compounds.

EVALUATION OF RESULTS

It was noted above that chrome compounds react with proteins via a reaction of the chromium atom with the side groups in the polypeptide chains. This view of the process involving the reaction of chrome compounds with proteins has been borne out

in the present research by our experiments in the tanning of collagen, silk fibroin, and a polyamide. The chrome compounds are fixed most by the collagen, less so by the silk fibroin. Polyamide fibers, which have no side chains with $-COOH$ or $-NH_2$ groups, do not react with chrome compounds.

The smaller amount of chrome compounds fixed by the silk fibroin than by the collagen may be explained as due to the lesser number of free amino and carboxyl groups in the silk fibroin. When we turn to the amino-acid composition, we see that the fibroin has much less of the diaminocarboxylic and monoaminocarboxylic acids than has the collagen.

According to Gustavson [7], chrome compounds react with silk fibroin at the peptide groups of the surface chains. He asserts that the peptide groups compensate for the absence of the active groups present in collagen.

In the present paper, our experimental data on the chrome-tanning of a polyamide have demonstrated that cationic and anionic chrome compounds do not react with peptide groups.

Hence, it cannot be accepted that chrome compounds react with peptide groups in silk fibroin.

The results of chrome-tanning formaldehyde-treated collagen (Table 3) indicate that the amount of fixed cationic chromic chloride does not depend upon whether the amino groups are free or blocked by the formaldehyde. In chrome tanning with anionic chromic sulfate, on the other hand, the amount of chrome compound fixed depends upon the state of the amino groups.

These facts indicate that when collagen is chrome-tanned with cationic chrom coordination compounds, the latter react principally with the carboxyl groups, whereas these compounds react with the amino groups when anionic chrome coordination compounds are used for chrome tanning.

Our experiments show a decrease in the amount of fixed cationic chromic sulfate compounds. At first glance, it would seem that this should not be so, inasmuch as the amount of cationic chrome compounds fixed does not depend upon whether the amino groups have reacted with the formaldehyde or not. An yet we actually do observe a decrease in the amount of cationic chromic-sulfate compounds fixed by the collagen. Earlier [7], the decrease in the fixation of cationic chromium was attributed to the probability that formaldehyde-treated collagen is less able to bind the hydrolyzed acid of the chrome solution, inasmuch as formaldehyde inactivates the basic groups in the protein.

This is not an exhaustive explanation, nor could it ever be generally applicable to chrome coordination compounds of various types. Our figures indicate that the behavior of the cationic chromic chloride is independent of whether the amino groups are free or have reacted with the formaldehyde. As for the decrease in the fixation of cationic chromic sulfate, that is due to a change in the composition and charge of the initial complex ion during the tanning process.

In an earlier paper [8], it was demonstrated experimentally that chrome compounds become overcharged during the tanning process, provided the anion groups of the accumulated acids are able to penetrate the inner sphere of the chrome coordination compound. This phenomenon may be due to the fact that the absorption of the basic chrome salt by the collagen disturbs the hydrolytic equilibrium, thus giving rise to additional quantities of acid in the tanning bath. The latter's anion groups penetrate the inner sphere of the coordination compound and change the composition of the complex ion as well as its charge.

Of the chrome compounds employed in our research, cationic chromic chloride suffers no change during tanning, since the ability of the chlorine ion to pene-

trate the inner sphere of the coordination compound is negligible under these circumstances.

As a result of the increasing quantity of sulfuric acid in the tanning solution, as compared to the residual chromium, the cationic chromic sulfate is able to change the composition of the complex ion and its charge during tanning; that is why the cationic chromic sulfate becomes anionic during the tanning process, and its reaction with formaldehyde-treated collagen begins to follow the pattern of anionic chrome compounds during the subsequent tanning period.

SUMMARY

1. The fact that a polyamide does not fix chrome compounds indicates that chrome coordination compounds do not react with peptide groups.

2. The fact that silk fibroin fixes less of the chrome compounds than does collagen is due to its having fewer amino and carboxyl groups in its side chains.

3. The chrome tanning of formaldehyde-treated collagen has proved that cationic chrome compounds react chiefly with the carboxyl groups of collagen, while anionic chrome compounds react with its amino groups.

The fixation of a smaller quantity of cationic chromic sulfate by formaldehyde-treated collagen is due to the fact that the chrome-tanning process involves a change in the composition and charge of the complex chromium ions, their reactions beginning to take on the pattern of anionic chrome coordination compounds.

LITERATURE CITED

[1] N.V.Chernov. Principles of Leather Quality. State Light Industry Press (1939).

[2] A. Kuntzel and Riess, Collegium, 635 (1936).

[3] S.I.Sokolov and R.I.Feldman. Colloid J. (USSR), VIII, 367 (1946).

[4] J. Bowes and R.H.Kenten, Biochem. J., 44, 142 (1949).

[5] I. Knunyants, Z. Rogovin, Yu. Rymashevskaya, and E. Khait, J. Gen. Chem., 17, 987 (1947).

[6] K.N.Gustavson. Handbuch der Gerbereichemie u. Lederfabrikation, 2, II, 180-184 (1939).

[7] K.N.Gustavson, Ind. Eng. Chem., 19, 244 (1927).

[8] I.P.Strakhov, Light Industry, 3, 14 (1949).

Received May 22, 1950

THE SPECIFIC GRAVITIES OF MOLTEN SALTS IN SYSTEMS OF CONGRUENTLY FUSING COMPOUNDS

I P Vereshchetina and N. P. Luzhnaya

There have been many research papers published on the specific gravities of molten salts. In addition to measurements of this property of individual salts, the variation of specific gravity with composition in systems consisting of two, three, and even four salts has been investigated [1].

Most researchers consider specific gravity as not very typical, as an almost purely additive property that does not enable one to draw any conclusions regarding the nature of the interaction among the system's components.

Shvartsman, for example [2], made a study of various properties of the melts in the $AgNO_3$ – AgI system, which has two congruently fusing compounds, and secured linear isotherms for the specific gravities that exhibited no appreciable deviations from additivity.

But in some instances, where the compounds formed within the system are clearly distinct, the specific-gravity isotherms depart markedly from the additive straight line.

Barzakovsky [3] recomputed the data of Mashovets and Lundina [4] on the specific gravity of the KCl – $MgCl_2$ system for molecular volumes and found a noticeable plateau on the specific-gravity isotherm at 700° for a KCl concentration of 50 mol %, which is the composition of carnallite.

In the KCl – $CaCl_2$, KCl – $CdCl_2$, and NaCl – $MgCl_2$ systems, the isotherms of molecular volumes exhibit a slight, though noticeable bend in the region of the corresponding compounds [3].

The present research was carried out with systems consisting of the halides and sulfates of potassium, thallium, and zinc. Some of the systems formed by these salts had been previously investigated by us by the thermal method, and we had also measured their conductivity in the molten state [5]. We found that sharply marked, congruently fusing compounds were formed in all these systems.

Investigation of the conductivity in the molten state at temperatures more than 100° above the melting points showed that the compounds formed within these systems exhibit sharply defined minima on the curves of specific conductance. We were interested in learning whether these compounds are manifested in any way on the "composition – specific gravity" curves.

EXPERIMENTAL

Operational procedure. The specific gravities were measured by the method of hydrostatic weighing, which is widely employed for measuring density at high temperatures. A platinum float, suspended by a fine platinum wire from the pan of an analytical balance, was immersed in a crucible containing the test salt mixture. The specific gravity of the mixture was determined from the ball's loss of weight. The instrument was graduated with chemically pure sodium and potassium nitrates. The furnace in which the crucible was heated was kept at a constant temperature by means of a contact galvanometer. The temperature did not vary more than 0.5° during measurements.

K_2Cl_2 – $ZnSO_4$ system. Our investigation of the conductivity of this system in the molten state showed that there were two sharply marked minima [5], corresponding to the composition of zinc kainite ($KCl \cdot ZnSO_4$) and another salt, apparently $3K_2Cl_2 \cdot ZnSO_4$ or a ternary compound.

The curves for the specific gravities in this system also exhibit a marked change in direction in the areas corresponding to the existence of kainite and another compound of the composition specified above (Fig. 1).

TABLE 1

Specific Gravity of the Molten K_2Cl_2 – $ZnSO_4$ System

Molar percent		$d_{475°}$	$d_{500°}$	$d_{525°}$	$d_{550°}$
K_2Cl_2	$ZnSO_4$				
58.11	41.89	2.157	2.141	2.126	2.106
57.18	42.82	2.174	2.157	2.141	2.125
56.41	43.59	2.177	2.162	2.140	2.125
54.61	45.39	2.193	2.178	2.158	2.146
49.06	50.94	2.270	2.263	2.241	2.222
45.00	55.00	2.335	2.317	2.298	2.284
40.15	59.85	2.416	2.400	2.393	2.364
35.00	65.00	2.536	2.525	2.506	2.479
33.23	66.77	2.546	2.533	2.511	2.503
31.72	68.28	2.562	2.539	2.521	2.512
30.73	69.27	2.581	2.563	2.537	2.532
28.29	71.71	2.616	2.603	2.581	2.583
24.74	75.26	2.693	2.689	2.671	2.643

The figures for the specific gravities at temperatures of 475, 500, 525, and 550° are listed in Table 1. As seen in Fig. 1, the measurements at 475° were made in supercooled melts, inasmuch as part of the composition and even kainite itself crystallize at higher temperatures. The composition of kainite, $KCl \cdot ZnSO_4$, corresponds to a clearly marked plateau in all four isotherms.

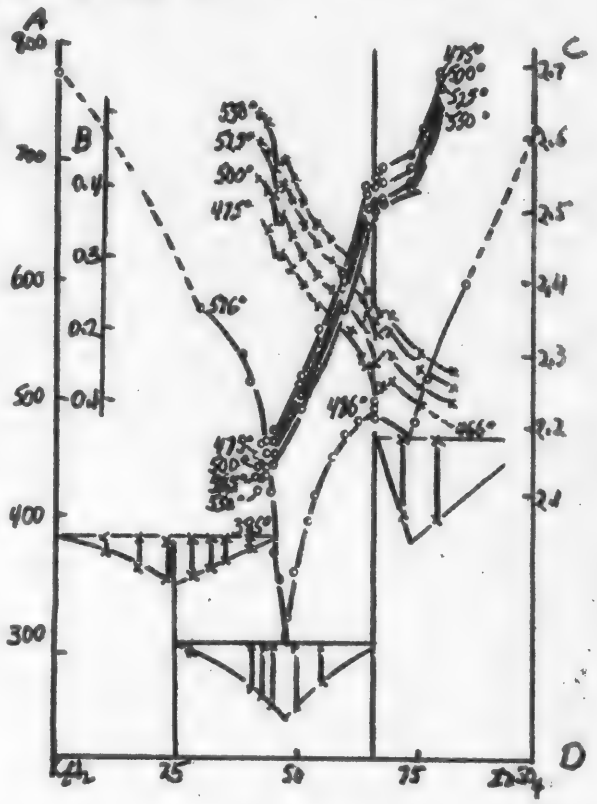

Fig. 1. Specific-gravity and conductivity isotherms of the K_2Cl_2 – $ZnSO_4$ System.

A-Temperature, °C; B-conductivity; C-specific gravity; D-molar %.

K_2Br_2 – $ZnSO_4$ System. Corresponding to the presence of a single compound of the kainite type ($KBr \cdot ZnSO_4$), the specific gravity isotherms display a single bend at the composition of this compound (Fig. 2). There is a sharp minimum at this point on the "composition – specific conductivity" curves.

Table 2 gives the specific gravities of melts of this system at 500, 525, and 550°. We were unable to employ lower temperatures because of the difficulty of producing supercooled states in this system.

Tl_2Cl_2 – $ZnSO_4$ System. Since the specific gravity of thallium chloride is much higher than that of zinc sulfate, the slope of the specific-gravity isotherm is opposite to that of potassium salts. Melts with a high percentage of TlCl have specific gravities in excess of 4.5.

Here, too, there is a slight change in the curvature of the curve near the composition of kainite ($TlCl \cdot ZnSO_4$), but it is less marked and somewhat shifted to the right of that compound's composition (Fig. 3).

TABLE 2

Specific Gravity of the Molten K_2Br_2 – $ZnSO_4$ System

Pt. No.	Molar percent K_2Br_2	Molar percent $ZnSO_4$	$d_{500°}$	$d_{525°}$	$d_{550°}$
1	60.00	40.00	2.597	2.575	2.559
2	54.48	45.52	2.642	2.622	2.611
3	49.88	50.12	2.681	2.662	2.655
4	45.42	54.58	2.705	2.683	2.667
5	33.40	66.60	2.778	2.765	2.753
6	31.91	68.09	2.806	2.789	2.784
7	26.38	73.62	2.861	2.848	2.837

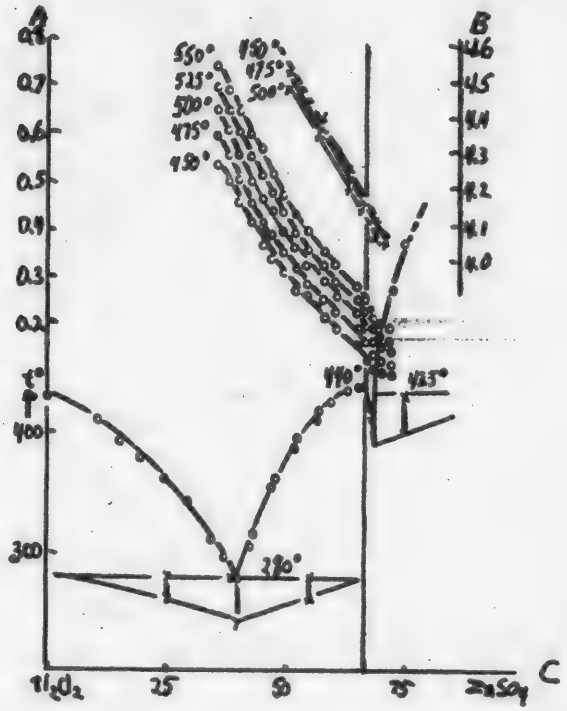

Fig. 3. Isotherms of specific gravity and conductivity of the Tl_2Cl_2 $ZnSO_4$ system.

A-Conductivity; B-specific gravity; C-molar %.

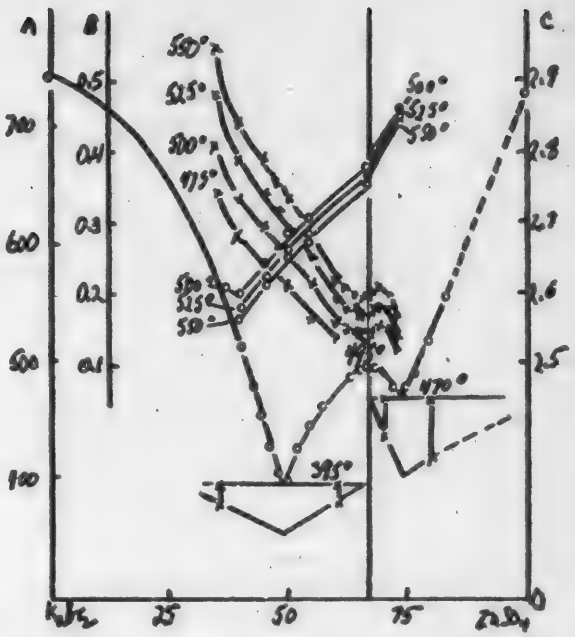

Fig. 2. Isotherms of specific gravity and conductivity for the K_2Br_2 – $ZnSO_4$ system.

A-Tmperature °C; B-conductivity; C-specific gravity; D-molar %.

TABLE 3

Specific Gravity of the Molten Tl_2Cl_2 $ZnSO_4$ System

Pt. No.	Molar per cent Tl_2Cl_2	Molar per cent $ZnSO_4$	$d_{450°}$	$d_{475°}$	$d_{500°}$
1	50.00	50.00	–	4.548	4.512
2	43.10	56.90	4.421	4.395	4.376
3	36.98	63.02	4.277	4.254	4.227
4	34.52	65.48	4.223	4.203	4.177
5	33.42	66.58	4.196	4.179	4.155
6	31.72	68.28	4.146	4.121	4.094
7	29.34	70.66	–	4.091	4.076

Table 3 gives the specific gravities of melts of the Tl_2Cl_2– $ZnSO_4$ system at temperatures of 450, 475, and 500°.

<u>K_2SO_4 – $ZnSO_4$ System</u>. This system contains two congruently fusing compounds: $ZnSO_4 \cdot K_2SO_4$ and $2ZnSO_4 \cdot K_2SO_4$. The former compound is hardly apparent on the specific-gravity isotherms (Fig. 4), though both compounds correspond to sharply marked minima on the specific-conductivity isotherms. The second compound is more clearly marked, there even being a slight plateau, at a composition of $2ZnSO_4 \cdot K_2SO_4$,

TABLE 4

Specific Gravity of the Molten K_2SO_4 – $ZnSO_4$ System

Pt. No.	Molar per cent K_2SO_4	Molar per cent $ZnSO_4$	$d_{500°}$	$d_{525°}$	$d_{550°}$
1	57.00	43.00	2.509	2.496	2.485
2	51.74	48.26	2.545	2.526	2.515
3	50.00	50.00	2.559	2.546	2.535
4	48.01	51.99	2.592	2.574	2.556
5	44.58	55.42	2.621	2.604	2.593
6	39.57	60.43	2.680	2.656	2.641
7	35.01	64.99	2.728	2.705	2.692
8	33.43	66.57	2.731	2.714	2.708
9	31.00	69.00	2.751	2.737	2.727
10	29.71	70.29	–	2.766	2.757
11	25.13	74.87	–	2.831	2.812

on the 500° isotherm, i.e., at a temperature that is only 16° above the compound's melting point.

Table 4 gives the specific gravities of melts of the K_2SO_4 – $ZnSO_4$ system at 500, 525, and 550°.

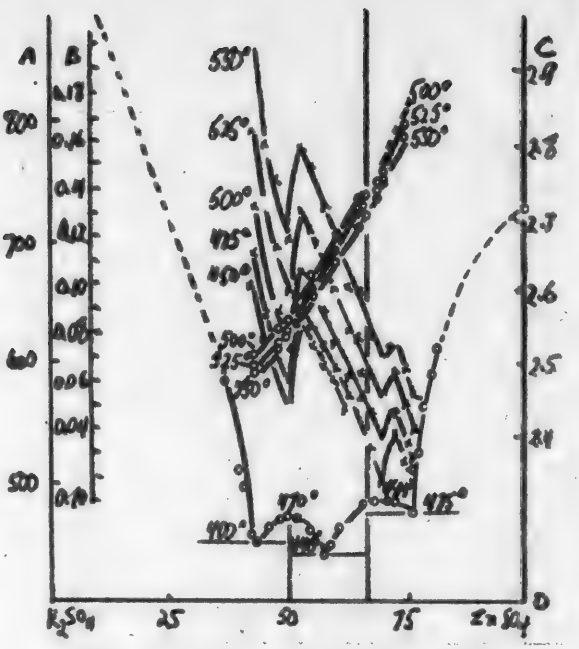

Fig. 4. Isotherms of specific gravity and conductivity of the K_2SO_4 – $ZnSO_4$ system.

A-Temperature °C; B-conductivity; C-specific gravity; D-molar %.

SUMMARY

1. Inspection of the diagrams of the four systems K_2Cl_2 – $ZnSO_4$, K_2Br_2 – $ZnSO_4$, Tl_2Cl_2 – $ZnSO_4$, and K_2SO_4 – $ZnSO_4$ at temperatures between 475 and 550° indicates that congruently fusing compounds are manifested more or less clearly on the "specific-gravity – composition" curves.

2. The specific gravity alone cannot be used as a sufficiently definite index of the presence of a compound in the system, even when the latter contains a clearly marked congruently fusing compound.

LITERATURE CITED

[1] A.G.Bergman, E.N.Varasova, N.P.Luzhnaya, and E.I.Lukyanova, Bull. Sect. Phys. Chem. Analysis, 11, 213 (1936).

[2] Shvartsman, Symposium in Honor of the 35th Anniversary of the Scientific Career of V.A.Plotnikov, 209. Kiev (1936).

[3] V.P.Barzakovsky, P.F.Antipin, and A.F.Alabyshev. The Electrochemistry of Molten Salts, 38. (1937).

[4] V. Mashovets and Z. Lundina, Trans. All-Union Aluminum and Magnesium Institute, 10 (1935).

[5] N.P.Luzhnaya and I.P.Vereshchetina, Trans. 2nd All-Union Conference on Theoretical and Applied Electrochemistry, 280 (1949).

Received May 16, 1950.

THE EFFECT OF THE GEOMETRICAL PARAMETERS OF THE ELECTROLYZER UPON THE DISTRIBUTION OF ELECTRIC ENERGY WITHIN IT

V. P. Mashovets, N. V. Pomotskaya, N. L. Lomarov and U. F. Turomshina

All-Union Aluminum and Magnesium Institute

The spatial distribution of the electric energy in an electrolyzer is closely reflected in its operation. The distribution of current density at the electrodes governs the thickness of the metal deposited on the cathode in electroplating; it also plays an important role in other electrochemical processes, inasmuch as the current efficiency depends on the current density. The distribution of the specific power throughout the electrolyte governs the heating in various zones of the electrolyzer, which is particularly important in the electrolysis of molten baths.

The field distribution is governed by the geometry of the electrolyzer as well as by electrochemical factors: the conductivity of the electrolyte, the current, and the polarization as a function of the current density.

The present paper discusses the influence of the geometrical factors in one particular case.

EXPERIMENTAL

The bath used had the form of a single-anode aluminum bath, though the results of our measurements cannot be applied quantitatively to an actual aluminum bath, inasmuch as the electrochemical conditions were quite different. We used an aqueous solution of 150 grams of $CuSO_4 \cdot 5H_2O$, 49 grams of H_2SO_4, and 50 grams of alcohol per liter, with copper electrodes. Direct copying of an aluminum bath, using molten cryolite at about 1000° entails almost insuperable experimental difficulties. The present paper must, therefore, be regarded merely as a first approximation. Even in this form, however, we can get interesting, even though only qualitative, indications of the influence of the various geometrical parameters upon the field distribution within the electrolyzer.

The experimental method of plotting the field has already been described by one of the present authors [1] and will not be set forth here. The electrolytic bath is shown in plan in Fig. 1. The ab part of the cathode corresponds to the exposed carbon wall of the bath, while the section bc represents the aluminum on the bottom of the bath. The de section of the anode corresponds to the vertical surface of the anode, and the section ef to its horizontal surface. In some of our tests the ab section of the cathode was replaced by a glass wall, a model of this sort corresponding to a bath in which the carbon wall is insulated by a lining of hardened electrolyte.

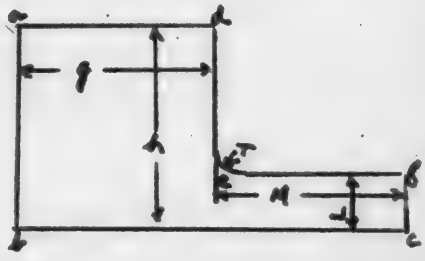

Fig. 1. Schematic plan of bath.

The following parameters were variable: Q – the distance from the anode to the side wall; H – the depth of the electrolyte; and L – the interelectrode distance in a real bath. Let us say that L = 2 cm, Q = 18-25 cm, and H = 9-14 cm, for example, the scale of the model is about 0.4 of natural size. The distance M is unimportant, as will be shown later; it was always taken as 12 cm. All measurements were made at a temperature of 25 ± 0.2° and a current I = 50 milliamps. All the other details of the measurements, as well as the method of plotting the field and working up the results, have been described previously [1].

In the subjoined tables the following notation has been employed:

j = current density; at the cathode, $j_{ave.C}$ = average current density, while j_a, j_b, and j_c are the current densities at the cathode points a, b (where it is a minimum), and c (where it is a maximum); at the anode, $j_{ave.A}$ = average current density, while j_d, j_e, and j_f are the current densities at the anode points d (where it is a minimum, except in the experiments with a small value of H), the anode corner e (where it is a maximum), and the anode point f (since the field is homogeneous in this zone, $j_f = j_c$, with the exception of the experiments in which L was very large); and I_{ab}, I_{bd}, and I_{dc} are the percentages of the current that pass through the respective sections of the cathode: ab (the "vertical wall"), bd, (the "horizontal" section "beyond the anode"), and dc (the "horizontal" section "beneath the anode").

The current density and the distribution of the current at the cathode are determined from the field map.

E is the total voltage across the bath (measured directly).

x is the resistivity of the electrolyte; it is given as the mean of the values determined from Equations (7) and (8);*

W is the power; W_0 is the overall power from Equation (9); W_e is the "ohmic" power, in the electrolyte; WA and WC are the anodic and cathodic "polarized" powers, from Equation (11);

$\frac{dW}{dV}$ is the differential specific power: max. at the corner of the anode, from Equation (15), min. at the corner of the cathode, from Equation (17), except in the bath with an insulated "side" wall ab, where $(dW/dV)_{min.} = 0$ (near point a).

$K_v = \left(\frac{dW}{dV}\right)_{max.} : \left(\frac{dW}{dV}\right)_{min.}$ is the variation factor of the distribution of the specific power;

$R_e = W_e/I^2$ is the effective ohmic resistance of the electrolyte;

C_e is the "ohmic constant" of the bath, from Equation (19).

S_e is the "derived" cross section of the electrolyte without allowing for polarization, from Equation (19), with S_0 the same quantity with polarization allowed for, from Equation (18) (using the "derived" interelectrode distance $l_e = l_0 = L$).

Influence of the Distance from the Anode to the "Side Wall", Q.

The choice of the distance form the anode to the side wall in an aluminum bath is governed by the following considerations. If this distance is too small, no lining is formed on the side wall, and it operates as a cathode. The aluminum deposited on the carbon cathode is combined into a carbide, and thus the current branching off to the side wall is wasted. When the distance between the anode and the side wall is too great, the increase in the dimensions of the bath increases its heat losses, and hence the specific energy consumption. This distance is chosen as 40 to 60 cm, depending upon the rating of the unit, in industrial baths for practical and design reasons.

In order to obtain clear results, the distance Q was varied within very wide limits in our experiments, ranging from 2 to 30 cm. The other parameters were

*All numbered equations are given in our preceding paper [1].

kept constant: L = 2 cm and H = 14 cm, while this was being done. The results are summarized in Table 1 (values that diverge excessively are given in parentheses), while the changes in the nature of the field and the current densities are shown in Figs. 2, 3, and 4.

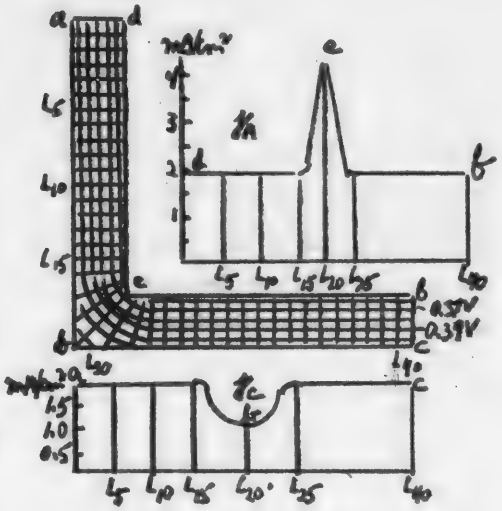

Fig. 2. Bath field at Q = 2, H = 14, and L = 2 cm, and curves of current density at the anode (j_A) and the cathode (j_C). In this and the following figures the scale of electrode length (along the axis of abscissas) has been reduced to half the linear scale of the bath field on the j_A and j_C curves.

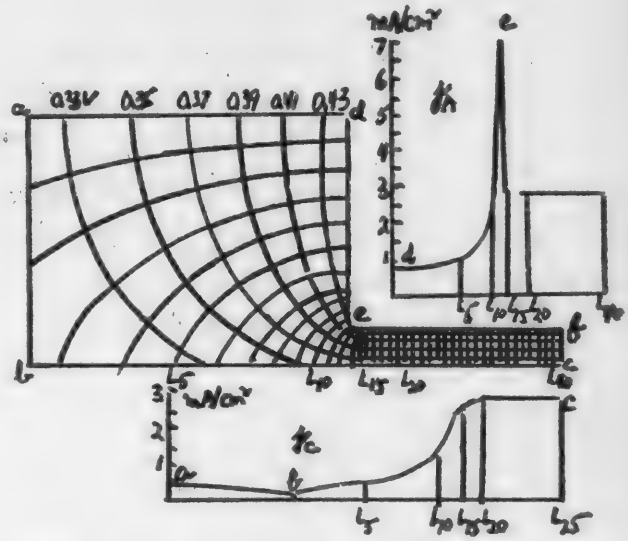

Fig. 3. Bath field at Q = 18, H = 14, and L = 2 cm, with curves of current density.

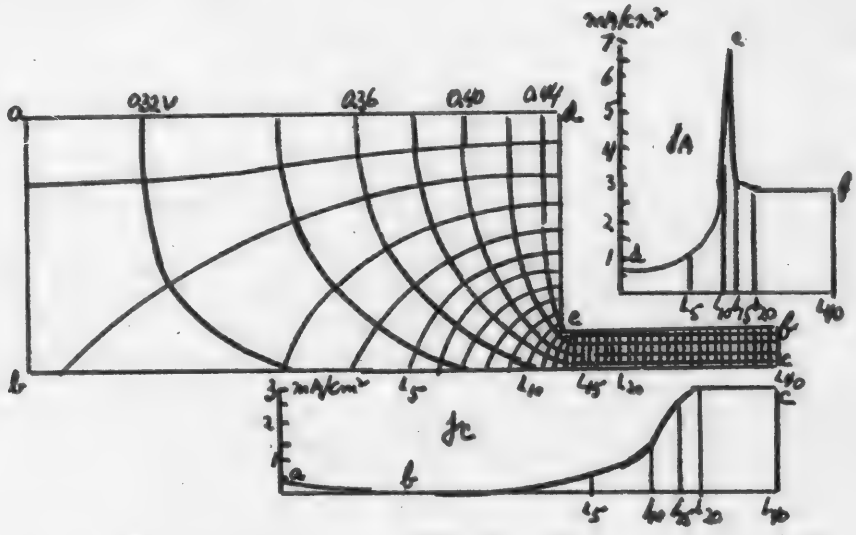

Fig. 4. Bath field at Q = 30, H = 14, and L = 2 cm, with curves of current density.

TABLE 1

Field Characteristics as functions of the "Anode – Side Wall" Distance Q

Bath No.	Q, cm.	Current density, milliamp/cm²						Cathode Current Distribution			E, millivolts	x·10³ in Ω·cm⁻¹
		Cathode			Anode							
		$j_{av.C}$	j_a	j_b	$j_c=j_f$	j_e	j_d	I_{ab}	I_{bd}	I_{dc}		
1	2	1.78	1.94	0.95	1.94	4.4	1.94	50.0	4.3	45.7	146.0	84.5
2	4	1.67	1.47	0.40	2.37	5.3	1.47	35.7	7.6	56.7	167.0	83.3
3	8	1.47	1.3	0.35	2.40	7.0	1.30	28.0	16.2	55.8	190.7	87.7
4	12	1.315	0.7	0.35	2.75	(5.4)	1.05	16.4	19.7	63.9	207.5	80.7
5	18	1.135	0.35	0.10	2.83	7.3	0.80	6.7	25.3	68.0	186.6	80.1
6	24	1.00	0.10	0.10	2.81	6.7	0.70	5.0	28.5	66.5	(176.3)	87.7
7	30	0.89	0.03	0.02	2.85	6.8	0.70	0.9	27.9	71.2	187.7	81.5
Bath with insulated wall ab												
4 i.	12	2.08	–	0.95	3.11	7.3	0.35	–	26.3	73.7	175.0	81.8
5 i.	18	1.67	–	0.60	2.86	7.25	0.55	–	31.3	68.7	161.9	84.4
6 i.	24	1.40	–	0.15	3.01	5.75	0.60	–	28.8	71.2	159.7	85.9

As the side wall is moved away (Q increases), the current density at that wall diminishes, especially in the lower portion of the wall (at the coal); j_c increases at the horizontal section of the cathode, beneath the anode.

The redistribution of the current at the cathode lightens the load on the "side wall"; the proportion of the current passing to the cathode beneath the anode, I_{dc}, increases. The current density diminishes at the peripheral section of the cathode (beyond the anode); but since the increase in Q increases the area of this section of the cathode, the proportion of the current carried by it, I_{bd}, rises. The anodic current density is likewise distributed less evenly.

All these changes are very prominent at low values of Q (< 12 cm); the effect of putting the side wall farther away is slight.

The changes in the power and in the "bath constant," C_e, are highly interesting. These quantities rise until Q = 12 cm, but when Q rises still higher, they begin to drop. At that distance the "side wall" plays so unimportant a role in the field distribution that its recession is masked by the rise in the "peripheral" section of the cathode. It is noteworthy that not only does the "ohmic" power rise with an increase in Q (up to Q = 12 cm), but the "polarization" power ($W_A + W_C$) does as well, though the mean cathode current density drops off, while that of the anode remains constant. This is due to the fact that the current density is distributed less evenly, and therefore, as Q increases, more and more of the current is carried by heavily loaded, and hence strongly polarized, sections of the electrodes.

The unevenness of the distribution of the specific power (K_v) becomes very high at large values of Q.

The derived cross section of the electrolyte, S_e and S_0, varies inversely with C_e, as follows from Equations (18) and (19). We shall consider the magnitude of the derived section later on.

In baths with an insulated "side wall" ab (cf Fig. 5 and Fig. 3, where baths

TABLE 1

L = 2 cm, H = 14 cm, $j_{ave.A}$ = 2.1 milliamp/cm^2

Power, W·10^{-3}			W_A+W_C (% of W)	dW/dV, W/cm^3·10^{-6}		K_V	R_e in Ω	C_e, cm^{-1}	Derived cross section, cm^2		Fig. No.
W_0	W_e	W_A+W_C		max.	min.				S_0	S_e	
7.30	2.82	4.48	61.4	229	21.4	10.7	1.13	0.095	8.1	21.1	2
8.35	3.15	5.20	62.3	338	3.8	89.0	1.26	0.105	7.2	19.1	
9.54	3.90	5.64	59.2	558	2.8	199	1.56	0.136	6.0	14.7	
10.37	4.37	6.00	57.5	(364)	3.0	(121)	1.75	0.141	6.0	14.2	
9.33	4.28	5.05	54.3	665	0.26	2550	1.71	0.137	6.7	14.6	3
(8.83)	(3.63)	5.20	(59.0)	512	0.23	2220	1.45	0.127	6.5	15.7	
9.39	4.25	5.14	54.8	567	0.01	56700	1.70	0.138	6.6	14.5	4
Bath with insulated wall ab											
8.75	4.18	4.57	52.2	652	–	–	1.67	0.136	7.0	14.7	
8.10	4.13	3.97	49.0	623	–	–	1.65	0.139	7.3	14.4	5
7.99	4.00	3.99	50.0	385	–	–	1.60	0.137	7.3	14.6	

with equal Q are compared), the cathode current density rises, of course. But the proportion of the current that passes through the "subanodic" portion of the cathode (I_{dc}) rises comparatively little, i.e., most of the "side wall" current is transferred to the "peripheral" portion of the cathode (I_{bd}). The "bath constant" C_e suffers practically no change, which indicates the very small part played by the "side wall" in the overall resistance of the bath for values of Q > 12 cm. The power ought to rise when the side wall is insulated; its slight drop is due, in part, to the increased specific conductivity and, in part, to probable errors in measurement.

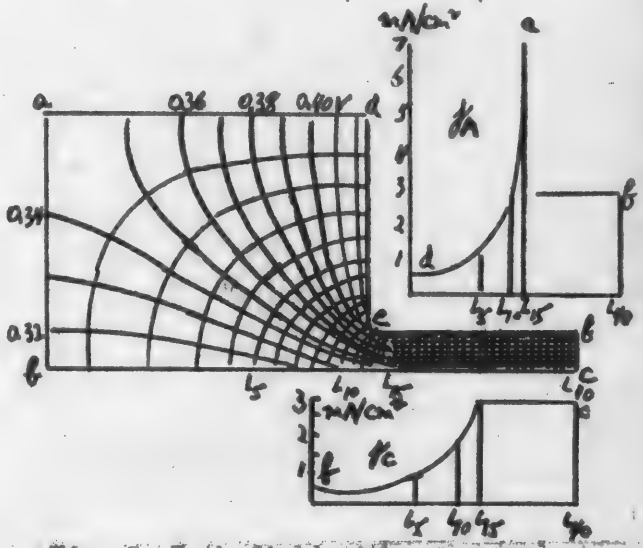

Fig. 5. Bath field with a nonconducting wall ab at Q = 18, H = 14, and L = 2 cm, with curves of current density.

Influence of H, the "depth of the electrolyte"

Raising the level of the electrolyte, and hence increasing the amount of the latter in the aluminum bath, results in more uniform operation. The thermal inertia increases, and the change in the electrolyte composition due to adding silica is diminished. On the other hand, raising the level increases the area of the bath's side wall, impairs the conditions for the formation of a lining on it, and thus entails the danger of current being wasted "on the side."

In modern baths, the depth of the electrolyte varies in practice from 15 cm in small baths to 30 and even 45 cm in large baths, in which the distance from the anode to the side wall is large.

TABLE 2

Field Characteristics as Functions of the "Depth of Electrolyte," H

Bath No.	H, cm	Current density, milliamp/cm²							Cathode current distribution			E, millivolts	$\varkappa \cdot 10^{-3}$ in $\Omega^{-1} \cdot cm^{-1}$
		Cathode				Anode							
		$j_{av.C}$	j_a	j_b	$j_e = j_f$	j_e	j_d	$j_{av.A}$	I_{ab}	I_{bd}	I_{de}		
8	3	1.51	0.05	0.04	3.54	7.2	5.44	3.90	0.2	17.3	82.5	219.5	87.7
9	9	1.28	0.10	0.09	3.1	7.1	0.85	2.66	2.4	23.7	73.9	(174.4)	72.6
5	14	1.135	0.35	0.10	2.83	7.3	0.80	2.10	6.7	25.3	68.0	186.6	80.1
10	20	1.00	0.40	0.07	2.63	5.0	0.50	1.67	11.8	27.0	61.2	153.2	86.1
11	30	0.83	0.55	0.07	2.50	4.6	0.45	1.26	21.5	20.3	58.2	143.2	79.8
		Bath with insulated wall ab											
9 i	9	1.67	–	0.20	3.06	5.45	(1.05)	2.66	–	27.5	72.5	189.7	81.2
5 i	14	1.67	–	0.60	2.86	7.25	0.55	2.10	–	31.3	68.7	161.9	84.4
10 i	20	1.67	–	0.60	2.90	4.85	0.35	1.67	–	32.5	67.5	171.2	83.3

In our tests, H was varied from 3 to 30 cm, Q being kept constant at 18 cm and L at 2 cm. The results are summarized in Table 2; the change in the nature of the field is visible in Figs. 6, 3, and 7. As H rises, the area of both electrodes increases, and the current density decreases accordingly. At the anode this decrease takes place over the entire surface; but at the cathode it occurs only at the "horizontal" part "beneath the anode." The current density rises at the parts of the cathode that are far from the anode, especially at the "side wall." That is why the current carried by the peripheral part of the cathode (I_{bd}), and especially by the "side wall" (I_{ab}), rises; the latter rise is due to a rise in the current density, as well as to an increase in the area of the "side wall".

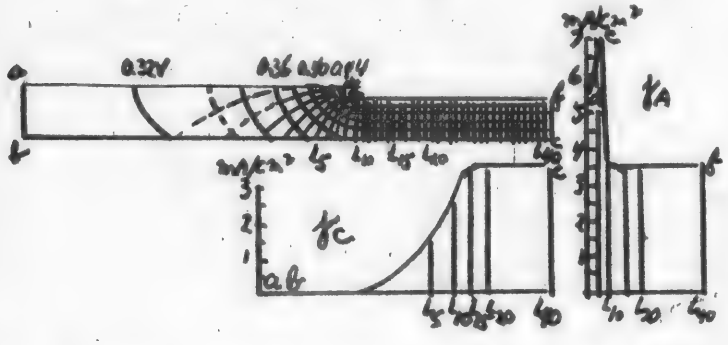

Fig. 6. Bath field at Q = 18, H = 3, and L = 2 cm, with curves of current density.

The power – the ohmic as well as the polarization power – diminishes, the latter dropping not only in absolute magnitude but also in per cent. This is due to the drop in the current density with the corresponding decrease in the polarization. The spatial distribution of the specific power is evened out, i.e., the variation factor K_V drops. The "bath constant" C_e drops, i.e., the resistance of the bath likewise drops; the derived cross section of the electrolyte rises accordingly.

When the "side wall" is insulated (Figs. 5 and 8, cf Figs. 3 and 7), the current density on the "vertical" part of the anode drops. The current density in the peripheral part of the cathode rises sharply. Therefore, the redistribution

TABLE 2

L = 2 cm; Q = 18 cm.

Power, $W \cdot 10^{-3}$			$W_A + W_C$ (% of W)	dV/dW, $W/cm^3 \cdot 10^{-6}$		K_V	Re in Ω	Ce_2, cm^{-1}	Derived cross section, cm^2		Fig. No.
W_0	W_e	W_A+W_C		max.	min.				S_0	S_e	
10.95	4.33	6.62	60.4	591	0.037	14800	1.73	0.152	5.2	13.2	6
(8.72)	(4.75)	(3.97)	(45.5)	694	0.22	3150	(1.90)	0.138	(7.9)	14.5	
9.33	4.28	5.05	54.3	665	0.26	2550	1.71	0.137	6.7	14.6	3
7.66	3.70	3.96	51.8	290	0.114	2540	1.48	0.127	7.6	15.7	7
7.16	3.90	3.26	44.1	266	0.12	2220	1.56	0.125	8.8	16.0	
Bath with insulated wall ab											
9.48	4.22	5.26	55.7	366	–	–	1.69	0.137	6.5	14.6	
8.10	4.13	3.97	49.0	623	–	–	1.65	0.139	7.3	14.4	5
8.56	3.53	5.03	58.7	283	–	–	1.41	0.117	7.05	17.1	8

of the current at the cathode actually boils down to the "side wall" current being switched to the peripheral "horizontal" part. There is practically no change in the current passing through that part of the cathode "beneath the anode." But at large values of H, any further increase in the "vertical" part of the anode has almost no effect upon the current distribution, and the proportion of the current carried by the peripheral and "subanodic" parts of the cathode remain practically unchanged.

When the "side wall" is insulated, a marginal effect is noted in the cathodic current distribution; the current density is higher at the edge of the cathode, at point b, than in adjacent parts of the cathode, loccated closer to the anode. This is readily seen in the cathode density curves of Figs. 5 and 8. The marginal effect is due to the fact that the tube of force serving the outermost parts of the cathode is widened in its central section, i.e., at point a, and hence has lowered resistance.

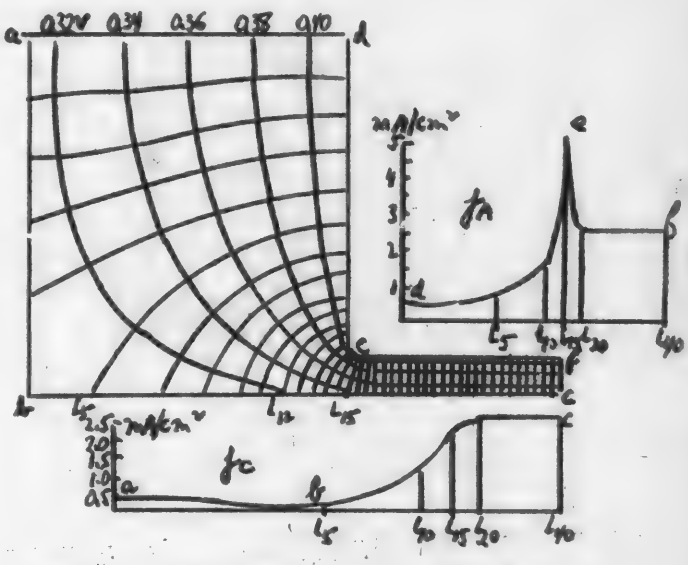

Fig. 7. Bath field at Q = 18, H = 20, and L = 2 cm, with curves of current density

The changes in the power, the "bath constant," and the derived cross section of the electrolyte caused by insulation of the "side wall" are negligible, lying within the limits of measurement error.

TABLE 3

Field Characteristics as Functions of the "Interelectrode Distance," L

Bath No.	L, cm	Current density, milliamp/cm²							Cathode current distribution			E, millivolts	$\varkappa \cdot 10^3$, $\Omega \cdot cm^{-1}$
		Cathode			Anode								
		j_a	j_b	j_e	j_f	j_e	j_d	$j_{ave.A}$	I_{ab}	I_{bd}	I_{dc}		
10	2	0.40	0.07	2.63	2.63	5.0	0.50	1.67	11.8	27.0	61.2	153.2	86.1
12	4	0.50	0.15	2.45	2.45	(7.7)	0.60	1.79	14.3	27.4	58.3	209.4	72.4
13	8	1.0	0.2	2.0	2.0	6.65	1.25	2.10	24.5	31.1	44.4	308.8	78.6
14	12	1.06	0.2	2.0	2.0	7.45	1.55	2.50	27.8	30.0	42.2	397.5	73.1
15	16	1.85	0.2	1.87	2.0	9.1	2.50	3.16	29.2	28.6	42.2	504.5	72.9
16	19	1.8	0.25	1.85	2.6	15.6	5.10	3.90	30.4	27.4	42.2	587.7	80.0
Bath with insulated wall ab $j_{ave.C} = 1.67$ mA/cm²													
10 i	2	–	0.60	2.90	2.90	4.85	0.35	1.67	–	32.5	67.5	171.2	83.3
13 i	8	–	0.90	2.45	2.45	7.1	0.85	2.0	–	44.6	55.4	337.1	83.0
15 i	16	–	12.0	2.28	2.28	9.4	2.45	3.16	–	51.2	48.8	536.4	78.7

Influence of the "interelectrode distance" L.

The distance from the horizontal surface of the anode to the surface of the metallic aluminum in the aluminum bath depends upon the thermal operation conditions of the bath, varying within very narrow limits in practice; 4.5 to 5.5 cm. In our tests L was varied from 2 to 19 cm, with H constant at 20 cm, and Q constant at 18 cm.

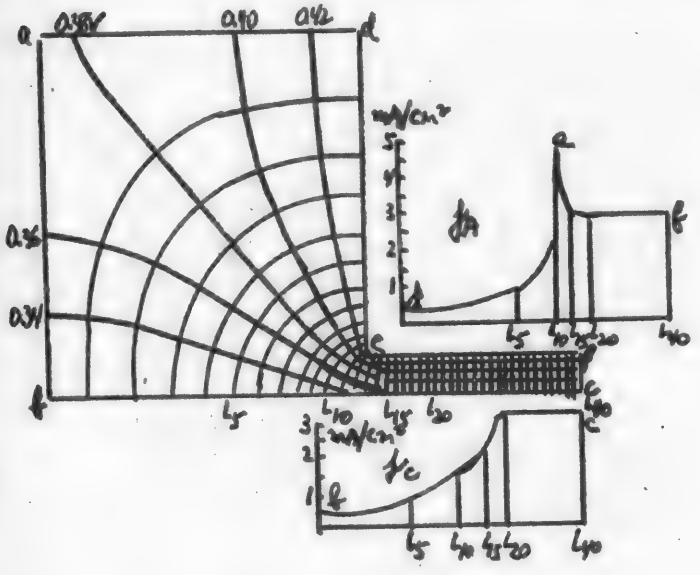

Fig. 8. Bath field with a nonconducting wall ab at Q = 18, H = 20, and L = 2 cm, with curves of current density.

This H:Q ratio is impossible in an actual aluminum bath. The large value of H was chosen to increase the possible range of values for L, thus providing a clearer picture of the influence of this variable.

The results are given in Table 3, the changes in the field being shown in Figs. 7 and 9.

As L increases, the anode area diminishes and the mean anodic current density rises. This rise occurs entirely in the "vertical" part of the anode and at the corner. The current density at the cathode is evened out, i.e., j_c drops at the "horizontal" part "beneath the anode" and j_a rises at the "side wall" so that when L approaches the value of Q, $j_a = j_c$. As the value of L is raised, the proportion of the current carried by the cathode "beneath the

TABLE 3

Q = 18 cm; H = 20 cm; $j_{ave.C}$ 1.0 milliamps/cm^2

Power, W·10^{-3}			W_A+W_C	dW/dV, W/cm^3·10^{-6}		K_V	R_e, in Ω	C_e, cm^{-1}	Derived cross section, cm^2		Fig. No.
W_0	W_e	W_A+W_C	% of W_0	max.	min.				S_0	S_e	
7.66	3.70	3.96	51.8	290	0.114	2540	1.48	0.127	7.6	15.7	7
10.47	7.09	(3.38)	32.3	(820)	0.62	1320	2.88	0.208	13.4	19.2	
15.44	11.50	3.94	25.5	563	1.02	550	4.44	0.348	17.5	23.0	
19.87	15.39	(4.48)	(22.5)	760	1.09	700	6.45	0.471	20.6	25.4	
25.22	21.73	(3.49)	13.8	1375	1.10	1250	8.47	0.616	21.8	25.9	9
29.39	25.47	3.92	13.3	3040	1.56	1950	10.25	0.821	20.2	23.1	
Bath with insulated wall ab $j_{ave.C}$ = 1.67 mA/cm^2											
8.56	3.53	5.03	58.7	283	–	–	1.41	0.117	7.05	17.1	8
16.80	12.10	4.70	27.9	607	≃	–	4.85	0.403	14.3	19.8	–
26.80	23.0	3.80	14.2	1120	–	–	9.20	0.721	19.1	22.2	10

anode" decreases, while that carried by the "side wall" rises, rapidly at first and then very slightly. The proportion of the current carried by the peripheral "horizontal" part of the cathode, I_{bd}, changes very little, passing through a flat maximum.

The voltage across the bath and the total power increases almost linearly. The rise in power is due solely to the ohmic losses: the "polarization" power remains practically constant, as its percentage of the total power diminishes.

The maximum current density at the corner of the anode and, hence, the maximum specific power, increase, doing so especially rapidly at large values of L. The minimum current density at the angle of the cathode and the minimum specific power likewise increase, though more slowly when L is large than at low values of L. As a result, the variation factor of the energy distribution, K_V, passes through a minimum at middle values of L.

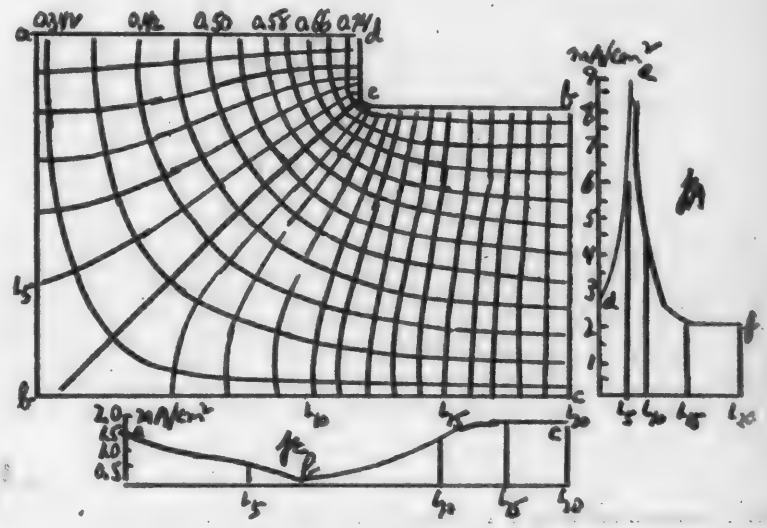

Fig. 9. Bath field at Q = 18, H = 20, and L = 16 cm, with curves of current density.

The "bath constant," C_e, like the ohmic power W_e, rises almost linearly. The derived cross section of the electrolyte was computed from Equations (18) and (19), on the assumption that the derived interelectrode distance l_0 = L. The derived

cross section rises rapidly at first, owing to the increase in the heavily loaded part of the cathode, after which it passes through a maximum and then falls off. The value of S_0 (allowing for polarization) approaches that of S_e (without allowing for polarization) as L increases, corresponding to a relative decrease in the importance of the polarization power.

When the "side wall" is insulated (Figs. 8 and 10, cf Figs. 7 and 9), there is practically no change in the current distribution at the anode; at the cathode, the current passing through the "side wall" is shifted principally to the peripheral "horizontal" portion, the current density and the percentage of the current rising relatively little at the "subanodic" part of the cathode. The voltage, power, ohmic resistance, and "bath constant" all increase when the "side wall" is insulated, slightly when L is small, and fairly considerably when L is large; this is understandable, since the role played by the "side wall" increases as the distance L is increased.

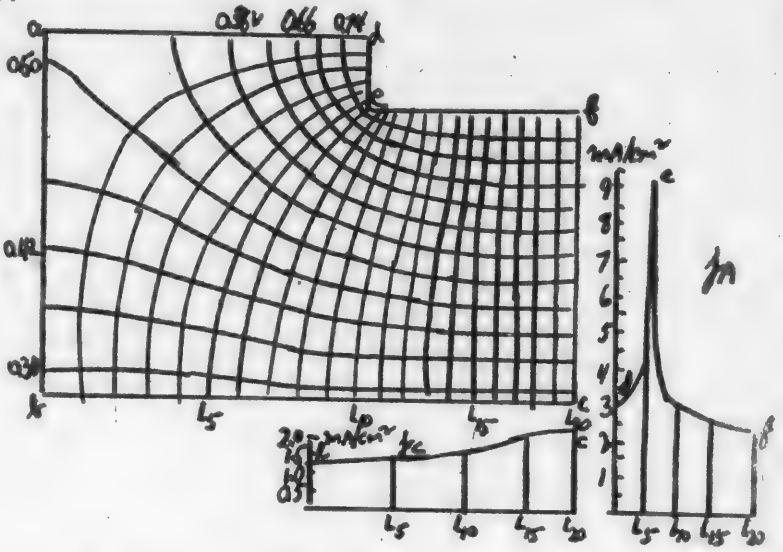

Fig. 10. Bath field with a nonconducting wall ab at Q = 18, H = 20, and L = 16 cm, with curves of current density.

"Derived Cross Section" of the Electrolyte.

In the design and technical calculation of electrolyzers the derived cross section of the electrolyte, S, is of considerable importance, the ohmic resistance of the electrolyzer being computed from it, viz:

$$R = \frac{l}{\varkappa S}.$$

Yet it is possible to calculate the derived cross section only when the electrodes are, for the most part, plane-parallel to each other or consist of a combination of plane-parallel elements, the interelectrode distance l being constant throughout the electrolyzer or throughout most of it (and even then the calculation is only approximate). The derived cross section of the electrolyte is then often calculated as the geometrical mean of the electrode areas:

$$S = \sqrt{q_C \cdot q_A}.$$

In aluminum baths, in particular, the areas of the heavily loaded parts of the electrodes, i.e., their horizontal portions, are taken, the interelectrode distance being taken as l.

Table 4 gives the total cathode and anode areas, q_{abc} and q_{def}, respectively, for some of the baths we tested, together with the areas of their "horizontal" parts, q_{bc} and q_{ef}, respectively (the chamfering at the corner of the anode being ignored in the latter quantity). The derived cross sections of the electrolyte are computed as the geometrical mean of the total areas for S' and of the "horizontal" areas for S". These values are compared with the derived cross sections S_e computed from the fields, plotted on the models, with only the ohmic power (and not the polarization power) allowed for.

TABLE 4

Bath No.	Principal parameters (in cm)			Electrode area (in cm^2)				Derived cross section, cm^2		
				Total		"horizontal part"				
	Q	H	L	Cathode q_{abc}	anode q_{def}	Cathode q_{bc}	anode q_{ef}	S'	S''	Se
1	2	14	2	28	23.6	14	12	25.7	13.0	21.1
3	8	14	2	34	23.6	20	12	28.3	15.5	14.7
5	18	14	2	44	23.6	30	12	32.2	19.0	14.6
6	24	14	2	50	23.6	36	12	34.4	20.8	15.7
7	30	14	2	56	23.6	42	12	36.3	22.5	14.5
8	18	3	2	33	12.6	30	12	20.4	19	13.2
9	18	9	2	39	18.6	30	12	27.0	19	14.5
10	18	20	2	50	29.6	30	12	38.5	19	15.7
11	18	30	2	60	39.6	30	12	48.7	19	16.0
12	18	20	4	50	27.6	30	12	37.6	19	19.2
13	18	20	8	50	23.6	30	12	34.4	19	23.0
15	18	20	16	50	15.6	30	12	27.9	19	25.9
16	18	20	19	50	12.6	30	12	25.1	19	23.1

The table indicates that the derived cross section S', which covers the total area of the electrodes, approaches the experimental value S_e only when Q is equal or close to the value of L (Baths Nos. 1, 15, and 16), and even then only very approximately. As for S'', it approaches S_e only in two cases (Baths Nos. 3 and 12, when $Q:L \cong 4$). In all the other cases, when Q is much larger than L, the part played by the "vertical" as well as by the peripheral "horizontal" parts of the cathode is so small that even the value of S", not to mention S', is much larger than S_e. Not only does the absolute magnitude of the calculated derived cross section S'' not agree with the experimental value S_e, but it does not reflect the actual trends in the changes of this latter quantity. Thus, S'' rises with an increase in Q above 8 cm, while S_e remains practically constant; as H increases, S" remains constant, while S_e increases, though slowly.

When the ratios of the principal parameters Q, H, and L are close to those obtaining in the real aluminum bath, as is the case in the Baths Nos. 5, 6, 7, 9, and 10, the derived cross section S_e is only slightly larger than the area of the "horizontal" portion of the anode, and is represented approximately by the following formula:

$$S_e = q_{ef} + 1.5\ L.$$

The insulation of the "side wall" has practically no effect upon the value of S_e, (provided Q is not too small and L is not too large), as is seen in Tables 1, 2, and 3.

In our models the quantity $M = q_{ef} = 12$ cm was chosen arbitrarily. If it is made larger, thus shifting the wall cf (Fig. 1), the only change will be an increase in the zone of the homogeneous field. If the same current density $j_c = j_f$ is then maintained at the added portions of the electrodes as exists in the zone of the homogeneous field, no change will occur in the nature of the field, nor in the power in the rest of the bath; hence, the difference $(S_e - q_{ef})$ will still be 1.5 L. Furthermore, since the model represents a cross section of half of the bath (the line cf serving as the axis), the difference between S_e and the anode area constitutes 3L for the whole bath. Finally, passing from the plane model

(the cross section) to the three dimensional bath, denoting the length of the anode by A and its width by B, and neglecting the complications at the corner of the anode, we may write:

$$S_e = (A + 3L)(B + 3L),$$

independent of the cathode dimensions. This expression may be recommended as a computational formula for the design of aluminum baths.

The quantity S_e makes no allowance for polarization. And yet polarization power, like the ohmic power, is consumed in the generation of heat. It would therefore be well to allow for the value of S_0, which was less than half of S_e in our models, when calculating the heat generated in the bath. In an aluminum bath, however, polarization is quite different (probably less) than when copper electrodes are used in a solution of copper sulfate. This means that the S_e:S_0 ratio will be different as well.

It should be stressed, moreover, that S_e, like S_0, is determined by the value of polarization as well as by the geometrical parameter of the electrolyzer; hence, the very concept of the "derived cross section" has merely a conventional, relative meaning.

SUMMARY

1. The method of mapping the electric field in solutions with complicated electrode configurations has been employed to ascertain the effect of the geometrical parameters of an electrolyzer upon the distribution of electric energy within it. A plane model of an aluminum bath with copper electrodes and an aqueous solution were used in the investigation.

2. A study has been made of the effect of the distance from the anode to the side wall, of the depth of the electrolyte, and of the interelectrode distance upon baths using operational and insulating side walls.

3. It has been shown that the method of determining the derived cross section of the electrolyte employed in engineering computations is unsatisfactory, and an approximate formula is proposed for computing this quantity. The very notion of a "derived cross section" is nothing but a convention.

LITERATURE CITED

[1] V.P.Mashovets, J. Appl. Chem., 23, 66 (1950).*

Received November 2, 1949.

*See CB translation p. 68 ff.

AN INVESTIGATION OF THE CATHODIC PROCESS IN SOLUTIONS OF NITRIC ACID AND IN THE HNO_3-H_2SO_4-H_2O SYSTEM

I. Oknin

Moscow Institute of Chemical Equipment

Soviet scientists have made comprehensive studies of the cathode process. The research of the A.N.Frumkin school is outstanding in this field [1]. Kabanov has measured the hydrogen overvoltage in acid media at high current densities (C.D), ranging up to 100 amps per cm^2 [2]. Iofa and Frumkin have investigated the hydrogen overvoltage in concentrated solutions of hydrochloric, hydrobromic, perchloric, and sulfuric acids [3,4,5]. Iofa and Stepanova have plotted curves of the hydrogen overvoltage in 1 - 10 N hydrochloric acid at temperatures ranging from -10 to +80° [6]. Many papers have been published on the cathode process in slightly acid, neutral, and alkaline solutions [7-16]. The Akimov school has made extensive investigations of the electrode processes in connection with their study of the processes involved in metal corrosion [17,18a,19-22]. Tomashov has discussed the general theory of the cathode process in oxidative media at great length [18b].

Solutions of nitric acid and the $HNO_3 - H_2SO_4 - H_2O$ system are acid, oxidative reaction media with a wide range of acidic and oxidative properties. The $HNO_3 - H_2SO_4 - H_2O$ system differs from solutions of pure nitric acid in that the concentration ratios of the oxidant and the hydrogen ions may be varied at will.

The curves of cathodic polarization in oxidative media consist of three sections: a high-potential section, where oxidative polarization predominates; a low-potential section where hydrogen polarization predominates; and an intermediate section, where there is a sharp change of potential, and oxidative concentration predominates [18b, 23]/

Different processes are adduced as the primary act in cathodic polarization of oxidative media: discharge of the hydrogen ions [24]; direct interaction of the oxidant with the cathode electrons [18b]; and the formation of metallic oxides [25-27].

The curves of cathodic polarization of a platinum electrode in nitric acid solutions of fairly high concentrations have a form that is typical of oxidative media. Owing to the catalytic action of nitrous acid, the section representing oxidative polarization grows longer when it is present. At concentrations below a certain value the potential of the platinum cathode drops evenly as the C.D. rises all along the polarization curve [24].

The hypothetical compound $H_2N_2O_5$ [28,29] and nitrogen dioxide NO_2 are considered to be oxidative depolarizers during the cathode process [30]. This is confirmed by the catalytic action of nitrous acid during the cathode process, these substances being formed during its reaction with nitric acid.

In the present research we proposed to obtain experimental data on the cathode process in solutions of nitric acid and in the HNO_3–H_2SO_4–H_2O system, to compare these results with certain features of the state of reaction media, and – with this comparison as a basis – to arrive at probable conclusions regarding the mechanism of the cathode process involved.

EXPERIMENTAL

Research method. The cathode polarization was measured at a temperature of 25.5±0.5°, at rest and with vigorous stirring (650 rpm). A large quantity of the reaction medium was used (500 cm^3) in order to prevent any appreciable change in its composition. The reaction medium was placed in an open glass beaker, in the center of which there was placed a glass stirrer. The electrodes and the connecting syphon were fastened to sleeves attached to a metallic ring above the beaker. A smooth platinum wire sealed into a glass tube served as the cathode. 1 cm of the wire, which had a diameter of 0.05 cm, projected from the tube. The connecting syphon was always full of a 2 N solution of sulfuric acid. The cathode potential was measured by the compensation method against a saturated calomel electrode. The measurements were made while an electric current passed through the electrode uninterruptedly, the C.D. being successively raised and then lowered. Before measurements were begun, the cathode was polarized at high C.D. for 10-15 minutes. This was done in order to secure an electrode surface that was as constant as possible throughout all the tests, as well as to drive out the nitrous and other gases in the reaction mixture by means of hydrogen.

The limiting cathode C.D. at which there is a sharp potential drop as the current is being gradually increased or a sharp potential rise as the current is being gradually diminished was found from the recorded curves of cathode polarization. We also made numerous measurements of the limiting cathode C.D. by observing the sharp drop and rise of the current.

Experimental data. We are unable to reproduce the curves of cathode polarization here, as they are much too numerous. They all have a shape that is characteristic of oxidative media, like the curves for solutions of nitric acid. Henceforth we shall use as characteristic of the cathode process the limiting cathode C.D. and cathode potentials at the smallest measured current densities (1-24 milliamp/cm^2). The respective data are listed in Table 1. In this table and henceforth throughout, I_{cb} and I_{ca} denote the limiting cathode C.D. at which a sharp potential drop takes place as the current is gradually increased: I_{cb} is the C.D. before the potential drop, while I_{ca} is the C.D. after the potential drop. I'_{cb} and I'_{ca} denote the limiting cathode C.D. at which the potential rises sharply as the current is being decreased: I'_{cb} – the C.D. before the rise, and I'_{ca} – the C.D. after the rise in potential.

Table 2 gives the data on the concentration of homopolar molecules of nitric acid, N_{NO_2OH}, and the specific conductivity, λ, as given in the literature, as well as the ratio of the concentration of homopolar molecules of nitric acid to the conductivity, N_{NO_2OH}/λ. The method of finding the concentration of homopolar molecules of nitric acid in ternary mixtures has been described in my preceding research [32]. The conductivity of the mixtures has been computed from the conductivities of aqueous solutions of the individual acids at 18° [33]. The partial conductivity of a given acid has been calculated from a tabulation of conductivities for solutions of the acid, using the conductivity corresponding to a molar concentration that equals the total acid concentration in the mixture, multiplied by a factor for the molarity of the given acid as a percentage of the total acid molarity. The total conductivity of the mixture was taken as equaling the sum of the computed partial conductivities.

In Table 3, the values of the limiting cathode C.D. are listed together with

Table 1. Data on the Limiting Cathode Current Densities and Cathode Potentials*

Mixt. No.	Comp. of mixt. mols/liter		cathode potential V at 1.24 mA/cm²		oxidative potential V [91]		Limiting cathode C.D., milliamp/cm²							
							At rest				While stirred			
	HNO_3	H_2SO_4	At rest	while stirred	0.003 mol/l HNO_2	1.0 mol/l HNO_2	I_{cb}	I_{ca}	I'_{cb}	I'_{ca}	I_{cb}	I_{ca}	I'_{cb}	I'_{ca}
1	12.9	0	+0.86	+0.82	+0.96	+0.87	8120	7500	6370	7500	10000	8430	8440	10000
2	10.3	3.6	+0.89	+0.86			>8120**				>7500**			
3	7.7	7.2	+0.86	+0.79			>6070**				>5200**			
4	5.2	10.8	+0.70	+0.70			657	468	313	344	340	375	363	313
5	2.6	14.4	+0.82	+0.96			607	563	525	563	480	660	657	481
7	10.3	0	+0.83	+0.79	+0.92	+0.84	3130	2690	156	206	950	750	81	113
8	8.3	2.9	+0.85	+0.84			3880	3440	407	470	5200	4120	875	1000
9	6.2	5.8	+0.87	+0.85			4560	3880	2880	3200	6180	5000	2260	2560
10	4.1	8.6	+0.86	+0.75			4070	3440	438	500	560	407	94	25
11	2.1	11.5	+0.77	+0.70			113	87.5	3.13	3.75	12.5	10.6	3.1	3.7
13	7.7	0	+0.83	+0.79	+0.88	+0.80	1040	843	18.8	25.0	14.4	11.9	4.4	5.6
14	6.2	2.2	+0.85	+0.83			1380	1130	313	457	100	75	56	81
15	4.6	4.3	+0.86	+0.84			1470	1000	12.5	6.25	812	593	188	282
16	3.1	6.5	+0.85	+0.82			1410	1060	81.3	113	1500	1000	81	106
17	1.54	8.6	+0.86	+0.76			500	407	12.5	25.0	263	200	6.3	12.5
19	5.2	0	+0.74	+0.15	+0.85	+0.76	125	93.6	<1.25	0	1.3	3.1	<1.3	0
20	4.1	1.4	+0.75	+0.70			225	175	<1.25	0	4.0	3.8	<1.3	0
21	3.1	2.9	+0.79	+0.74			325	250	3.13	3.13	3.1	5.0	≈0	0
22	2.1	4.3	+0.83	+0.78			370	275	1.25	0.63	6.3	9.4	3.1	3.1
23	1.04	5.8	+0.82	+0.78			200	156	0	0	3.1	5.2	1.3	0
25-29	2.6-0.52	0-2.9	<0	<0	+0.81	+0.72	0	0	0	0	0	0	0	0

*The notation in this and subsequent tables is explained in the text.

**We cite the maximum current densities available from a group of storage batteries. No potential drop was observed at these current densities.

TABLE 2

Data on the concentration of Homopolar NO_2OH Molecules and Specific Conductivity

Mixture No.	$\underline{N}_{NO_2OH}$, mols/liter	$\lambda \cdot 10^4$, $\Omega^{-1} \cdot cm^{-1}$	$\frac{N_{NO_2OH}}{\lambda}$
1	9.6	5300	18.2
2	9.3	3910	24
3	7.35	2786	26
4	5.05	1907	26
5	2.5	1418	18
7	6.5	6400	10.2
8	6.35	5200	12.2
9	5.52	3917	14.1
10	3.84	2830	13.6
11	2.0	1860	10.7
13	3.6	7450	4.83
14	3.7	6540	5.7
15	3.85	5510	7.0
16	2.5	4470	5.6
17	1.35	3480	3.9
19	1.30	7700	1.70
20	1.30	7490	1.74
21	1.30	7040	1.85
22	1.00	6560	1.53
23	0.60	5980	1.0
25-29	0		

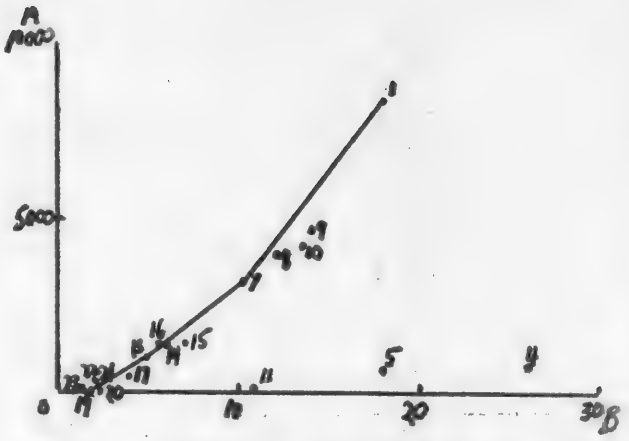

Fig. 1. Limiting cathode C.D. $\underline{I}_{cb}$ (A) plotted as a function of the ratio of the concentration of homopolar nitric acid molecules to the conductivity $\underline{N}_{NO_2OH}/\lambda$ (B) for solutions of nitric acid and ternary mixtures at rest.

The numerals in this and subsequent diagrams denote the mixture numbers. Straight lines are used to connect the individual points for nitric acid solutions.

the concentration of homopolar molecules of nitric acid, the concentration of hydrogen (or nitrate) ions, and with their ratio for solutions of nitric acid. In this table the overall nitric acid concentration is denoted by N_{HNO_3}. All the figures listed in Table 3 are direct experimental values.

The limiting cathode C.D. is plotted against the characteristics of state of of the reaction mixtures in Figs. 1-3 for ternary mixtures and in Figs. 4-6 for nitric acid solutions.

The characteristic features of the cathode process, as measured at a platinum electrode in mixtures containing a fairly high concentration of nitric acid, are as follows. The cathode potentials of different mixtures do not differ much at the smallest C.D. used in the measurements. Nor do these potentials differ much from the equilibrium potentials of a platinum electrode in nitric acid solutions (Table 1).

In most cases, the limiting cathode C.D., measured with increasing current, were much higher than those measured with a falling current (Table 1). But the larger the ratio of the concentration of homopolar nitric acid molecules to the conductance $\underline{N}_{NO_2OH}/\lambda$, the smaller this difference. Thus, there is almost no difference in all the mixtures of the first series (Mixtures 1-6), in which $\underline{N}_{NO_2OH}/\lambda$ = 18-26 (Table 2). The difference is slight in Mixture 9, in which the $\underline{N}_{NO_2OH}/\lambda$ ratio is a maximum for Series 2 (Mixtures 7-12) and equals 14.1. The limiting cathode C.D. measured in mixtures at rest is higher than when measured when stirred. But here, too, the larger the ratio of the concentration of homopolar nitric acid molecules to the conductance $\underline{N}_{NO_2OH}/\lambda$, the smaller this difference. All the mixtures of Series 1, Mixtures 8 and 9 of Series 2, and Mixtures 15 and

TABLE 3

Comparison of the Experimental Data on the Limiting Cathode C.D. with the Concentration of Homopolar NO_2OH Molecules, the Concentration of Hydrogen Ions, and with the Ratio between them for HNO_3 Solutions

N_{HNO_3} mols/liter	N_{NO_2OH} mols/liter	N_{H^+}, mols/liter	$\frac{N_{NO_2OH}}{N_{H^+}}$	$\log\frac{N_{NO_2OH}}{N_{H^+}}$	At rest			When stirred		
					I_{cb} mA/cm²	I'_{cb} mA/cm²	$\log I'_{cb}$	I_{cb}, mA/cm²	I'_{cb}, mA/cm²	$\log I_{cb}$ / $\log I'_{cb}$
12.9	9.6	3.3	2.9	0.462	8120	6570	3.817	10000	8440	4.000 / 3.926
10.3	6.5	3.8	1.71	0.234	3130	156	2.192	950	81	2.977 / 1.908
7.7	3.6	4.1	0.88	-0.056	1040	18.8	1.274	14.4	4.4	1.158 / 0.644
5.2	1.3	3.9	0.33	-0.48	125	< 1.3	< 0.096	1.3	< 1.3	0.114 / < 0.114
2.6	0	2.6	0	-∞	0	0	-∞	0	0	-∞ / -∞
8.23	4.2	4.03	1.04					1600 *		3.2 *
6.15	2.16	4.00	0.54					200 *		2.3 *
5.13	1.28	3.85	0.33					16 *		1.2 *
4.11	0.49	3.62	0.135					0.5 *		-0.3 *
3.09	0	3.09						0 *		-∞ *

16 of Series 3, with the maximum values of the $\frac{N_{NO_2OH}}{\lambda}$ ratio for their respective series, yield values of the limiting cathode C.D. that are in close proximity, Mixtures 1, 8, and 9 even exhibiting higher values for the stirred mixture than for the mixture at rest. No limiting cathode C.D. was observed in Mixtures 25-29. Nor did Ellingham [24] find it to exist in a 3.09 N nitric acid solution (Table 3). At the same time, the concentration of homopolar nitric acid molecules is nearly zero in these mixtures (Tables 2 and 3).

As we pass from the first series to the last, we observe a parallel change of the limiting cathode C.D. and the concentration of hompolar nitric acid molecules in those mixtures in which the ratio of the concentrations of sulfuric to nitric acids is similar, such as Mixtures 3, 9, 15, and 21. The conductance of such mixtures constantly increases as we pass from the first series to the last.

In the first three mixtures of two of the series, Mixtures 7, 8, 9, 13, 14, and 15, the limiting cathode C.D. rises sharply as we move from the first series to the third, though the concentration of homopolar nitric acid molecules changes but little. This sharp rise in the limiting cathode C.D. is accompanied by a marked decrease in conductance.

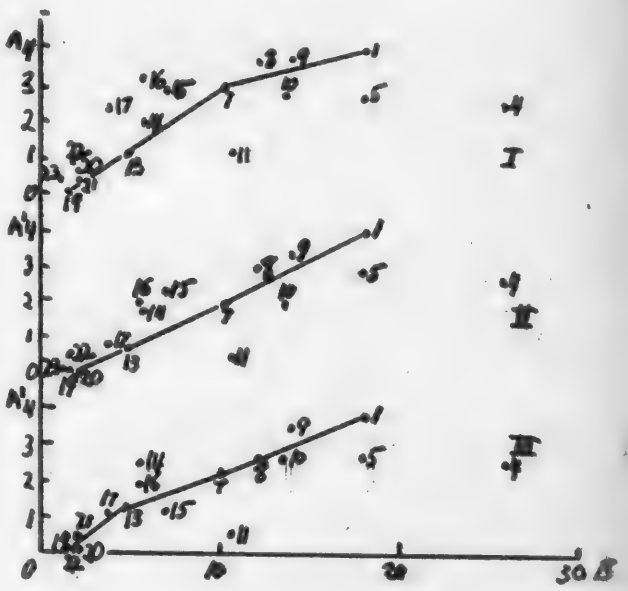

Fig. 2. Logarithm of the limiting cathode C.D. (A and A') plotted as a function of the ratio between the concentration of the homopolar nitric acid molecules and the conductivity $\frac{N_{NO_2OH}}{\lambda}$ (B).

Log I_{cb} (A) - logarithm of the limiting cathode C.D. as the current is raised; log I'_{cb} (A') - logarithm of the limiting cathode C.D. as the current is decreased.

I and II represent stirred media (in this and subsequent diagrams; III represents media at rest.)

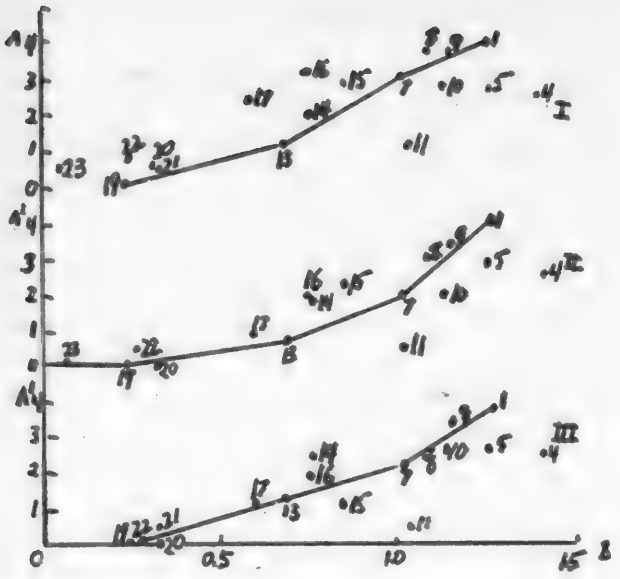

Fig. 3. Logarithm of the ultimate cathode C.D. (A and A') plotted as a function of the logarithm of the ratio of the concentration of nitric acid molecules to the conductivity log $\underline{N}_{NO_2OH}/\lambda$ (B).

(A) Log I_{cb}; (A') log $\underline{I}^{\circ}_{cb}$.

A definite parallelism exists between the limiting cathode current density and the ratio of the concentration of homopolar nitric acid molecules to the conductance, both for mixtures in the separately considered series and for mixtures in different series, whose acid-concentration ratios are similar (Tables 1 and 2).

In the nitric acid solutions the hydrogen-ion concentration changes but little, in comparison to the concentration of homopolar nitric acid molecules. In these solutions, the change in the limiting cathode C.D. parallels that of the concentration of homopolar molecules and of the latter's ratio to the hydrogen-ion concentration (Table 3).

The quantitative variation of the limiting cathode C.D. with the ratio of the concentration of homopolar nitric acid molecules to the conductance or to the hydrogen-ion concentration is rather complex, differing for various stirring conditions or changes in cathodic polarization (Figs. 1 - 6).

In mixtures at rest, this function does not depart very much from a straight line for nitric acid solutions or for a ternary mixture, when polarization is occurring with increasing current, and hence the liberated hydrogen is not being subjected to agitation (Figs. 1 and 4).

With vigorous mechanical stirring or when the hydrogen liberated is being stirred – when polarization is occurring with decreasing current – the following is observed in solutions of nitric acid. When polarization occurs with a rising current, there is an approximately straight-line relation between the logarithm of the limiting cathode C.D. and the logarithm of the ratio of the concentration of homopolar nitric acid molecules to the hydrogen-ion concentration (Figs. 3, I and 6, I). When polarization takes place with a falling current – whether the solution be stirred or at rest – the logarithm of the limiting cathode C.D. is a straight-line function of the ratio of the concentration of homopolar nitric acid molecules to the hydrogen-ion concentration as well as to the conductance (Figs. 2, II, III and 5, II, III). The same sort of relationship between the limiting cathode C.D. and the ratio of the concentration of homopolar nitric acid molecules to the

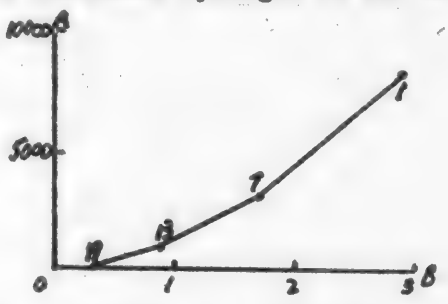

Fig. 4. Limiting cathode C.D. $\underline{I}_{cb}$ (A) plotted as a function of the ratio of the concentration of homopolar nitric acid molecules to the concentration of hydrogen ions $\underline{N}_{NO_2OH}/N_H^{\circ}$ (B) for solutions of nitric acid at rest.

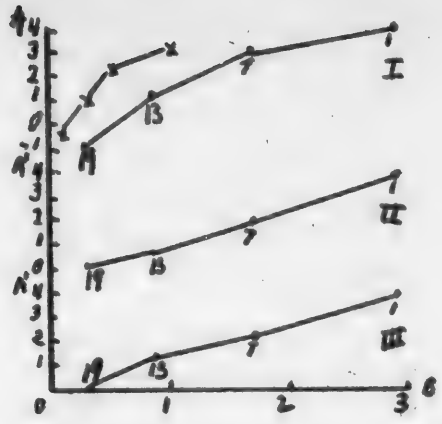

Fig. 5. Logarithm of the limiting cathode C.D. (A and A') plotted as a function of the ratio of the concentration of homopolar nitric acid molecules to the concentration of hydrogen ions $\frac{N_{NO_2OH}}{N_H}$ (B) for solutions of nitric acid. (A) Log $\underline{I}_{cb}$; (A') Log $\underline{I}'_{cb}$;

The crosses in this diagram and in Fig. 6 represent the measurements made by Ellingham [24].

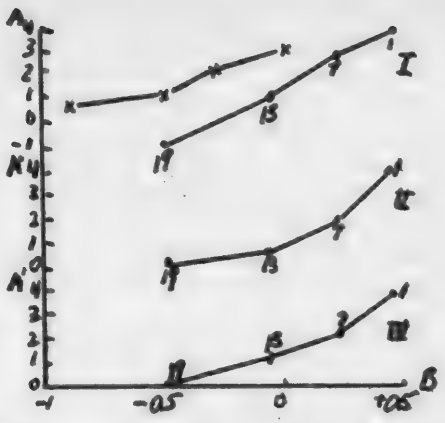

Fig. 6. Logarithm of the limiting cathode current density (A and A') plotted as a function of the logarithm of the ratio of the concentration of homopolar nitric acid molecules to the concentration of hydrogen ions $\log \frac{N_{NO_2OH}}{N_H}$ (B) for nitric acid solutions.

(A) $\log \underline{I}_{cb}$; (A') $\log \underline{I}'_{cb}$;

conductance is observed for ternary mixtures as well; but here the experimental points are widely scattered on the graph (Figs. 2 and 3). This is due to the great complexity of such systems and of the cathode processes taking place within them, as well as to the greater unreliablity of the data on the concentration of homopolar molecules of nitric acid and on the conductance.

EVALUATION OF RESULTS

Our experimental results enable us to draw several conclusions regarding the mechanism of the cathode process in nitric acid solutions and in the $HNO_3 - H_2SO_4 - H_2O$ system.

The fact that the limiting cathode C.D. is zero when there are no homopolar nitric acid molecules in nitric acid solutions or in the $HNO_3 - H_2SO_4 - H_2O$ system, the proximity of the values of the cathode potential at low C.D. values and of the oxidative potential in nitric acid solutions, and the fact that the changes in the limiting cathode C.D. parallel those in the concentration of homopolar nitric acid molecules when there is no change (or a change only in one direction) in the effect of the hydrogen ion concentration – all this goes to show that the homopolar molecules of nitric acid are the principal oxidative cathode depolarizers in these reaction media.

Furthermore, the experimental data indicate that, together with the homopolar nitric acid molecules, the hydrogen ions also participate in the cathode process, both at high as well as at low cathode potentials. Both of these depolarizers compete for the cathode electrons, inasmuch as the action of one impairs and suppresses the action of the other. This is indicated by the drop in the limiting cathode C.D. that occurs when the hydrogen-ion concentration increases while the concentration of homopolar nitric acid molecules is kept constant, as

well as by the straight-line relationship between the limiting cathode C.D. and the ratio of the concentration of homopolar nitric acid molecules to the hydrogen ion concentration. The following mechanism of the cathode process is found to agree with the experimental data. When the surface of the electrode is at a high potential, a layer of sulfuric and nitric acid anions is in close proximity to it. When this is so, the NO_3' ions take no part in the cathode reaction. Interaction with the electrons of the cathode surface is also very difficult for the hydrogen ions. That is why it is chiefly the NO_2OH molecules that react with the cathode electrons directly at low C.D. values, producing HNO_2 and O" or OH'. The latter react with the hydrogen ions that flow toward them, forming water.

As the C.D. increases, thus causing an increase in the rate at which the homopolar nitric acid molecules are used up, the hydrogen ions begin to play a larger part in the primary cathode process. When the ratio of the rate of depolarization by the hydrogen ions to the rate of depolarization by the homopolar nitric acid molecules reaches a certain value, hydrogen atoms accumulate at the cathode, and the potential drops from a value that approximates the cathode potentials in the oxidation-reduction system $NO_2OH - HNO_2$ to a value that approximates the cathode potentials in the $H^\circ - H(H_2)$ system. As we proceed from high current densities to low ones, the sharp potential rise that occurs when the limiting cathode C.D. is reached may be regarded as the result of reaching a definite value of the inverse ratio of the depolarization rates.

It is natural to suppose that the greater the ratio of the homopolar nitric-acid molecule concentration to the hydrogen-ion concentration, and the higher the cathode potential, the greater will be the ratio of the rate of oxidative depolarization to the rate of hydrogen depolarization.

It follows directly from this suggested mechanism of the cathode process that there is a straight-line relationship between the limiting cathode C.D. and the ratio of the concentration of nitric acid molecules to the hydrogen-ion concentration. Since the ratio of the rate of oxidative depolarization to the rate of hydrogen depolarization will be higher at high potentials than at low, the limiting cathode C.D. measured as the current rises must be higher than that measured as the current falls. The decrease in the limiting cathode C.D. during stirring may be due to the rate of hydrogen depolarization increasing more than the rate of oxidative depolarization. Nitrous acid raises the cathode potential or maintains it at a rather high level. When it accumulates at the electrode in media at rest, the limiting cathode C.D. in such media must be higher than in media that are stirred. But, as the nitrous acid is accumulated at the cathode only up to a certain limiting concentration, it is unable to effect any major change in the ratio of oxidative depolarization to the rate of hydrogen depolarization. This corresponds to the slight effect upon the limiting cathode C.D. of stirring conditions or of the direction of polarization in media in which the ratio of the concentration of homopolar nitric acid molecules to the hydrogen-ion concentration is large. In media at rest, it is more likely that the rates of depolarization processes are determined by the rates of diffusion of the depolarizers and their concentrations which are proportional to these rates. It follows, therefore, that under these conditions, the limiting cathode C.D., which is governed by the ratio of the rate of depolarization by homopolar nitric acid molecules to the rate of depolarization by hydrogen ions according to this supposition, ought to be proportional to the ratio of the concentrations of these depolarizers. At intensive stirring the rates of the depolarization processes are not controlled by the rates of diffusion of the depolarizers, and the relationship between the limiting cathode C.D. and the ratio of the concentrations of the depolarizers in question must be more complex. Both of these conclusion are likewise in conformity with our experimental data.

The catalytic action of nitrous acid upon the process of oxidative cathode depolarization may be explained as due to its giving rise to molecules and nitrate ions of homopolar molecules of nitric acid. The high concentration of nitrate ions at the surface of the cathode favors this; this is so when the potential of the cathode is high, and when the absolute and relative concentrations of these anions in the solution are high, plus the permanently high surface concentration of the nitrous acid primarily formed. Moreover, conditions must be such as to make it possible for homopolar molecules of nitric acid to be formed. Under these conditions the catalytic action of nitrous acid in the process of cathodic depolarization of a platinum electrode is exhibited both in solutions of nitric acid and when noble metals, such as copper, are dissolved in it [24,30]. Our investigation has shown that the limiting cathode C.D. is much larger at rest than with stirring (which removes the nitrous acid from the cathode surface) in mixtures that have a relatively high percentage of nitric acid that is sufficiently dissociated plus a comparatively low percentage of sulfuric acid, while at the same time containing homopolar nitric acid molecules.

As for catalysis in nitric acid solutions, the notion of their internal state advanced by Halban and Eisenbrand [34] deserves serious consideration. Their investigation of the absorption spectra of nitric acid in various solvents led them to conclude that aqueous solutions of nitric acid up to 10 N concentration contain a negligible number of homopolar NO_2OH molecules (up to $2.4 \cdot 10^{-3}$ mol/liter). According to these authors, in this concentration range, the hydrogen and nitrate ions do not associate into homopolar molecules, but rather into associated ion-pairs, such as $H_3O^+ \cdot NO_3^-$. The concept of the association of the hydrated ions H^+ and NO_3^- into ion-pairs instead of their forming homopolar NO_2OH molecules is supported by the high degree of hydration of nitric acid. According to Kuzmin, in 6.16 N, 9.79 N, and 14.50 N nitric acid solutions, 1 mol of acid combines with 3.0, 2.5, and 1.6 mol of water, respectively [35].

If this is the state of nitric acid solutions, their weak depolarizing activity at high cathode potentials becomes understandable. It is, moreover, natural that it is not the homopolar molecules that are catalytically activated, but, rather, the nitrate ions, whether free, or associated with hydrated hydrogen ions, or both. The mechanism of the catalytic action of nitrous acid may be represented as the result of this action of its molecules upon nitrate ions, reinforcing their negative field and resulting in the detaching of protons from the H_3O^+ ions, existing in associated ion-pairs or free, supplied to the cathode by electrolysis. As we have stated in our brief survey of the literature, several foreign authors, including Joss, Evans, and others, consider secondary products – the hypothetical compound $H_2N_2O_5$ and NO_2, which are not direct components of the reaction medium – to be the oxidative cathode depolarizers in nitric acid solutions. According to Evans, the NO_2 depolarizer is formed as the result of the reaction of nitrous acid with the molecules of nitric acid. As these authors see it, therefore, the homopolar molecules of nitric acid cannot be active cathode depolarizers. In our opinion, this last assertion is contrary to the facts and is due to their making an insufficient allowance for the real state of affairs in nitric acid solutinns when cathodic action is going on. It is not the molecules of nitric acid, but rather the nitrate ions that are catalytically activated, as is indicated by a comparison of the extent of the catalytic action of nitrous acid with the state of the reaction medium that reacts with the cathode.

SUMMARY

1. Experimental data have been secured on the cathodic polarization of a platinum electrode in solutions of nitric acid and in the nitric acid – sulfuric acid – water system. The experimental data on the cathodic process are compared

with the characteristics of the state of the reaction mixture. Theoretical conclusions are deduced regarding some of the problems related to the mechanism of the cathode process.

2. The limiting cathode C.D. becomes a measurable quantity only after homopolar molecules of nitric acid appear in the reaction media.

3. The limiting cathode C.D., measured under various experimental conditions, is a linear function of the concentration of homopolar nitric acid molecules and an inverse linear function of the hydrogen-ion concentration and of the conductance of the medium.

4. The limiting cathode C.D.s measured in mixtures at rest are higher than those measured in agitated mixtures; likewise, those measured with rising current values are larger than those measured while the current is being reduced. These differences diminish or vanish, however, when the ratio of the concentration of homopolar nitric acid molecules to the hydrogen-ion concentration or to the conductance grows larger.

5. The homopolar molecules of nitric acid are an oxidative cathode depolarizer in solutions of nitric acid and in the nitric acid – sulfuric acid – water system.

6. The hydrogen ions participate alongside the homopolar nitric acid molecules in the primary process of cathodic depolarization, at high potentials as well as at low.

7. It is probable that the limiting cathode C.D. in these systems is governed by the ratio between the rates of cathodic depolarization by the homopolar nitric acid molecules and the hydrogen ions.

8. The catalytic action of nitrous acid in the high-potential cathode process may be interpreted as resulting from the formation of homopolar molecules of nitric acid at the cathode surface when molecules of nitrous acid act upon free nitrate ions or upon nitrate ions associated with hydrated hydrogen ions.

LITERATURE CITED

[1] B.V.Ershler, Bull. USSR Acad. Sci., Div. Chem. Sci., 3, 245 (1946).

[2] B.Kabanov, Acta Physicochim., 5, 193 (1936).

[3] Z.A.Iofa, J. Phys. Chem. 13, 10, 1435 (1939).

[4] Z.A.Iofa, and A.N.Frumkin, J. Phys. Chem. 18, 7-8, 268 (1944).

[5] Z.A.Iofa, J. Phys. Chem. 19, 3, 117 (1945).

[6] Z. Iofa and V.Stepanova, J. Phys. Chem. 19, 3, 125 (1945).

[7] V. Kheifets and N.E.Polyakova, J. Appl. Chem. 22, 8, 801 (1949).

[8] A. Murtazaev, J. Phys. Chem. 23, 10, 1247 (1949).

[9] Yu.G.Siver and B.N.Kabanov, J. Phys. Chem. 23, 4, 428 (1949).

[10] Z.A.Iofa, Ya.B.Shimshevich, and E.P.Andreeva, J. Phys. Chem. 23, 7, 828 (1949).

[11] V.S.Bagotsky, Proc. USSR Acad. Sci., 58, 7, 1387 (1947).

[12] M.A.Loshkarev and A.A.Krukova, J. Phys. Chem. 23, 12, 1547 (1949).

[13] A.N.Krasilshchikov, J. Phys. Chem. 18, 11-12, 537 (1944).

[14] A.N.Krasilshchikov, J. Phys. Chem. 20, 10, 1187 (1946).

[15] A.N.Krasilshchikov and V.A.Andreeva, J. Phys. Chem. 20, 10, 1199 (1946).

[16] A.N.Krasilshchikov, J. Phys. Chem. 23, 3, 332 (1949).

[17] G.V.Akimov. Theory and Research Methods of Metal Corrosion. 119-135 passim. Moscow-Leningrad (1945).

[18] N.D.Tomashov. Corrosion of Metals with Oxygen Depolarization, a) 96-179; b) 49-95; c) 50, 61, 76. Moscow-Leningrad (1947).

[19] G.V.Akimov and G.B.Clark, Proc. USSR Acad. Sci., 58, 8, 1669 (1947).

[20] G.B.Clark and G.V.Akimov, Proc. USSR Acad. Sci. 58, 9, 1973 (1947).

[21] I.L.Rozenfeld and G.V.Akimov, Proc. USSR Acad. Sci. 67, 5, 879 (1949).

[22] N.D.Tomashov, G.P.Sinelshchikov, and M.A.Vedeneeva, J. Phys. Chem., 23, 3, 289 (1949).

[23] I.Oknin, J. Appl. Chem. 18, 494 (1945).

[24] H.J.T.Ellingham, J. Chem. Soc., 1565 (1932).

[25] A.Travers et R. Diebold, Bull. Soc. chim. France, (5), 5, 690 (1938).

[26] Y. Yamamoto, Bull. Inst. phys. chem. Research (Abstr.), 15, 12, 69 (1936).

[27] E.S.Hedges, J. Chem. Soc., 561 (1930).

[28] E.J.Joss, J. Phys. Chem.,(London), 30, 1222 (1926).

[29] S. Glasstone and A. Hickling, Electrolytic Oxidation and Reduction, 224 and 235 (1935).

[30] U.R.Evans, Trans. Faraday Soc., 40, 120 (1944).

[31] R.J.Monk and B.J.Ellingham, J. Chem. Soc., 125 (1935).

[32] I.Oknin, J. Appl. Chem. 23, 12 (1950).

[33] Landolt-Bornstein, Tabellen, 1074 (1923).

[34] N.V.Halban and J. Eisenbrand, Z. phys. Chem., 131, 433 (1928).

[35] A.I.Kazmin, J. Phys. Chem., 11, 585 (1938).

Received March 17, 1950

A PHOTOCOLORIMETRIC METHOD OF DETERMINING SMALL QUANTITIES OF MILK SUGAR*

M. N. Tulchinsky

Chair of General and Analytical Chemistry,
Leningrad Institute of the Refrigeration and Dairy Industry

In our preceding report [1] we suggested the use of the hexavalent chromium ion in an alkaline medium as a reagent for reducing saccharine substances and demonstrated the straight-line relationship between the amount of hexavalent chromium reduced and the concentration of lactose. When solutions of reducing sugars are heated with salts of hexavalent chromium in an alkaline medium, the color changes to green, Cr^{6+} being changed to Cr^{3+}. A study of this color indicated that its intensity increases with a growing concentration of the reducing sugar substance. The green color of the reaction mixture may be measured with a photocolorimeter, by recording the galvanometer readings of the changes in the voltage of the photoelectric current in the circuit. The relationship between the galvanometer readings and the green coloring of the reaction mixture makes it possible to compute the amount of sugar present.

With these relationships as a basis we have endeavored in the present paper to elaborate a photocolorimetric method for determining small quantities of milk sugar.

EXPERIMENTAL

Effect of the alkali concentration in the reaction medium and the length of time the reaction mixture is heated upon the intensity of the green coloring. In developing a photocolorimetric method of measuring small quantities of milk sugar we had to determine the effect of the concentration of alkali in the reaction mixture upon the production of the most intense and stable colors in the solution. We used a solution of sodium carbonate to make the reaction mixture alkaline, since a caustic alkali produces a brown tint that masks the green.

The investigation of the effect of the soda concentration upon the solution color was conducted as follows: 6 ml of a 0.25 N solution of K_2CrO_4, 3 ml of a solution containing 6 mg of lactose, and various volumes (from 0.5 to 3.0 ml) of a 2N solution of Na_2CO_3 were placed in a test tube of uniform diameter and wall thickness, with a capacity of 15-16 ml. The volume of the reaction mixture was kept at 12 ml, so that as the amount of soda solution varied up to 3 ml, a corresponding volume of distilled water was added to make up the difference. The reaction mixture was heated over a boiling water bath for 15 minutes.

The intensity of the green color of the solutions was measured with a photocolorimeter, [2]. The method of measurement is described below.

The effect of varying the concentration of soda upon the intensity and stability of the green is shown in Fig. 1.

The curve plotted in Fig. 1 shows that the extent of the reduction of

*Report II of a series on this topic.

hexavalent chromium and, hence, the intensity of the solution's green color increases with a rising percentage of Na_2CO_3, reaching a maximum at a salt concentration of 0.42 N in the reaction mixture (2.5 ml of a 2 N Na_2CO_3 solution in 12 ml).

Any further increase in the soda concentration causes no change in color, so that we used 3 ml of a 2N Na_2CO_3 solution in 12 ml of the reaction mixture, the Na_2CO_3 concentration being 0.50 N.

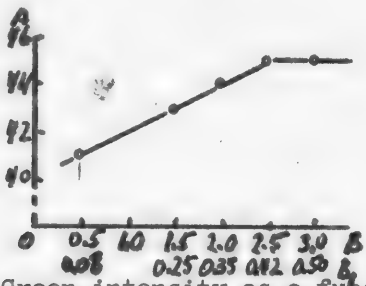

Fig. 1. Green intensity as a function of the soda concentration. Quantity of lactose: 6 mg.

A-Galvanometer readings, in scale divisions; B-ml of 2N Na_2CO_3 solution per 12 ml of reaction mixture; B_1-amount of soda in the reaction mixture, expressed in normalities.

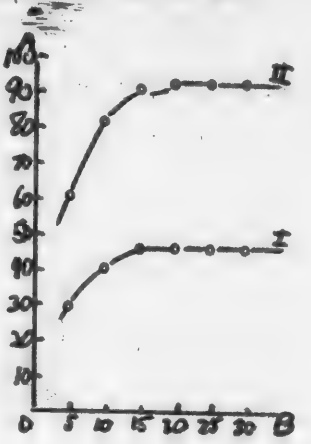

Fig. 2. Green intensity as a function of the time the reaction mixture is heated, for different concentrations of lactose.

A-Galvanometer readings, in scale divisions; B-heating time, min. Quantity of lactose: I-6mg; II-12mg.

We then examined the effect of the length of time the reaction mixture was heated upon the intensity of the green. We ran these tests with two different amounts of lactose: 6 mg and 12 mg, in 12 ml of reaction mixture, containing 3 ml of a 2 N Na_2CO_3 solution. 6 ml of a 0.25 N solution of potassium chromate was added. The reaction mixture was heated over a boiling water bath for periods ranging from 5 to 30 minutes. Our results are shown in the curves reproduced in Fig. 2. The shape of these curves indicates that the reduction of hexavalent chromium by lactose of the specified concentrations is practically complete within 15 minutes.

Effect of the lactose concentration upon the intensity of the green color of the reaction mixture as determined by a photocolorimeter. Establishing the conditions (soda concentration and heating time) required for producing the most intense and stable color in the reaction mixture enabled us to turn to an examination of the nature of the relationship between the concentration of lactose and the intensity of the reaction mixture's color, as determined by a photocolorimeter.

These tests were run as follows: 6 ml of a 0.25 N K_2CrO_4 solution, 3 ml of a 2 N Na_2CO_3 solution, and 3 ml of the lactose solution being tested were placed in a 15-16 ml test tube (with uniform diameter and wall thickness). The reaction mixture was heated over a boiling water bath for 15 minutes, after which the photocolorimetric measurements were made.

Our results for pure lactose preparations (Table 1 and Fig. 3) bear out the results obtained in our preceding report [1], namely: that the solution color changes with the lactose concentration. The difference between various concentrations may be recorded by means of the galvanometer readings. Analysis of the curve shown in Fig. 3 indicates that the solution color obeys Beer's law.

TABLE 1

Relationship between Intensity of Solution Color and Lactose Concentration

Mg of lactose in 12 ml of reaction mixture	Galvanometer reading, scale divisions. 1 Division = $105 \cdot 10^{-6}$ V
0	0
1	7.5
2	14
4	30
6	46
9	69
12	90

Fig. 3. Solution color intensity as a function of the lactose concentration.

A-Galvanometer readings, scale divisions; B-mg of lactose.

Method of Determination. 1) Extracting milk sugar from objects to be analyzed. One of the basic requirements that must be met by unknown solutions if the amount of a substance they contain is to be determined colorimetrically is that they be colorless until they are reacted with the reagent that produces the coloring [3]. That is why we employed solutions of $Al_2(SO_4)_3$, NaOH, and NaF as coagulators to eliminate the proteins when making determinations of the milk sugar in milk and other objects that contained proteins.

Colorless filtrates of the objects to be analyzed that contained milk sugar were secured as follows: 1 ml of milk, measured with an accuracy of 0.01 ml, or a corresponding quantity of another test substance with the same lactose content, was transferred to a dry 25-ml Erlenmeyer flask, and 11 ml of distilled water, 1 ml of a 10% $Al_2(SO_4)_3$ solution, 1 ml of a 0.45 N NaOH solution, and 1 ml of a saturated solution of NaF were added. The reaction medium must not be alkaline, and the volume of the mixture must total 15 ml.

The milk sugar concentration must not exceed 0.4%. The contents of the flask were shaken together and then allowed to stand for 15 minutes. The mixture was then filtered twice through the same filter.

The solution thus prepared was completely transparent and colorless, like distilled water.

2) Preparation of colored solutions. The following method was adopted for preparing colored solutions, based upon the reaction described above.

6 ml of a 0.25 N K_2CrO_4* solution (1.6185 g of K_2CrO_4 in 100 ml of solution), 3 ml of a 2 N Na_2CO_3** solution, and 3 ml of the filtrate of the solution under test are placed in each of a set of 15-16 ml test tubes of uniform inside diameter and wall thickness. The amount of lactose in 12 ml of reaction mixture must not exceed 12 mg. The contents of the test tubes are mixed well, after which the tubes are immersed in a boiling water bath and heated in the boiling bath for 15 minutes, the level of the water in the bath being above the level

*The K_2CrO_4 should be prepared from recrystallized $K_2Cr_2O_7$ [4].

**In preparing the 2N soda solution, one must know the amount of water in the $Na_2CO_3 \cdot H_2O$ crystal hydrate, which is conveniently done by desiccating a weighed amount of the soda crystal hydrate to constant weight at 180°.

of the reaction mixture in the test tubes. When the 15 minutes are up, the test tubes are lifted from the water bath, closed with stoppers, cooled with water to room temperature, and wiped dry on the outside.

The solutions thus prepared, the green colorings of which differ in intensity, depending upon the percentage of milk sugar, are ready for photocolorimetric determinations.

3) Photocolorimetric measurement of colored solutions and determination of their milk sugar content. The color of solutions of varying intensity, prepared by the method described above, can be measured with various types of photocolorimeters. The volume of the reaction mixture will, of course, depend upon the capacity of the photocolorimeter cell, containing the following solution proportions: 2 volumes of a 0.25 N K_2CrO_4 solution, 1 volume of a 2 N Na_2CO_3 solution, and 1 volume of the solution under test.

In the present paper we shall describe the procedure employed with a test-tube photocolorimeter using selenium photoelectric cells, designed by B.V.Ozimov, [2], based upon a differential circuit (Fig. 4). (See Plate I, page247).

Constant voltage in the circuit, to produce uniform incandescence of the light-source lamp L is maintained by the current stabilizer S (to lower the voltage, the transformer T is connected into the circuit).

Before measurements are begun the galvanometer is set to zero by means of control solutions. This is done by placing 6 ml of a 0.25 N K_2CrO_4 solution, 3 ml of a 2 N Na_2CO_3 solution, and 3 ml of distilled water in each of two identical test tubes.* The contents of the test tubes are stirred well, the test tubes are placed in the instrument's sockets, the switch Sw is turned on, lighting up the lamp L, and the light flux is regulated by the diaphragm D until the galvanometer needle stands at zero, after which the switch is turned off. Then the test solution is poured into an exactly similar, dry test tube, and the latter is placed in one of the sockets, replacing the control test tube; the photocolorimeter lamp is turned on, and the galvanometer deflection is read off. The same determination is made with a solution whose color is due to a known concentration of lactose (the standard solution) under the same conditions.

Lactose preparations contain water of crystallization. The percentage of sugar in these preparations must therefore be determined (say, by the Bertrand method), and the resultant data used in preparing a solution of the wanted concentration.

In preparing a standard solution enough lactose must be used so that the color produced will cause almost full-scale deflection of the galvanometer needle.

The amount of milk sugar in the unknown solution is determined by calculation, starting with the deflections of the galvanometer needle corresponding to the known lactose concentration in the standard solution and to the concentration in the solution under test. For example, if 12 mg of lactose produces a deflection of 90 scale divisions, the amount of lactose in a solution whose color produces a deflection of 46 scale divisions can be calculated from this proportion:

$$x = \frac{12 \cdot 46}{90} = 6.13 \text{ mg of lactose.}$$

The periodic preparation of a standard colored solution of lactose ** may

*The selection of these test tubes is described in a paper by B.V.Ozimov [2].

**The color of the standard solution produced by lactose was measured during the course of a month; it was found to be unchanged. The solution was kept in stopped test tubes exposed to light.

be replaced by using a standard based on mineral salts. The color of such salt solutions is very stable. Flerov and Ozimov [5, 6] have employed mineral salts extensively to imitate colored solutions, with a view to securing stable colors.

In our research we made use of a solution of $NiSO_4$ containing a 0.2 N solution of HCl. The color of such a solution must produce a deflection of the galvanometer needle that equals the deflection produced by the standard lactose solution.

When using an artificial standard prepared from mineral salts, it is first necessary to establish the null point of the galvanometer against the control solution (6 ml of a 0.25 N K_2CrO_4 solution, 3 ml of a 2 N Na_2CO_3 solution, and 3 ml of distilled water), as specified above; then the deflections of the galvanometer needle produced by the standard and unknown solutions must be found, and the lactose content found from their ratio as indicated above.

We employed a round LGU galvanometer with a 100-division scale, each division corresponding to $105 \cdot 10^{-6}$ volt.

In our measurements, a deflection of the galvanometer needle by one scale division corresponded to the color of a solution produced by about 0.1 mg of lactose in 12 ml of the reaction mixture.

When measuring unknown solutions with higher lactose concentrations and, hence, more intense green, it is well to employ control solutions corresponding to the known concentrations of lactose to establish the galvanometer null point (it is convenient to use $NiSO_4$ or $NiCl_2$ standards). Then the galvanometer readings for the standard and the unknown solutions are read off, and the computation made as above.

Determining milk sugar by the photocolorimetric and the Bertrand method. We then made a comparison of the photocolorimetric method for determining small quantities of lactose with the Bertrand method of determining them. Our results are listed in Table 2. The figures in the table indicate that the discrepancies

TABLE 2

Comparative Determination of Milk Sugar by the Photocolorimetric and Bertrand Methods

Object under analysis	Photocolorimetric method			Bertrand method		
	Quantity of subs. used for one determination, g	% lactose	Discrepancy between parallel determinations	Quantity of subs. used for one determination, g	% lactose	Discrepancy between parallel detmns.
Cow's milk	0.2	3.89 3.91	0.02	2.5	3.98 4.02	0.04
Cow's milk	0.2	5.10 5.05	0.05	2.5	5.08 5.15	0.07
Milk sugar (crude)...	0.008	94.7 95.1	0.4	0.08	94.0 94.5	0.5

between parallel determination when our method is used are no larger, but are even somewhat smaller, than with the Bertrand method. When minute quantities of crude milk sugar are analyzed, the discrepancies between the parallel determinations increased in both methods. The percentage of lactose in various objects was the same when measured by both methods, but in one determination by the photocolori-

metric method the quantity of analyzed substance was one-tenth of the quantity used in the Bertrand method.

An advantage of the photocolorimetric method over the Bertrand method is the feasibility of determining small amounts of sugar; in addition, it is more convenient, simpler, and requires less time for each determination, thus saving labor time, which is especially valuable when several analyses are involved. The fact that it is possible to measure extremely minute quantities of sugar by the photocolorimetric method ought to make it appeal to biologists, breeders, physicians, and workers in the food industry.

The method may also be employed to determine other reducing sugars, such as: glucose, maltose, fructose, as well as saccharose after its inversion.

SUMMARY

1. A photocolorimetric method of determining small quantities of milk sugar has been elaborated, based on a reaction suggested by the author, using the reduction of sugars by hexavalent chromium in an alkaline medium.

2. In our measurements, the colors produced in this reaction obey Beer's law.

3. The photocolorimetric method makes it possible to determine tenths of a milligram of sugar.

4. The photocolorimetric method possesses the following advantages over Bertrand's method: the feasibility of determining small quantities of sugar, the simplicity and convenience of measurement, and the shorter time required for each determination.

5. The reduction of hexavalent chromium in an alkaline medium may be utilized for the photocolorimetric determination of other sugars as well.

LITERATURE CITED

[1] M.N.Tulchinsky, J. Appl. Chem. 23, 2, 176 (1950).*

[2] B.V.Ozimov, J. Applied Chem. 23, 2, 166 (1950). **

[3] D.G.Joe. Colorimetry, 17 (1935).

[4] Yu.V.Karyakin. Pure Chemical Reagents, 208 (1938).

[5] K.V.Flerov, Chem. Social. Agric., 2, 96 (1937).

[6] K.V.Flerov and B.V.Ozimov, J. Gen. Chem. 18, 1, 18 (1948).

Received April 13, 1950

---

*See CB translation p. 181 ff.

**See CB translation p. 171 ff.

BRIEF COMMUNICATIONS

THE SOLUBILITY OF SODIUM NITRITE AND NITRATE IN WATER WHEN SODA IS PRESENT

I. N. Kuzminykh and E. L. Yakhontova

Mendeleev Institute of Chemical Technology, Moscow, Awarded the Order of Lenin

Solutions prepared by having nitrogen oxides absorbed by soda, which are used for the recovery of crystalline sodium nitrite, contain $NaNO_2$, $NaNO_3$ and Na_2CO_3 simultaneously. The solubility of each of these salts in water is common knowledge. The literature likewise contains detailed data [1] on the mutual solubility of $NaNO_2$ and $NaNO_3$ in water. As for data on the way in which soda affects the solubility of the nitrite and nitrate in water, there is either no mention of them in the literature (for the $NaNO_2 - NaNO_3 - Na_2CO_3 - H_2O$ system) or the data are incomplete (for the $NaNO_2 - Na_2CO_3 - H_2O$ system). The inadequacy of the data hampers the rational organization of the technological process.

In order to fill this gap, we* have measured the solubility of $NaNO_2$ and $NaNO_2 + NaNO_3$ in the presence of various quantities of Na_2CO_3. These measurements were made in the 10-30° temperature range, which corresponds to the terminal crystallization temperature. The experiments were made by means of the polythermal method (suggested by V.F. Alekseev [2] in 1877). In this method the saturation temperature is read off visually: when the initial crystal appears as the solution is cooled, and when the last crystal disappears as the solution is heated. The mean of the two readings is taken. This method gives good results at temperatures up to 30-35° and has been repeatedly used to determine solubilities.

EXPERIMENTAL

$NaNO_2 - Na_2CO_3 - H_2O$ System. The literature contains data for two solubility isotherms in this system: 30° (Atroschenko [3,4]) and for 23.1° (J. Bureau [5]). Unfortunately, the composition of the equilibrium phases was not determined in Atroschenko's experiments, and, hence, his data give no idea of what crystals separate out when any given solution is cooled to 30°. This makes the Atroschenko diagram unusable for solving problems involving the crystallization of the nitrite from solutions containing Na_2CO_3. Bureau's isotherm for 23.1° indicates that sodium nitrite is a solid equilibrium phase only for solutions that contain no more than 6.5% Na_2CO_3; beyond that there is the isothermal invariant point, where there are two solid phases – the nitrite and the soda hydrate ($Na_2CO_3 \cdot H_2O$, according to Bureau). The fact that Bureau's figures on the solubility of the nitrite in water (45.25% $NaNO_2$) disagree appreciably with the values generally given in the reference works (45.9% $NaNO_2$) is worthy of note.

*The laboratory technician A. G. Kuznetsova and the students V. Goryacheva, N. Bubnova, V. Smirnova and V. Cherkashina assisted in the experimental work.

All these impelled us to remeasure the solubility of $NaNO_2$ in water when Na_2CO_3 is present and to plot the isotherms for the temperatures lying between 10 and 30°, which are required for computing the crystallization of the nitrite. Pure preparations of $NaNO_2$ and Na_2CO_3 were prepared for these experiments. At first, by way of training, we determined the solubility of $NaNO_2$ in water at various temperatures; our results were in good agreement with the handbook data.

Solutions of $NaNO_2 + NaNO_3$, the bottom phase of which is $NaNO_2$, are of interest in preparing the crystalline nitrite. We therefore prepared solutions that were saturated with $NaNO_2$, but were not saturated with soda (from small Na_2CO_3 concentrations to the eutonic point) for use in our measurements.

Our procedure was as follows: 10 ml of a soda solution of known concentration,* was placed in a test tube fitted with a stirrer; then enough $NaNO_2$ was added to produce a saturation temperature of about +8°. Then small quantities of $NaNO_2$ were successively added to the test tube, and each time the saturation point of the resulting solutions was read off visually. When the equilibrium temperature reached 35°, the experiment was stopped; measurements at higher temperatures are inaccurate (owing to the evaporation of the water in the test tube).

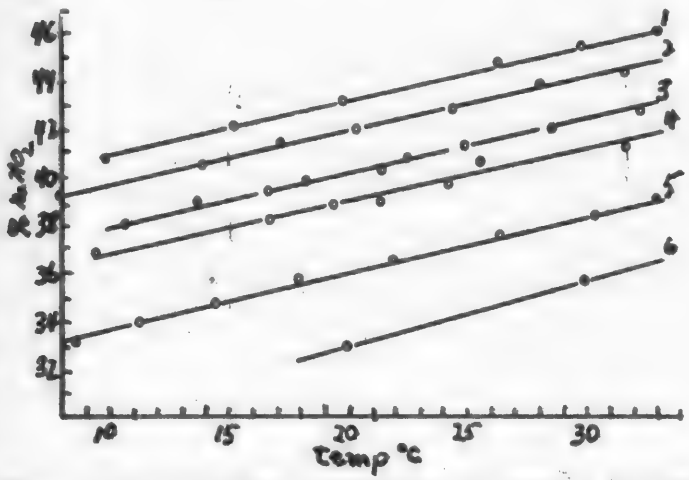

Fig. 1. Solubility polytherms of sodium nitrite in water when soda is present.

Na_2CO_3 concentration in the original solution, containing no soda: 1-3.0; 2-5.54; 3-8.63; 4-10.46; 5-12.59; 6-15/14.

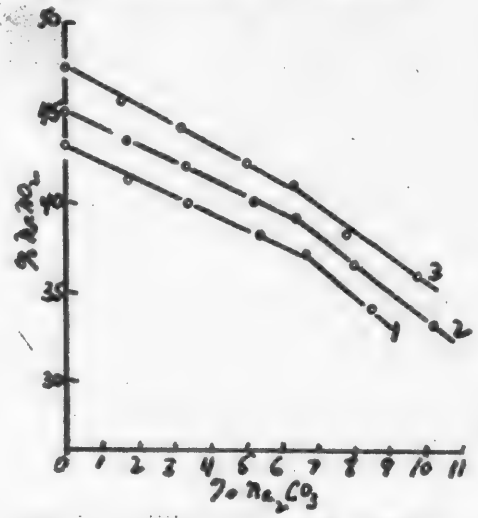

Fig. 2. Solubility of sodium nitrite in water with soda present.

Temperatures, °C: 1-10; 2-20; 3-30.

The test results are shown in Fig. 1 in the shape of 6 polythermal curves. These data were used to plot the solubility isotherms of $NaNO_2 - Na_2CO_3 - H_2O$ for 10, 20, and 30° (Fig. 2). There is a bend in the isotherms at 6-7% of Na_2CO_3 in the solution, indicating the appearance of a new bottom phase – soda hydrate – at that point. Pure nitrite crystallizes out of solutions to the left of these isothermal invariant points. The solubility curves in Fig. 2 indicate that when soda was dissolved in saturated $NaNO_2$ solutions, it exercised a salting-out effect on the nitrite.

<u>$NaNO_2 - NaNO_3 - Na_2CO_3 - H_2O$ System.</u> When nitrogen oxides are absorbed by a soda solution, we usually get a mixture of the nitrite and the nitrate. If we are to deal with crystallization problems, we must have figures on the effect of the soda upon the mutual solubility of $NaNO_2$ and $NaNO_3$ in water. Since there were no such figures in the literature, we made a series of measurements, using the same polythermal method of exploring equilibria in aqueous solutions.

*3.0, 5.54, 8.63, 10.46, 12.59, 15.14% Na_2CO_3.

The results of our measurements are shown in Figs. 3 and 4 as a series of isotherms for 15 and 25°. Each isotherm consists of two branches, which meet at the isothermal invariant point; the left-hand branch (the $NaNO_2$ side) gives the composition of solutions from which the crystalline nitrite separates out upon cooling; the right-hand branch applies to solutions saturated with the nitrate. The isotherms in both figures differ in the percentage of Na_2CO_3 in the solution.

The top isotherm in each diagram represents the case where the solutions of $NaNO_2$ and $NaNO_3$ contain no soda. In plotting these isotherms, we had at our disposal; first, the handbook data [1] on the solubilities in the $NaNO_2 - NaNO_3 - H_2O$ system at 0, 21, and 52°, from which we obtained the data for the temperatures we were interested in by interpolation; and second, the data we had obtained experimentally by measuring the solubilities. The two sets of figures were in good agreement with each other.

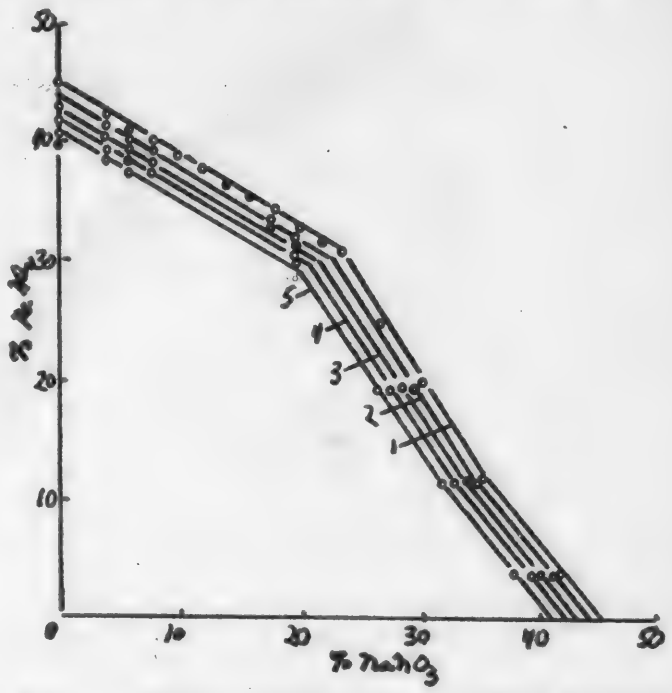

Fig. 3. Mutual solubility of sodium nitrite and nitrate in water when soda is present. Temperature: +15° C.

% in solution: 1-0; 2-1; 3-2; 4-3; 5-4.

The remaining isotherms (Figs. 3 and 4) represent different percentages of soda in the solutions:, 1, 2, 3, and 4% of Na_2CO_3. We see that the equilibrium concentrations of the nitrite (left-hand branch) and the nitrate (right-hand branch) diminish as the percentage of soda in the solution rises.

These figures were obtained by preparing 49 solutions containing different proportions of $NaNO_2$ and $NaNO_3$. The saturation temperatures of these solutions was determined, after which small quantities of Na_2CO_3 were added to them and the equilibrium temperature read off visually in each case. This enabled us to plot a polythermal curve, exhibiting the effect of adding Na_2CO_3 upon the saturation temperature, for each of the original solutions. We thus plotted 49 experimental polytherms, which resembled those shown in Fig. 1. Of this total, 37 represented the area of crystallization of $NaNO_2$, the others representing the crystallization area of the nitrate.

As we know, the graphical representation of the equilibria in four-component systems is very difficult. From the practical standpoint, we are merely interested, however, in solutions whose bottom phase consists of the nitrate or the nitrite or whose bottom-phase is an isothermal invariant mixture (i.e., solutions that are not saturated with soda). Therefore, to make use of the graphs easier, we expressed the influence of Na_2CO_3 by plotting several isotherms in a row, the isotherms differing in the percent of Na_2CO_3 in the solution (1, 2, 3, and 4%). We did this by making use of our experimental polytherms and determining the compositions of the $NaNO_2 + NaNO_3$ solutions that are saturated

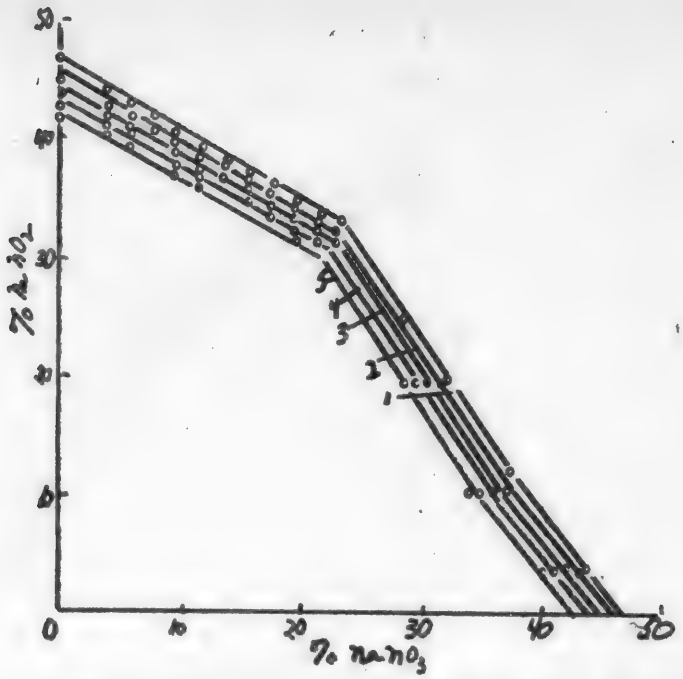

Fig. 4. Mutual solubility of sodium nitrite and nitrate in water when soda is present. Temp. = 230°.

% in solution: 1-0; 2-1; 3-2; 4-3; 5-4.

with the nitrite or the nitrate at the given temperature (15 or 25°) and at each given Na_2CO_3 concentration. A series of auxiliary curves was plotted to facilitate this treatment of the experimental material by making it possible to find the desired values by means of graphic interpolation; these data were then employed to plot the isotherms in Figs. 3 and 4.

SUMMARY

The solubility of $NaNO_2$ and $NaNO_2$ + $NaNO_3$ in water when Na_2CO_3 is present has been investigated by the polythermal method. Solubility isotherms of the $NaNO_2$ – Na_2CO_3 – H_2O system have been plotted at 10-30° for the concentration range in which the bottom phase consists of the nitrite. Isotherms have been plotted for the temperature range 15-25°, representing the effect of the Na_2CO_3 concentration in the solution (1-4%) upon the mutual solubility of $NaNO_2$ and $NaNO_3$ in water.

LITERATURE CITED

[1] Technical Encyclopedia, Handbook, VII, 105 (1936).

[2] V.F.Alekseev, J. Russ. Phys.Chem.Soc, 1877, 208.

[3] V.I.Atroschenko, J. Chem. Ind., 1, 26, (1938).

[4] V.I.Atroschenko and S.I.Kargin. The Technology of Nitric Acid, 160. State Chemical Press (1949).

[5] J. Bureau, Ann. Chim., 8, 97-142 (1937).

Received April 26, 1950.

THE SOLUBILITY OF NAPHTHALENE IN COAL-TAR OILS

M. M. Potashnikov

As we know, the extraction of naphthalene from coal tar products is based upon crystallization, distillation, and pressing processes. The crystallized oil, the distillate, and the pressing product secured as the result of these processes constitute coal-tar oils that are saturated with naphthalene at these process temperatures. We therefore have to know the solubility of naphthalene in coal-tar oils at various temperatures for design purposes as well as for the establishment of the optimum operating conditions in industry.

There is extremely little to be found in the literature on the solubility of naphthalene in coal-tar oils. The reference literature [1] cites figures secured by German researchers in 1923, which cover only a limited temperature range, 0 to 40°C, on the one hand, and are not of much use, on the other, since they were based upon the coal-tar oils secured from German plants, which differ, as we know, from our domestic coal-tar oils.

The present research aimed at determining the solubility of naphthalene in light-middle and heavy (absorbing) oils, produced from the coal tar of domestic by-product coke plants, at temperatures ranging from 0 to 75°C.

EXPERIMENTAL

The solubility of naphthalene was determined in the instrument depicted in Fig. 1. Pure naphthalene and the oil under test were placed in the beaker 1, which was immersed in beaker 2, filled with water, the latter in turn being immersed in a water bath 3 that was heated electrically. The water bath was heated gradually, being regulated in such a fashion that the change in temperature of the contents of beaker 1 and of the water in beaker 2 was about 1°C in 3 minutes, as measured by the thermometers 4.

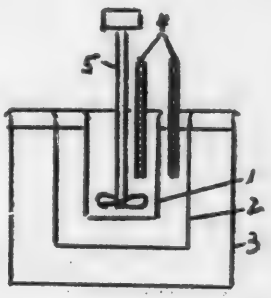

Fig. 1. Device for determining the solubility of naphthalene.

1-Beaker; 2-beaker containing water; 3. water bath; 4-thermometers; 5-stirrer.

The oil-naphthalene mixture was vigorously stirred by the stirrer 5, new batches of naphthalene or oil being added as the mixture was heated or cooled, so that neither of the phases was allowed to disappear – the solid during heating and the liquid during cooling. The combination of gradual change of temperature and vigorous stirring of the oil and naphthalene made it possible to attain a state of equilibrium rather quickly.

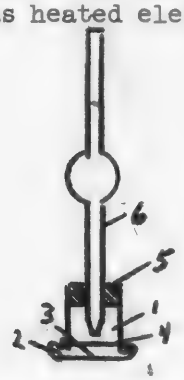

Fig. 2. Filtering Device.

1-Glass cylinder; 2-bent edge of cylinder; 3-filter; 4-thread; 5-stopper; 6-pipet.

The rate at which a state of equilibrium was reached was determined by keeping the oil-naphthalene mixture at a given temperature and taking samples of the liquid phase at short intervals of time (1-2 minutes), the per cent naphthalene in these samples being determined. Equilibrium was reached when the concentration of naphthalene in successive samples of the liquid phase ceased to rise.

It was found that the oil is saturated with naphthalene fairly rapidly – within 3 to 8 minutes – at various temperatures lying within the 0 - 75°C range. The oil-naphthalene mixture was kept at the given temperature for 15 minutes in all of these tests in order to ensure reliable results.

A Mohr pipet was used in taking samples of the liquid phase: oil saturated with naphthalene.

To prevent the capture of finely dispersed particles of naphthalene, produced during vigorous stirring, the tip of the pipet, which was immersed in the liquid, was fitted with a special filtering device, depicted in Fig. 2. This device consisted of a glass cylinder 1, the lower edge 2 of which was bent outward and covered with a filter 3 made of dense filter paper, secured by a thread 4 tied over the bent edge of the cylinder. The cylinder was mounted on the pipet 6 by means of a tight stopper 5 that sealed off the upper opening of the cylinder.

When the oil saturated with naphthalene was drawn up into the pipet, it was filtered through the filter paper, keeping out the minute particles of naphthalene.

After the sample had been taken, the filter device was removed from the pipet, washed with benzene, and dried for use in subsequent determinations, while the contents of the pipet were warmed up and transferred to a tared beaker for determining the amount of naphthalene in the oil.

The naphthalene concentration was determined by the usual method: from the crystallization temperature of a mixture consisting of a weighed amount of the unknown oil and a weighed amount of pure naphthalene in a Zhukov apparatus [2]. The concentration of naphthalene in the oil under test was determined from the crystallization temperature.

In our investigation we used light-middle and heavy (absorbing) oils derived from coal tar secured from one of the tar-treating installations of a by-product coke plant. The phenols were removed from these oils by washing them with 20% NaOH, the organic bases being removed by washing them with 30% H_2SO_4.

The oils used in this investigation had the following properties after the phenols and the bases had been removed and the oils had been desiccated.

		Light-middle Oil	Heavy (absorbing) Oil
Specific gravity at 20°C		1.027	1.051
Temp., °C, at which boiling begins .		195	224
Distillation temperature, °C	10%.....	209	233
	20	215	236
	30	217	238
	40	219	241
	50	222	245
	60	226	250
	70	231	259
	80	239	269
	90	251	285
	95	267	306

The tests were run at temperatures spaced 5° apart in the 0-75°C range. Stops were made at these temperatures at which equilibrium of the oil and the naphthalene was reached, samples of the liquid phase being taken, as the mixture temperature was successively raised from 0 to 75°C and as it was successively cooled from 75 to 0°C. Naphthalene was added in the first series of tests, as the temperature was raised, while oil was added in the second series of tests as the mixture cooled.

The data on the solubility of naphthalene secured in these tests are listed in the table.

TABLE

Temp. °C	Solubility of naphthalene, % by weight			
	In light middle oil		In heavy (absorbing) oil	
	During heating	During cooling	During heating	During cooling
0	9.99	9.81	9.60	9.80
5	12.50	12.37	11.12	11.56
10	14.65	15.25	13.88	14.12
15	16.87	17.22	17.16	17.33
20	20.65	20.20	20.00	19.66
25	22.68	22.91	22.83	24.20
30	26.23	27.02	28.92	29.54
35	29.74	29.70	31.94	32.02
40	33.33	34.02	36.02	36.97
45	37.20	37.75	42.53	42.48
50	42.56	43.38	47.96	48.80
55	48.80	47.98	54.81	54.30
60	60.27	60.40	61.60	60.82
65	71.19	70.83	69.30	70.49
70	80.32	79.44	79.27	79.66
75	90.02	90.47	91.66	91.37

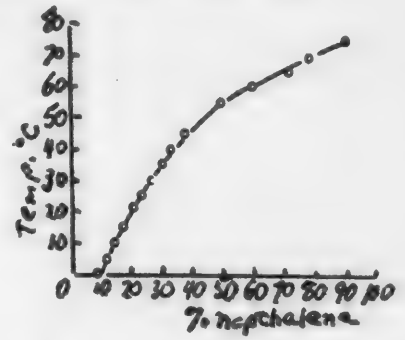

Fig. 3. Solubility of naphthalene in light-middle oil as a function of the temperature.

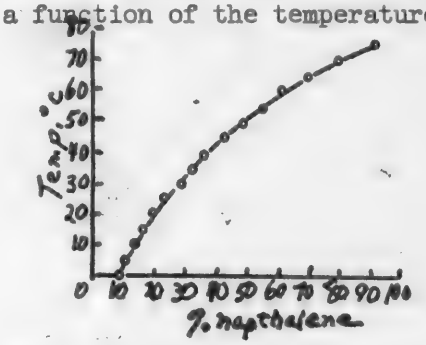

Fig. 4. Solubility of naphthalene in heavy (absorbing) oil as a function of the temperature.

The experimental values fit the curves plotted in Figs. 3 and 4. Comparison of these data indicates that the solubility of naphthalene in light-middle oil is pretty much the same as that in heavy (absorbing) oil in the 0-25°C and 60-75°C temperature ranges.

The solubility of naphthalene in the heavy oil is higher than in the light-middle oil in the 25-60°C range.

The shape of these curves indicates that solutions of naphthalene in light-middle and heavy oils are not ideal solutions. The solubility rises markedly above 55°C.

SUMMARY

1. A study has been made of the solubility of naphthalene in light-middle and heavy (absorbing) oils secured from coal tar.

2. It has been found that the solubility of naphthalene is about the same in both oils in the 0-25° and 60-75°C temperature ranges.

3. Solutions of naphthalene in light-middle and heavy oils are not ideal ones. The naphthalene solubility rises particularly rapidly above 55°C.

LITERATURE CITED

[1] Coke-Chemistry Handbook, IV, United State Scientific and Technical Press (1939).

[2] L.D.Gluzman and I.I.Edelman. Supervision of Coke By-Product Production, 322-324. Metallurgical Press (1946).

Received April 13, 1950.

THE SATURATION VAPOR PRESSURES OF β-PICOLINE, γ-PICOLINE, AND 2,6-LUTIDINE

I. L. Liplavk and E. P. Boliter

One of the products of the by-product coke industry, the β-picoline fraction, contains three major substances: β-picoline, γ-picoline, and 2,6-lutidine.

The recovery of these products from the β-picoline fraction is an extremely difficult task, owing to the proximity of the boiling points of these substances: β-picoline b.p. = 143.2°; γ-picoline b.p. = 145°; and 2,6-lutidine b.p. = 144.6°.

Hence, rectification under normal conditions cannot be employed to separate the β-picoline fraction into more highly enriched fractions. The absence of any data on the vapor pressures of these components makes it impossible to fix the conditions under which rectification of this product might be improved.

That is why the major objective of the research reported on in this paper has been determination of the saturation vapor pressures of β-picoline, γ-picoline, and 2,6-lutidine at various temperatures. It is apparent that this research is required for solving the practical problems facing the coke by-product industry. Moreover, the results obtained are of scientific interest as well, since there are no figures on the saturation vapor pressures of these compounds in the scientific, technical, or reference literature at the present time.

EXPERIMENTAL

Recovery of β-picoline, γ-picoline, and 2,6-lutidine. Pure substances were required for securing reliable data on their saturation vapor pressures. As we know, it is impossible to secure them synthetically, inasmuch as the presently available syntheses yield mixtures of all these substances at once, and it is as difficult to separate them as it is in the industrial β-picoline fraction.

Making use of the fact that these substances have radically different temperatures of crystallization: -21.2° for β-picoline; +3.2° for γ-picoline; and -6.5° for 2,6-lutidine, we resorted to the method of fractional crystallization. We first ascertained the general nature of the structural diagram, composition vs. crystallization temperature, for the mixture being tested. Since we had no pure substances available, this diagram was plotted indirectly, without definite data on concentrations, from the fractionation of the β-picoline fraction, tapping off one-degree fractions. But, in view of the fact that direct fractionation of the β-picoline fraction does not yield enriched intermediate fractions, we fractionated the hydrochlorides of the β-picoline fraction. We know from the literature [1] that the boiling point of β-picoline hydrochloride is 233°, that of γ-picoline hydrochloride is 240°, and that of 2,6-lutidine hydrochloride

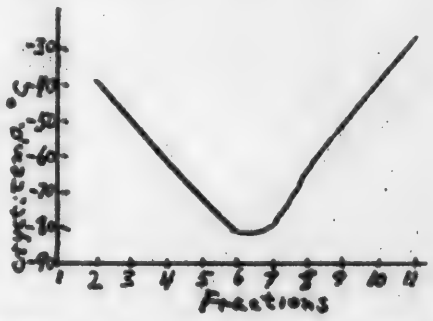

Fig. 1. Crystallization temperature of one-degree intermediate fractions.

is 245°. These differences in the boiling points of the salts enabled us to obtain intermediate fractions enriched with one component or another in a rectifying column with an efficiency of 16 theoretical trays.

The intermediate fractions were tapped off at one-degree intervals, after which the fractions were decomposed with alkali and the resulting bases carefully desiccated and distilled. The figures on the crystallization temperatures of the intermediate fractions exhibit a well-defined minimum when passing from intermediate fractions enriched with β-picoline to those enriched with γ-picoline (Fig. 1).

Thus, separation of one of the components of the mixture in question by means of fractional crystallization required that the concentration of the components not be that of the minimum. The authors were unable to compute this concentration or to determine it experimentally: all they could do was to adopt the premise that fractions as highly enriched as possible had to be employed for fractional crystallization.

The fraction enriched with 2,6-lutidine was secured from the β-picoline fraction by precipitating the latter with urea and repeatedly recrystallizing the resultant coordination compound of 2,6-lutidineurea [2]. The resulting 2,6-lutidine had a crystallization temperature of -11°.

An enriched fraction of γ-picoline was secured from the same β-picoline fraction which was freed of its 2,6-lutidine by precipitating the γ-picoline with calcium chloride. This method [3] makes use of calcium chloride's property of forming a complex salt with γ-picoline alone. After the 2,6-lutidine and the γ-picoline had been separated from the β-picoline fraction, the residue contained a base enriched with β-picoline.

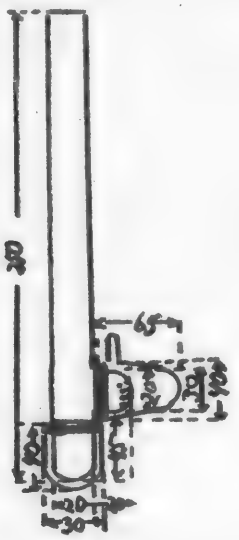

Fig. 2. Device for fractionally crystallizing the unknown mixture.

Fractional crystallization was carried out in a device (Fig. 2), consisting of a test tube with a side bulge, the spherical surface of which contained numerous tiny openings. The bottom of the test tube was covered with a glass housing to ensure uniform cooling. The lateral bulge was also covered with a housing connected to a vacuum pump in order to remove the crystals from the solution. The liquid was poured into the test tube, and a thermometer was inserted through the stopper. The liquid was stirred with the thermometer. Temperature discontinuties and arrest points indicated the onset of crystallization. As the temperature was lowered still further, the device was taken out of the freezing mixture, and the crystals were brushed toward the side bulge by means of a tiny glass spatula. The vacuum pump was turned on at the same time, and the crystals were filtered out.

Each successive operation raised the crystallization temperature, at first by 2-3°, and then by 1° or less. The crystallization temperature of the fraction enriched with 2,6-lutidine was thus raised to -6.5°. Further crystallization did not produce any change in the crystallization temp., the freezing point of the filter and the residue remaining the same, i.e., -6.5°. The constants of the resulting substance are given in Table 1.

As a rule, the purity of substances recovered from coal-tar bases is measured by the melting points of their salts – picrates, chloromercurates, etc. But theoretical considerations, as well as the accumulated experience of analysis of

the bases compelled us to abandon this method as inadequate. We used, instead, another method, involving the determination of all the physical properties, principally the crystallization temperature of the substance itself, and in plotting time – crystallization temperature curves of the resulting substances. The existence of a plateau on the cooling curve (Figs. 3, 4, and 5), together with the totality of physical properties listed in Table 1, which agree with the data cited in the literature, indicated that the prepared substances were wholly pure.

TABLE 1

Physical Properties of 2,6-Lutidine, β-Picoline, and γ-Picoline

Name	Specific gravity at 20°C	Refractive index at 20°C	Boiling point, corrected to 760 mm	Crystallization temperature, °C
2,6-Lutidine...	0.9150	1.4996 (at 16° C)	144.7	-6.5
γ-Picoline.....	0.9572	1.5052	145.0	+3.0
β-Picoline.....	0.9520	1.5040	143.2	-21.2

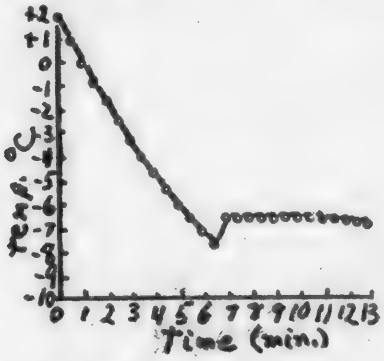

Fig. 3. Crystallization cooling curve of 2,6-lutadine.

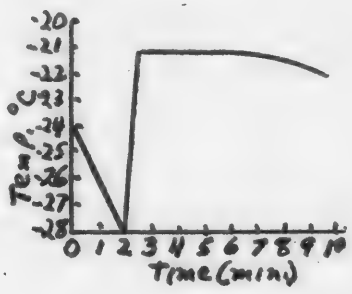

Fig. 4. Crystallization cooling curve of β-Picoline.

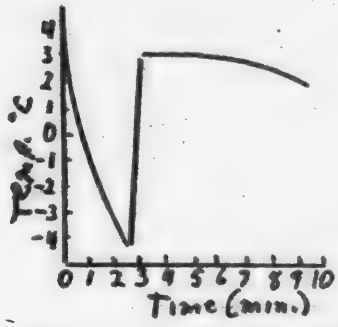

Fig. 5. Crystallization cooling curve of γ-picoline.

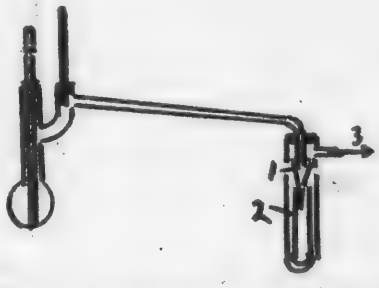

Fig. 7. Apparatus layout for vacuum distillation.

1-Funnel; 2-ampoule; 3-branch tube to vacuum pump.

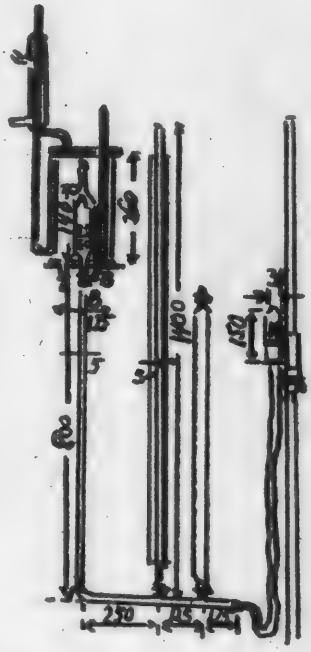

Fig. 6. Device for determining the saturation vapor pressure of β- and γ-picolines and 2,6-lutidine.

A-Measuring vessel; B-side branch; K-mercury container.

Determining the saturation vapor pressures of β- and γ-picolines and 2,6-lutidine. The vapor pressures were determined by the static method in a Sorell-NATI apparatus [5], largely modified by the present authors. These modifications enabled us to measure the vapor pressure with an accuracy of 0.01 mm mercury

column. The apparatus layout is shown in Fig. 6.

The principal element of the apparatus is the measuring vessel A, which is provided with a side branch tube B. The top terminates in a neck with a ground-glass stopper. The bottom of the vessel is connected to the side branch via a three-way stopcock, which, in turn, is connected to a manometer, a buret, and an open movable container for mercury K. The measuring vessel is placed in a closed bath with two windows on opposite sides. The temperature of the bath was kept constant by boiling a suitable liquid in it.

The whole apparatus was filled with chemically pure mercury. The measuring vessel was filled from an ampoule, thus ensuring a complete vacuum in the measuring vessel and eliminating any contact with the air, which might moisten the substance under test. In practice, the measuring vessel was filled as follows: the substance under test was placed in a small flask, from which it was distilled directly into the ampoule at a vacuum of 2-3 mm (Fig. 7). The ampoule was a flask with a capacity of 5-7 cm^3, with an elongated neck and a flat bottom; there were several projections in its walls, by means of which the ampoule was held in the neck of the measuring vessel. Figure 8 shows the position of the ampoule in the measuring vessel. When the ampoule was half full, the heating of the distilling flask was stopped, and the substance was allowed to solidify under the same vacuum. Then the vacuum was disconnected, the ampoule was filled to the top with mercury, and it was again placed under vacuum. This was done to remove any air adsorbed to the mercury, especially at the mercury-test liquid boundary.

Fig. 8. Measuring vessel with ampoule (A).

After all the air had been removed, the vacuum was turned off, and the ampoule was turned upside down. The mercury did not pour out of the ampoule, but formed a reliable seal, owing to the small diameter of the ampoule's neck (3 mm), on the one hand, and the high surface tension of mercury, on the other. While in this position, i.e., neck downward, the ampoule was immersed in the mercury within the measuring vessel. Then the ampoule was completely buried in the mercury by closing the top stopper, the ground-glass surface of which had been coated with vacuum grease; closing of the measuring vessel forced some of the mercury out. Lowering the movable container K lowered the level of the mercury in the measuring vessel, and the resulting vacuum caused the liquid to flow out of the ampoule. Then the measurements were made as in the Sorrell - NATI apparatus. The level in tube B was read off with a cathetometer; the reading on the manometer scale was likewise made with a cathetometer. The overall precision of measurement was 0.01 mm Hg. But we reduced the precision of measurement to 0.1 mm mercury column because the bath temperature was determined to within 0.1°.

Table 2 gives the saturation vapor pressures of β-picoline, γ-picoline, and 2,6-lutidine at various temperatures.

The curves of the change in the saturation vapor pressures of β-picoline, γ-picoline, and 2,6-lutidine are depicted in Fig. 9.

The general nature of the variation of the saturation vapor pressures of the substances under test with temperature conforms to the Clausius-Clapeyron equation, since this function is represented by straight lines when plotted on semilogarithmic paper, as shown in Fig. 10.

We see from the curves in Fig. 9 that the vapor pressures of β-picoline

TABLE 2

Saturation Vapor Pressures of β-Picoline, γ-Picoline, and 2,6-Lutidine in mm of Mercury as a Function of the Temperature.

2,6-Lutidine		γ-Picoline		β-Picoline	
Temp., °C	Vapor pressure	Temp., °C	Vapor pressure	Temp., °C	Vapor pressure
17.0	11.6	15.8	14.8	15.5	13.0
56.6	56.0	64.7	80.1	64.6	77.0
64.6	85.3	78.2	109.5	72.2	107.2
78.9	147.7	108.4	227.8	106.6	256.4
108.9	416.6	135.3	590.8	133.5	622.6

and γ-picoline are in close proximity throughout the temperature range investigated. Their vapor pressures differ widely, however, from that of 2,6-lutidine, especially in the 70-130° range. It is in this same temperature range that the vapor pressures of β-picoline and γ-picoline diverge most.

Hence, our data indicate that the most efficient way of separating the β-picoline fraction is to fractionate it at reduced pressures of the order of 200-300 mm. These conditions are most effective for the recovery of 2,6-lutidine, since the difference between its boiling point and those of the picolines is then 20°.

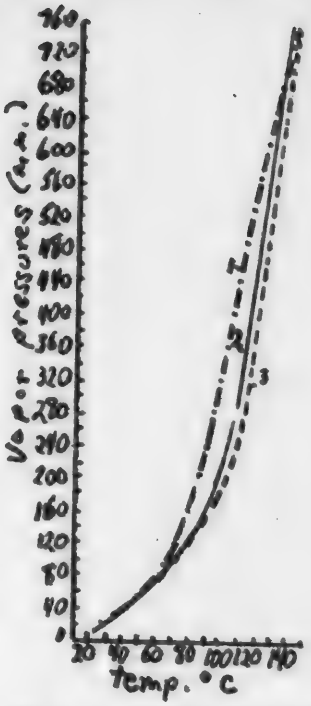

Fig. 9. Vapor pressure as a function of temperature.
1-2,6-Lutidine; 2-β-picoline; 3-γ-picoline.

Fig. 10. Vapor pressures of β-picoline and -picoline as a function of temperature.
1-β-picoline; 2-γ-picoline.

SUMMARY

1. Data on the saturation vapor pressures of β-picoline, γ-picoline, and 2,6-lutidine, which have not been available in the scientific, technical, or reference literature up to the present, have been secured for the first time.

2. The feasibility of separating the β-picoline fraction industrially by low-pressure rectification has been demonstrated.

LITERATURE CITED

[1] Chem. Abs. 612⁷ (1946).
[2] G.Rietnof, U.S., 2, 376, May 15 (1945).
[3] F.E.Reimers, U.S., 2, 366, 502, Dec. 14 (1943).
[4] Riethof, Richards, Savitt, Othmer, Ind. Eng. Chem., Anal. Ed., 18, 458 (1946).
[5] M.M.Kusakov. Methods of Determining the Physical and Chemical Characteristics of Petroleum Products, 309. United Scientific and Technical Press. (1936).

Received April 2, 1950

THE EFFECT OF THE CONCENTRATION OF ACIDS UPON THEIR ATTACKING CARBON STEELS

S. A. Balezin and T. I. Krasovitskaya

We know that the rate with which steel dissolves in sulfuric acid rises with increasing concentration of the acid up to a certain value, after which it drops off sharply. The maximum corrosion effect occurs with 11-14 N acid. All the tested steels become passive in an acid of higher than 17 N normality. The "dissolution rate vs. nitric-acid concentration" curve exhibits a maximum like the curve for sulfuric acid. The rate of corrosion of carbon steels in hydrochloric acid rises continuously though not evenly with a rise in the latter's concentration – slowly at low concentrations (0.5-4 N) and rapidly later on (4-7 N).

But the only research that has been done on the practically important problem of the quantitative relationship between acid concentrations and acid attack has been confined to sulfuric acid, and the figures cited by Ram [1] and Novikov [2] – the only researchers in the field – do not agree.

Ram found that the relationship he had determined between the rate of dissolution and the concentration of sulfuric acid could be represented by the formula:

$$\rho = K\left(\frac{a^n}{\eta}\right),$$

where ρ is the rate at which the steel dissolves; a is the activity of the acid, computed for each acid concentration separately by means of the activity coefficient, in accordance with the Lewis and Rendall theory [3]; η is the relative viscosity of the acid solutions; and K and n are constants.

Novikov [2], making a study of more dilute acid solutions, found that Ram's equation did not apply to H_2SO_4 solutions with a concentration below 3 N, and proved that it was theoretically unfounded, demonstrating that the viscosity of acid solutions does not affect their ability to attack a metal. Novikov's own experimental data led him to propose a different equation, relating the rate at which steel is dissolved (ρ) to the activity of the sulfuric acid (a):

$$\rho = Ka^{2/3},$$

which holds good over a wide concentration range.

It has been the aim of the present research to check the Novikov formula derived by him for sulfuric acid, and to endeavor to establish quantitative relationships between the activity and the attack of other acids.

EXPERIMENTAL

In the present paper 8 grades of steel, of different carbon content, have been tested. The data of their analyses are listed in Table 1.

The steels were exposed to the action of chemically pure sulfuric, hydrochloric, and acetic acids. The gravimetric method of analysis was used. The results are given in Table 2 and in Figs. 1, 2, and 3.

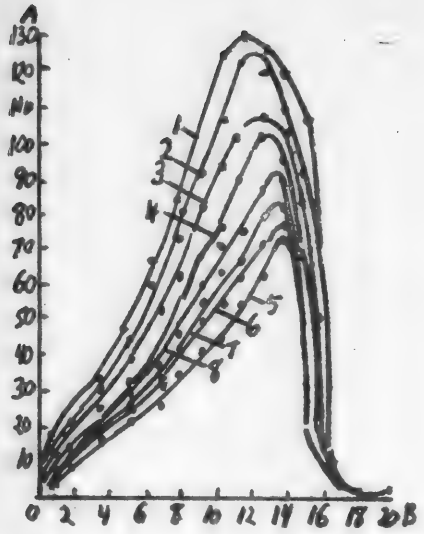

Fig. 1. Rate at which steels dissolve as a function of the H_2SO_4 concentration.

A-Rate of corrosion, grams/m^2/hr; B-normality of the acid.

% carbon in the steel: 1-0.9; 2-0.78; 3-0.6; 4-0.45; 5-0.05; 6-0.1; 7-0.19; 8-0.32.

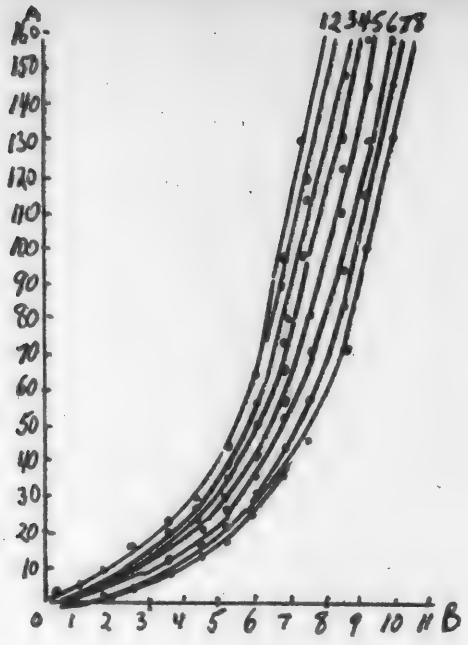

Fig. 2. Rate at which steels dissolve as a function of the HCl concentration.

A-Rate of corrosion, grams/m^2/hr; B-normality of the acid.

% carbon in the steel: 1-0.9; 2-0.78; 3-0.6; 4-0.45; 5-0.32; 6-0.19; 7-0.1; 8-0.05.

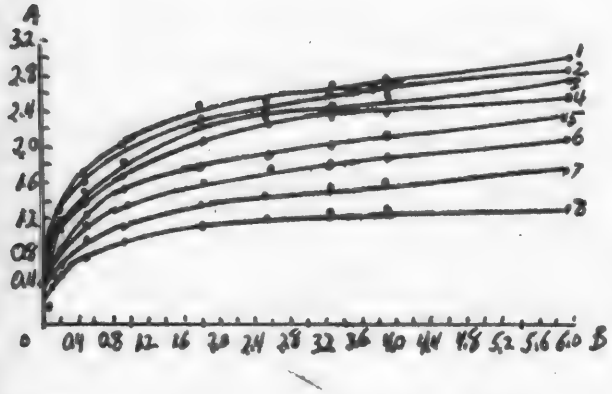

Fig. 3. Rate at which steels dissolve as a function of the CH_3COOH concentration.

A-Rate of corrosion, grams/m^2/hr; B-normality of the acid.

% carbon in the steel: 1-0.9; 2-0.78; 3-0.6; 4-0.45; 5-0.32; 6-0.19; 7-0.1; 8-0.05.

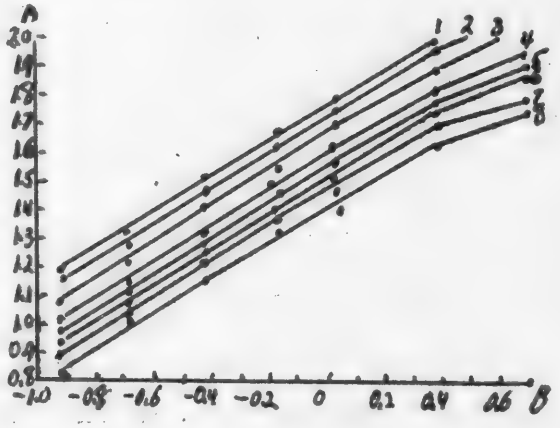

Fig. 4. Logarithm of the rate of steel dissolution as a function of the logarithm of H_2SO_4 activity.

A-Logarithm of the corrosion rate; B-logarithm of activity. % carbon in the steel: 1-0.9; 2-0.78; 3-0.6; 4-0.45; 5-0.32; 6-0.19; 7-0.1; 8-0.05.

TABLE 1

Analysis Data of the Tested Steels

Grade of steel	Per cent (by analysis)					
	C	Si	Mn	P	S	Cu
1	0.05	0.14	0.49	0.030	0.025	0.24
2	0.1	0.17	0.46	0.030	0.027	0.21
3	0.19	0.19	0.40	0.032	0.029	0.28
4	0.32	0.21	0.39	0.032	0.028	0.24
5	0.45	0.25	0.42	0.034	0.027	0.27
6	0.6	0.23	0.44	0.030	0.025	0.30
7	0.18	0.24	0.43	0.029	0.023	0.22
8	0.9	0.18	0.38	0.027	0.030	0.25

TABLE 2

Rate at which Steels Dissolve in Various Acid Solutions (in Grams/M_2/Hr)

Acid	Acid concentration	Per cent carbon in steel							
		0.05	0.1	0.19	0.30	0.45	0.60	0.78	0.90
Sulfuric ..	0.975	6.66	8.33	9.10	9.10	10.6	11.5	14.2	16.3
	1.905	9.50	9.95	12.1	12.8	13.9	17.2	20.2	21.1
	3.63	16.3	17.1	18.8	18.8	22.4	26.0	29.8	32.5
	5.22	21.0	25.0	27.5	29.2	30.2	39.2	43.9	46.0
	6.67	27.2	31.0	36.1	37.4	41.0	53.8	59.0	60.0
	8.00	36.2	44.5	46.6	49.9	60.7	72.5	79.1	83.0
	9.25	41.0	50.2	52.7	60.4	67.9	81.6	91.0	101.0
	10.4	46.6	56.2	62.3	69.7	77.3	93.0	107.4	125.0
Hydrochloric	3.68	8.60	9.41	10.8	13.0	16.8	19.0	20.2	22.5
	4.36	12.5	14.1	16.3	19.6	24.3	27.1	29.8	30.3
	5.32	17.0	20.0	23.6	27.6	35.0	39.9	43.2	45.1
	6.10	24.8	26.4	43.7	41.9	50.7	57.8	63.3	64.5
	6.87	38.0	39.8	50.3	56.6	71.0	67.7	91.2	94.1
	7.25	58.7	64.0	71.0	81.6	98.0	114	119	127
	8.50	72.8	87.4	95.5	109.0	131	148	168	174
	9.22	101	114	130	160	179	212	253	278
	9.90	130	146	155	190	231	253	278	309
	10.46	163	170	180	240	315	330	380	430
	10.85	190	247	264	289	356	399	449	516
Acetic	0.01	0.110	0.134	0.163	0.181	0.212	0.252	5.261	0.272
	0.02	0.172	0.209	0.250	0.282	0.314	0.334	0.346	0.355
	0.05	0.301	0.463	0.612	0.694	0.761	0.798	0.835	0.931
	0.10	0.425	0.551	0.700	0.821	0.880	0.987	1.010	1.035
	0.198	0.573	0.700	0.842	0.957	1.03	1.08	1.14	1.19
	0.486	0.750	0.910	1.09	1.23	1.37	1.46	1.52	1.55
	0.945	0.921	1.11	1.34	1.50	1.66	1.78	1.81	1.90
	1.80	1.08	1.32	1.56	1.78	2.00	2.14	2.21	2.28
	2.55	1.18	1.45	1.73	1.96	2.20	2.35	2.40	2.52
	3.27	1.25	1.55	1.94	2.05	2.33	2.50	2.58	2.66

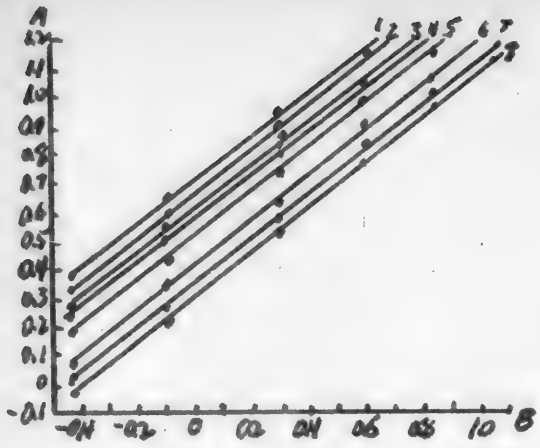

Fig. 5. Logarithm of the rate of steel dissolution as a function of the logarithm of HCl activity (activities corresponding to concentrations ranging from 0.5 to 4 mols per liter H_2O).

A-Logarithm of the corrosion rate; B-Logarithm of activity. % carbon in the steel: 1-0.9; 2-0.78; 3-0.6; 4-0.45; 5-0.32; 6-0.19; 7-0.1; 8-0.05.

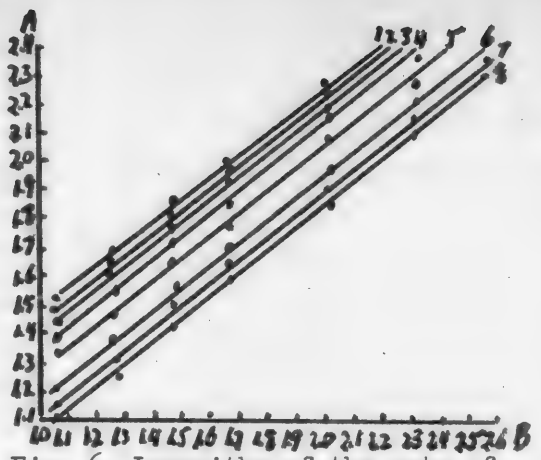

Fig. 6. Logarithm of the rate of steel dissolution as a function of the logarithm of HCl activity (activities corresponding to concentrations ranging from 5 to 14 mols per liter H_2O).

A-Logarithm of the corrosion rate; B-logarithm of activity. % carbon in the steel: 1-0.9; 2-0.78; 3-0.6; 4-0.45; 5-0.32; 6-0.19; 7-0.1; 8-0.05.

These results fully agree with those cited in the literature, as far as sulfuric and hydrochloric acids are concerned. There are no such data in the literature for acetic acid.

Figures 4, 5, 6, and 7 depict the relationship between the logarithms of acid activity and the logarithms of the rate of steel dissolution.

The fact that the relationship between the activity logarithms and the logarithms of the corrosion rate is expressed as a straight line for all the acids tested proves that the following formula is correct:

$$\rho = K \cdot a^n,$$

where ρ is the rate of steel corrosion; a is the acid activity; and K and n are constants.

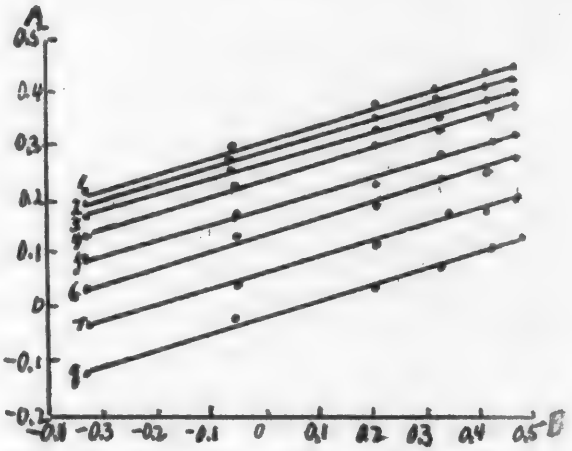

Fig. 7. Logarithm of the rate of steel dissolution as a function of the logarithm of CH_3COOH activity.

A-Logarithm of the corrosion rate; B-logarithm of activity. % carbon in the steel: 1-0.9; 2-0.78; 3-0.6; 4-0.45; 5-0.32; 6-0.19; 7-0.1; 8-0.05.

The observed drop in the values of the rate of steel corrosion from the formula values for sulfuric acid at concentrations above 9.25 N (Table 2, Fig. 4) is evidently due to the appearance at this concentration of the factors that lead to passivation of steels in the acid as the latter's concentration continues to rise.

The fact that the "log a - log ρ" straight lines are all parallel for the same acid is evidence that the constant n does not depend on the grade of steel. The value of the constant n was found from the tangent of the slope of the

"log $\underline{a}$ – log ρ" straight lines. The value of $\underline{n}$ is 0.67 for sulfuric acid, which demonstrates that Novikov's formula $\rho = K \cdot a^{2/3}$ holds good for all the grades of steel tested. We used our experimental data to calculate the values of $\underline{n}$ for hydrochloric and acetic acids, $\underline{n}$ being found to equal 0.85 for hydrochloric acid and 0.33 for acetic acid.

Hence, the value of $\underline{n}$ is a characteristic of the acid. Knowledge of this constant is of considerable practical importance, as it enables one to compute the rate at which steel dissolves at any activity, provided the value of the constant $\underline{K}$ has been determined experimentally.

The value of the constant $\underline{K}$ depends upon the nature of the acid and upon the composition of the steel. The value of this constant is given by the intercepts of the "log $\underline{a}$ – log ρ" straight lines on the axis of ordinates.

When steels are dissolved in sulfuric acid, the coefficient $\underline{K}$ rises from 25.39 to 53.5 with a rising % C in the steel (which corresponds to a change in the value of log $\underline{K}$ from 1.415 to 1.767).

When steels are dissolved in hydrochloric acid, the coefficient $\underline{K}$ rises from 1.88 to 4.59 with a rising % C in the steel (log $\underline{K}$ varies from 0.276 to 0.667).

When steels are dissolved in acetic acid, the coefficient $\underline{K}$ rises from 1.08 to 1.93 with a rising % C (log $\underline{K}$ varies from 0.033 to 0.285).

The way in which the constant $\underline{K}$ varies with changes in the % C in the steel is understandable. Indeed, as Krasovitskaya has shown, the rate of dissolution of carbon steels at a single concentration of sulfuric, hydrochloric, or acetic acid rises uninterruptedly with a rising % C in the steel.

It follows from the formula $\rho = K \cdot a^n$ that $\underline{K}$ is simply the dissolution rate of steel in an acid solution whose activity ($\underline{a}$) equals one.

SUMMARY

Investigation of the rate of dissolution of eight grades of steel, of different carbon content, in sulfuric, hydrochloric, and acetic acids of various concentrations has shown that the activity of sulfuric, hydrochloric, and acetic acids ($\underline{a}$) is related to their rate of attack of carbon steels throughout a wide concentration range by the general formula:

$$\rho = K \cdot a^n ,$$

where $\underline{K}$ and $\underline{n}$ are constants. For sulfuric acid the value of $\underline{n}$ is 0.67; for hydrochloric acid, $\underline{n}$ = 0.85; and for acetic acid, $\underline{n}$ = 0.33.

LITERATURE CITED

[1] S. Ram, Isom.Soc.Chem.Cud, 54, 107 (1935).

[2] S.K.Novikov, Sci. Rep., Lenin State Polytech. Inst., Moscow, 44, 42 (1947).

[3] Lewis and Rendall, J. Am. Chem. Soc., 43, 1112 (1921).

Received March 24, 1950.

DOUBLE SUBSTITUTIONS OF METHYL KETONES IN FURFURYLIDENE KETONES

V. I. Tikhonova

Chair of General Chemistry, Saratov State Institute of Medicine

In the study of the reactivity of various organic compounds, several investigations have been made of the double substitutions involving carbonyl compounds. The first papers in this field were those by Chelintsev and Nikitin [1] on the reactions involving double substitutions of aldehydes in the condensation products with acetone. They showed that the aliphatic aldehydes displace furfural, while furfural itself displaces aromatic aldehydes. The difference between the activity of the aldehydes in these reactions is quite considerable: furfural, for example, is five times as active as benzaldehyde, while the differences between other aldehydes is even greater [2].

Thereafter, a number of research workers established processes involving the double displacement of ketones from hydrazones, semicarbazones, and bisulfite compounds. Neuberg and Collatz, for example, have described their observations of the displacement of some ketones by others from their hydrazones [3]. But the literature contains no description of the double substitution of ketones in their condensation products with aldehydes.

We endeavored to effect the double substitution of ketones in their condensation products with furfural. We used acetone, methyl ethyl ketone, methyl propyl ketone, and acetophenone in these reactions.

There is not much difference between the activities of these methyl ketones in this reaction. Their relative activities are as follows:

Acetone	>	Methyl ethyl ketone	>	Methyl propyl ketone	>	Acetophenone
100		83.6		75.1		68.5

Such slight difference in activity made the employment of these compounds in double substitution reactions extremely difficult.

The reactions of ketones with aldehydes in the presence of an alkali result in the formation of high-molecular unsaturated ketones. Many of these unsaturated ketones form colored products when dissolved in concentrated solutions of strong acids. This phenomenon of halochromism is particularly striking in the condensation products of acetone and acetophenone with furfural. The possibility of checking the change in concentration of the products of the condensation of ketones with furfural colorimetrically enables us to observe the dislodging of one ketone by another in these condensation products.

EXPERIMENTAL

To effect the displacement of acetophenone by acetone we prepared the pure condensation product of acetophenone and furfural – furfurylideneoacetophenone:

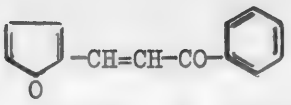

(I)

We did this by condensing furfural with acetophenone by the Costaneski method [4].

Equimolar amounts of furfural and acetophenone were dissolved in alcohol, and a suitable amount of an aqueous KOH solution was added to the solution. The reaction mixture was agitated and then allowed to stand for 2 hours. Diluting the solution with water yielded the oily condensation product, which was separated out in a separating funnel. The resultant oil was washed repeatedly with water and then dissolved in ether. The ether solution was desiccated above $CaCl_2$, and the ether was driven off. We endeavored to secure the pure furfurylidenoacetophenone by simply distilling the desiccated oily product at 317° and atmospheric pressure [4]. The oil resinified above 200°, however, and carbonized at 270-280°. We then resorted to distillation at 11 mm vacuum and 187°C.

The purity of the product was then checked. We were interested in having it completely free of furfural. This was done by reacting the product with aniline in the presence of acetic acid. When we made the "aniline test," the furfural reaction turned out positive – a red color was produced.

In order to secure a furfurylidenoacetophenone that was completely free of furfural, we repeated the condensation of furfural with acetophenone, varying the condensation conditions somewhat. We used an excess of acetophenone, employing 3 molecules of the ketone to 2 molecules of furfural. The mixture was allowed to stand overnight. The aniline test of the resulting pure product indicated that there was absolutely no free furfural present.

Substitution of Acetone for Acetophenone

Reaction of furfurylidenoacetophenone with acetone in an acid medium. We dissolved a drop of the furfurylidenoacetophenone we had prepared in 10 ml 60% sulfuric acid; the solution was an amber color. We added a drop of acetone to it. Within 10 to 15 minutes the yellow color of the solution turned to red, and within a few hours the color of the mixture was characteristic of the condensation product of furfural and acetone: difurfurylidenoacetone (II). It was obvious that the furfurylidenoacetophenone had been converted into the corresponding condensation product of furfural and acetone.

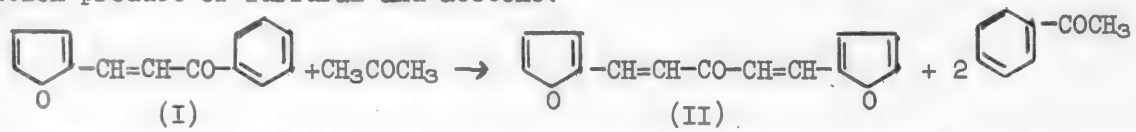

(I) (II)

Hence, under these conditions acetone replaces acetophenone in the latter's condensation products with furfural.

To provide further proof of this conclusion, we made the following test: we prepared furfurylidenoacetone and reacted it with acetophenone in an acid solution.

For this condensation we prepared a mixture of equal volumes (1 ml each): a 0.002 molar aqueous solution of furfural; a 0.020 molar aqueous solution of acetone; and a 50% solution of caustic potash.

Fifteen minutes after the reaction began, the reaction mixture was dissolved in 30 ml of 60% sulfuric acid at 50° C (water bath). By this time the reaction of the acetone with the furfural under the given alkaline conditions was already complete. One drop of pure acetophenone was added to the resultant red solution. Calculation indicates that when this is done the molar acetophenone:acetone ratio is approximately 15:1. No change in color was observed, however, even after 30 minutes had elapsed. Then two more drops of pure acetophenone was added to the

mixture; after 5-6 hours had passed, comparison of the mixture's color with that of a control solution showed that the intensity of its red color had weakened somewhat. Hence, in an acid medium the substitution process involves principally the replacement of the acetophenone by acetone.

We also carried out this reaction of replacing acetophenone by acetone in an alkaline solution.

Reaction of furfurylidenoacetophenone with acetone in an alkaline medium. For these experiments we prepared a weak alcoholic solution of furfurylidenoacetophenone, whose concentration was such that dissolving 1 ml of it in 10 ml of 60% sulfuric acid turned the solution an intense yellow. The reaction was carried out with different concentrations of acetone. Since the reaction product is a saturated diketone:

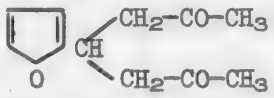

(III)

that is incapable of halochromism with an acid when the molar excess of acetone over the furfural is very high, we had to confine ourselves to a slight excess of acetone in our experiments [5].

We used 0.020 molar and 0.005 molar aqueous solutions of acetone in our experiments. These molar ratios of the ketone to the aldehyde yield unsaturated ketones as condensation products [6]:

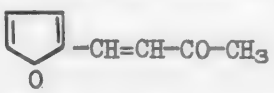

(IV)

Furfurylidenoacetone

and

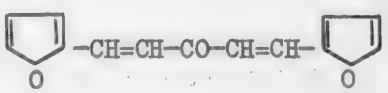

(II)

Difurfurylidenoacetone

We prepared the following mixtures for the tests: the first mixture consisted of equal volumes of an alcoholic solution of furfurylidenoacetophenone, a 0.020 molar aqueous solution of acetone, and a 60% aqueous solution of caustic potash; the second (the control mixture) consisted of equal volumes of an alcoholic solution of furfurylidenoacetophenone, water, and a 60% aqueous solution of caustic potash.

Small flasks containing these mixtures were placed in a water bath at 50°. Fifteen minutes later samples of each mixture were taken and dissolved in ten times their volume of 60% sulfuric acid. The color of the control mixture (without any acetone) was yellow, while the color of the mixture containing acetone differed appreciably from that of the control mixture by displaying a trace of red. This proved that unsaturated condensation products of furfural and acetone had been formed.

Thirty minutes later new samples were taken and dissolved in the acid; they exhibited the same picture, the red color of the first mixture being deeper by now.

We secured similar results when we repeated these tests, using lower concentrations of acetone, down to 0.005 mol.

Hence, acetophenone is displaced by acetone from furfurylidenoacetophenone in an alkaline medium as well.

Displacement of Methyl Propyl Ketone by Acetone

We have pointed out above that methyl propyl ketone is only 25% less active than acetone in a reaction with furfural, while methyl ethyl ketone is only 17% less active. Nevertheless, we endeavored to substitute acetone for methyl propyl ketone in the condensation products of furfural with the first of these ketones. Alkali as well as acid were used in these tests.

We used a mixture of equal volumes of a 0.005 molar aqueous solution of

furfural and a 0.020 molar aqueous solution of methyl propyl ketone in these tests. 5 ml of 60% caustic potash was added to 10 ml of the mixture. The reaction mixture was placed in a 50° water bath for 30 minutes. Then 2 ml of the solution was dissolved in 20 ml of 60% sulfuric acid. The color of the acid solution was a barely perceptible yellow-green. A few drops of pure acetone was added to it. The solution exhibited no change of color in the course of 2 hours.

A reaction mixture of equal volumes of the following solutions was prepared to test the substitution reaction in an alkaline mixture: a 0.005 molar aqueous solution of furfural, a 0.020 molar aqueous solution of methyl propyl ketone, and a 60% caustic potash solution. Thirty minutes after the reaction set in 3 ml of a 0.020 molar aqueous solution of acetone was added to 6 ml of this mixture. By this time there was no free furfural in the reaction mixture, as the aniline test was negative. The solution was left for another 30 minutes in the water bath. A sample of the reaction mixture was dissolved in 10 times its volume of 60% sulfuric acid. The solution was colored slightly red, which is characteristic of the condensation products of furfural and acetone.

We were able to produce a more intense color of a similar acid solution when we added a smaller concentration of acetone to the condensation products of methyl propyl ketone and acetone (in an alkaline medium). This reduced the acetone – furfural molar ratio, which results, as we have shown, in the formation of unsaturated ketones that are capable of halochromism.

Thus, we were able to substitute acetone for methyl propyl ketone in these products only in an alkaline medium. We were unable to observe such replacement when an acid is present.

The reactions described by us, involving the substitution of other methyl ketones by acetone in their condensation products with furfural, are based upon the differences in the activity of these ketones. The greater the difference in reactivity, the easier it is to substitute one ketone – the more active one – for another. It is extremely difficult to effect this sort of reaction with adjacent homologs, such as acetone and methyl ethyl ketone; in these cases the determining factor becomes the relative quantities of these ketones present in the reactions.

Methyl ethyl ketone is only 17% less active than acetone in the furfural reaction. But when it is used in very large excess over the acetone, the acetone can be partially displaced from its corresponding condensation product with furfural. We prepared a dilute solution of difurfurylidenoacetone in 60% sulfuric acid, and then added 0.25 ml of pure methyl ethyl ketone to 10 ml of this solution; after 30-40 minutes had elapsed (at 40-50°), a slight change in the tint of the solution color could be noticed, its violet hue being lost. This is an indication of the partial substitution of methyl ethyl ketone for the acetone.

SUMMARY

1. A qualitative reaction has been carried out involving the substitution of acetone for acetophenone in the primary condensation product of furfural and acetophenone. The reaction was carried out in an acid as well as an alkaline medium.

2. The process involved in the substitution of acetone for methyl propyl ketone in the primary condensation product of that ketone with furfural has been investigated. Owing to the slight difference between the chemical activity of these two compounds in the reaction with furfural, we were able to detect this substitution only in an alkaline medium.

LITERATURE CITED

[1] V.V.Chelintsev and E.K.Nikitin, J.Gen.Chem. 2, 3, 224 (1932).
[2] V.V.Chelintsev and E.K.Nikitin, J.Gen.Chem. 10, 6, 1453 (1940).
[3] Neuberg and Collatz, C, 11, 2227, 557 (1932).
[4] Costaneski, Padrajanski, Ber., 29. 2249 (1896).
[5] V.I.Tikhonova, J.Appl.Chem. 22, 9, 1014 (1949).
[6] E.K.Nikitin, J.Gen.Chem. 5, 1279 (1935).

Received May 29, 1950

A COMPOUND HELIX AS A CATALYST CARRIER

N. Z. Kotelkov

Chair of Chemistry, Saratov Agricultural Institute

It has been established, as the result of numerous experiments, that only a top layer some 200-300 mμ thick of a solid catalyst is active in catalytic processes, so that pure catalysts have an inactive mass that actually acts as a carrier for the catalytically active atoms or molecules. Moreover, a pure contact agent is caked and recrystallized during catalysis, thus losing its activity. These unwelcome phenomena may be effectively counteracted or eliminated by mounting the catalyst on a suitable carrier.

With this in mind, as well as to make the fullest possible use of the catalyst and to increase its active surface, we employed compound helixes as carriers, made up, depending upon the nature of the catalysis process, of pure metal wire (copper, aluminum, iron) or of alloy wire (nichrome, fekhral, nickeline, manganin, etc.).

EXPERIMENTAL

Manufacture of the spiral. A wire 0.5-0.7 mm in diameter and 672 to 480 cm long, with a surface of 105.5 cm^2, was wound into a close helix with an inner diameter of 2.3 mm (Fig. 1, a, b, c, d, and e – helixes of copper, aluminum, iron, nichrome, and nickeline wire. See Plate, page 245). The resulting helix was then wound into a compound helix, 6.5-7.5 cm long, with an inner diameter of 6 mm, consisting of 16-18 turns (Fig. 2, a, b, c, d, and e, compound helixes made of copper, iron, aluminum, nickeline, and nichrome wire. See Plate, page 245).

The compound helix was mounted inside the usual (quartz) catalysis tube. The temperature was measured with a thermocouple, one junction of which was placed inside the helix; a quartz plug was fitted in the other end of the helix. When helixes of high resistance alloys were used, heating was effected directly by means of the electric current passing through the helix. Constant temperature can be maintained by use of a thermoregulator, the accuracy of regulation being heightened by the helix's low thermal inertia.

Effective use of the helixes. Platinum, palladium, alumina, and various Saratov and Voronezh clays were used as catalysts mounted on the helixes. Helixes with catalysts applied to them are shown in Fig. 3 (see Plate, page 245), where a, b, c, and d are compound helixes: a – aluminum, coated chemically with alumina; b – nichrome, coated thermally with platinum; c – nichrome, coated with alumina; d – nichrome, coated with clay.

Platinum and palladium were applied thermally, totaling 0.05-0.07% of the carrier by weight [1,2,3], representing a total of 0.007-0.009 g for a nichrome helix weighing 13.35 g.

A comprehensive study has been made [4,5] of the catalytic dehydrogenation of cyclohexane over Pt and Pd, using various carriers.

In the present paper we made a study of the dehydrogenation of cyclohexane and the oxidation of hydrogen above the same metals, applied to a nichrome helix (Tables 1 and 2).

TABLE 1

Dehydrogenation of Cyclohexane Above Platinized Asbestos and a Platinized Nichrome Helix

Test No.	Experimental Conditions		Amount of platinum deposited on the carrier	Volume of helix, ml	Surface of helix, cm^2	Per cent dehydrogenation
	Temp., °C	Rate of feed, ml/min				
	350	0.2	10 g on asbestos			100
4	350	0.02	0.0056 g on simple nichrome helix	1.42	71.13	27.2 - 28.5
19	350	0.02	the same, but after the helix had been carbonized [2]	1.42	71.13	67 - 73
49	350	0.05	0.007 g on compound helix	1.58	105.5	40.2
50	400	0.05	ditto	ditto	ditto	72.3
53	350	0.05	ditto, but after the helix had been "carbonized"	"	"	100

TABLE 2

Oxidation of Hydrogen with Palladinized Asbestos and Palladinized Nichrome Helix

Test No.	Temperature, °C	Per cent hydrogen by volume in air-hydrogen mixture	Amount of palladium deposited on the carrier	Quantity of carrier, g	Surface of carrier, cm^2	Percent oxidation at gas-mixture feed rate of 4 liters/hour
1	78	3	0.034 g on asbestos	0.5	–	100 (slight local overheating)
2	100	10	ditto	0.5	–	100 (slight local overheating)
3	78	3	0.0013 g on helix	1.91	15	100 (no over heating)
4	100	10	ditto	1.91	15	100 (slight local overheating).

As we see in the table, the efficiency of the proposed design is $\frac{10}{4 \cdot 0.007} =$ = 357 times higher than that customarily employed for dehydrogenating cyclohexane, and $\frac{0.034}{0.0013} = 26$ times higher for the oxidation of hydrogen. It is apparent that

the increase in efficienc is still greater when the weight of the pure catalysts is compared with that of the same catalysts deposited on compound helixes.

This effect may be explained as due to the influence of the crust of oxides on the nichrome surface upon the structure of the thermally deposited platinum. As a result, the contact mass acquires a finely dispersed structure, providing the maximum possible number of active centers under the given conditions and inhibiting caking and the recrystallization of the catalyst mass. An explanation of the favorable effect of this "carbonizing" upon the dehydrogenation of cyclohexane has been given in a previous paper [2], and we shall not dwell upon it here.

The advisability of depositing the dehydrating catalysts, alumina and clay, upon a nichrome helix is illustrated in Table 3.

TABLE 3

Dehydration of Isopropyl Alcohol Above Alumina and Voronezh Fire Clay (rate of feed = 0.05 ml per min.)

Test No.	Temp., °C	Catalyst	Volume of helix, ml	Surface of helix, cm^2	Per cent dehydration
62	250	13.93 g of clay in pellets			99.67
63	300	ditto			99.97
237	300	0.46 g of clay, deposited on a compound helix	1.58	105.5	99.42
239	250	1.02 g of clay, deposited on a compound helix	1.58	105.5	99.89
240	275	ditto	1.58	105.5	100
241	350	ditto	1.58	105.5	100 *
137	250	13.93 g of alumina in pellets			67.06
138	300	ditto			98.67
196	250	1.06 g of alumina deposited on a compound helix	1.58	105.5	69.55
197	300	ditto	1.58	105.5	98.89

As we see from the table, the efficiency of the proposed process exceeds that of the customary one by 13.93/1.02 = 1400% at 250° and 13.93/0.46 = 3000% at 300°, in the dehydration of isopropyl alcohol with clay.

About the same efficiency is observed with alumina deposited on the exterior of the helix. As for the alumina produced chemically as a porous layer on an aluminum helix, this type of deposit causes the efficiency to rise $\frac{3.5}{0.0125} \simeq$ 280 times.

TABLE 4

Dehydration of Isopropyl Alcohol with Alumina (alcohol feed rate = 3 ml per hour)

Test No.	Temp., °C	Amount of alumina, g	Per cent dehydration
113	350	3.4966 as pellets	94.15
114	400	ditto	99.94
363	350	0.0125, deposited on an aluminum helix	96.90
364	400	ditto	99.98

In this case, 0.0125 g of aluminum oxide was deposited on the aluminum helix chemically instead of using 3.4966 g of it in the form of pellets. Moreover, the percentage dehydration is somewhat higher above the helix (Table 4).

Helixes made of high-resistance wire are directly heated by an electric

* With a feed rate of 0.1 ml per min.

current of 1.7-2.5 amp, instead of in a tubular electric furnace, using 7.5-10 amp at the same voltage. This effects a saving of 400% and more of electric energy. Heating the helix by passing a current through it makes it possible to follow the catalysis process visually without disassembling the apparatus – all that is necessary is removing the asbestos insulation from the catalysis tube; this is a factor of great importance in laboratory investigations.

SUMMARY

1. It has been found that in several cases it is advisable to employ compound helixes made of suitable metals or alloys as a carrier for catalysts.

2. A compound helix made of nichrome is a good carrier: a) for platinum and palladium, since the presence of an oxide crust prevents caking and recrystallization; and b) for alumina and clay, owing to the thermal stability of the helix and the fact that it can be heated by an electric current passing through it.

3. An aluminum helix chemically coated with alumina is a good dehydration catalyst.

LITERATURE CITED

[1] M.S.Gershenovich and N.Z. Kotelkov, J. Appl. Chem. 11, 253 (1938).

[2] N.Z.Kotelkov, J. Appl. Chem. 15, 193 (1942).

[3] N.Z.Kotelkov, J. Anal. Chem., 5, 48 (1950).

[4] N.D.Zelinsky, Bull. USSR Acad. Sci., 1929, 29.

[5] Yu.K.Yurev, J. Phys. Chem. 5, 393 (1934)

Received May 3, 1950

PROTECTING IRON AGAINST CORROSION

UNDER ATMOSPHERIC CONDITIONS BY COATINGS OF OIL*

A. Ya. Drinberg and M. G. Rokhlin

Lensoviet Institute of Technology, Leningrad

In a previous report [1] we discussed the general trend of chemical and physical changes observed during the aging of oil films when exposed to the air. In considering the changes occurring in the film itself, neither we not a number of other research workers [2] took into account the changes in its protective, anticorrosion properties.

There is hardly room for doubt that the duration of the anticorrosion protection of metals is one of the most important properties to be considered in the use of paint vehicles and oil paints. Moreover, there is no direct connection between the changes in the mechanical properties of the films and their protective properties. Indeed, numerous cases have been described in which the film continued to provide excellent protection against corrosion despite rapid changes in its mechanical and chemical properties. For example, coats of red lead in linseed oil [2,3] quickly turn brittle, their elongation and elasticity falling off sharply, while their protective properties are maintained for a long time. The same holds true of all paints based on polymers of divinylacetylene [4] and nitropentaphthals [5]. On the other hand, highly plastic coatings based on cellulose esters [6], without oil priming coats, and many other film-forming materials, as well as coatings with a pigment base, which exhibit a lesser change of their mechanical properties when their films are aged, provide poor corrosion protection, and the service life of such coatings is shorter.

The present paper describes experiments on the preparation of various unpigmented oil coatings and the testing of their ability to protect iron against corrosion under atmospheric conditions. Subsequent reports will deal with the changes in the mechanical and anticorrosion properties of these films that occur with age, as well as with the aging of pigmented films.

EXPERIMENTAL

The vegetable oils selected for these experiments were first refined, their major physical and chemical characteristics corresponding to the technical specifications (All-Union Standards, People's Commissariat for the Food Industry, 1939, Nos. 378, 305, 307/ST-6, and No. 1488). The data on their principal physical and chemical characteristics are listed in Table 1.

The mean molecular weight was determined by Rast's camphor method. The esters of pentaerythritol and the fatty acids were synthesized as follows. First, the oils were saponified in the usual manner with caustic potash and alcohol. The resulting soaps were then treated with sulfuric acid. The sulfuric acid was washed out of the fatty acids thus produced, which were desiccated and then esterified with pentaerythritol to yield the corresponding esters.

* Report IX of a series on the polymerization and drying of oils and esters of the fatty acids.

TABLE 1

Physical and Chemical Characteristics of Vegetable Oils

Vegetable oil	Molecular weight	Specific gravity at 20°	Viscosity at 20°, (° Eng.)	Refractive index at 20°	Color equivalent in mg of iodine	Saponification No. mg KOH	Hübl No.	Acid Number, mg KOH
Tung oil	837	0.940	7.5	1.519-1.525	45	195.2	148.9	2.4
Linseed oil ..	842	0.936	6.5	1.482-1.484	16	193.4	176.1	1.1
Cottonseed oil	860	0.922	6.8	1.464-1.472	120	192.5	120.1	0.4

The purity of the initial pentaerythritol was tested by the Reid benzaldehyde method; it was found to be 92% pure. Its melting point was 244°. It contained 0.08% moisture.

The data on the synthesis of the pentaerythritol esters of the acids recovered from the vegetable oils are listed in Table 2.

TABLE 2

Data on the Synthesis of Pentaerythritol Esters

Initial vegetable oil	Acids recovered	Acid number of the acids recovered	Esterification temperature, °C	Duration of esterification, hours	Acid No. of the resulting pentaerythritol esters
Linseed oil	Oleic, Linoleic, Linolenic, Saturated acids	191.8	170-185	14.0	7.0
Cottonseed oil	Oleic, Linoleic, Saturated acids	90.4	175-185	14.5	8.0

The physicochemical characteristics of the pentaerythritol esters are listed in Table 3.

TABLE 3

Physicochemical Characteristics of Pentaerythritol Esters

Pentaerythritol ester	Molecular weight	Specific gravity at 20°	Visocity at 20°, (° Eng.)	Refractive index	Color equiv in mg iodine	Hübl No.	Saponification No. mg KOH	Acid No., mg KOH
Linseed oil	1260	0.947	9.0	1.483-1.487	58	149.2	196.5	7.0
Cottonseed oil	1300	0.956	8.9	1.470-1.475	170	109.5	190.0	8.4

The iodine numbers are somewhat low, apparently because minor oxidative and polymerizing processes, which were hard to avoid during the synthesis process, took place in the pentaerythritol esters.

It is obvious that the molecular weights of the pentaerythritol esters are

raised somewhat (10 to 15%) over their theoretically computed values (1110-1140) for the same reason.

The paint vehicles were prepared by mixing the siccative with the slightly heated (40-50°) respective oil in certain proportions, which were the same for all the oils, so that they contained the equivalent of 0.13% of metallic cobalt.

The comparative data on the total drying time for the paint vehicles and the oils are given in Table 4.

TABLE 4

Data on the Time Required For the Complete Drying of Paint Vehicles and Oils

Time for complete drying of vegetable oils at 20°, days			Time for complete drying of paint vehicles made from vegetable oils, at 20°, hours		
Tung oil	Linseed oil	Cottonseed oil	Tung oil	Linseed oil	Cottonseed oil
4.5	6	Does not dry out	1.5	24-26	45 days (peels off)
Time for complete drying of pentaerythritol esters at 20°, days			Time for complete drying of paint vehicle of pentaerythritol esters at 20°, hours		
-	Linseed oil	Cottonseed oil	-	Linseed oil	Cottonseed oil
-	2.5	10	-	5-6	14-15

Three methods were used to determine the durability of the oil films for the sake of comparison, viz.: a) testing them under natural atmospheric conditions; b) testing them in an apparatus for accelerated aging, a "weatherometer"; and c) a rapid test in a "high speed apparatus",

The following indexes were employed to check the changes that occur in oil films during aging, i.e., from the instant they begin to dry until they break down: a) the anticorrosion protection they afford; b) the elementary composition of the films during various aging stages; c) the extent of their conversion into three-dimensional polymers; d) loss in weight; e) mechanical properties, including their elasticity (reversible deformation of the free film), the impact and bending strength of the film, and the hardness of the film; and f) the external appearance of the film: change in color, appearance of cracks, peeling, and similar indications of aging.

With the exception of the principal index - indicating the anticorrosion properties - each of the indexes listed above, taken by itself, cannot be regarded as an exhaustive indication of the state or the properties of the aging film. Hence, simultaneously determining several indexes enabled us to get an idea of the mechanical and physico-chemical properties of the film, and thus of its value as a coating.

We usually employed a single-layer coating with a film thickness of 20-30 μ in order to facilitate the diffusion of oxygen and, hence, to accelerate the oxidation processes that bring about the other aging effects.

The iron sheets used in making up the samples were carefully cleaned and degreased before a coating was applied. After covering the edges with a protective aluminum coating, the sheets were dried at 20°, and 15 days after application of

the film they were sent to the "roof" station for exposure, where they were mounted at an angle of 45°. They were exposed to atmospheric action for 6 months – from May to October.

The extent of corrosion of the iron surface underneath the film when the samples were aged under normal atmospheric conditions is given in per cent in Table 5.

TABLE 5

Per Cent Corrosion of Samples Underneath Coatings Under Normal Atmospheric Conditions

Length of exposure, months	Paint vehicle				
	Linseed pentaerythritol ester	Cottonseed pentaerythritol ester	Tung oil	Linseed oil	Natural linseed oil
1	0	0	0	0	0
2	Specks	0	0	Specks	Specks
3	2 - 3	0	Specks	2 - 3	5
4	5	Specks	10	8 - 10	10
5	20	5	30	20 - 25	20
6	30	10	60	40 - 50	40

Table 5 shows that after 6 months of exposure the least corrosion occurred under the "cottonseed" pentaerythritol-ester paint vehicle, while the most corrosion occurred underneath the tung oil.

Investigation of the properties of films when tested in an accelerated aging apparatus (the Leningrad Institute of Technology "Weatherometer"). Iron sheets 5 x 10 cm in size and 0.4 and 0.2 mm thick, coated with an oil film 25 ± 1 μ thick, were subjected to these tests. The edges of these sheets were coated with a bituminous varnish, and their backs were coated with No. 138 oil-glyptal priming to protect the oil coating under test from corroding action commencing at the unprotected portions of the iron's surface.

On the 15th day after the sheets had received their oil coatings, they were placed in the apparatus and tested for their resistance to corrosion. The apparatus is shown diagramatically in the subjoined drawing.

The following procedure was set up to test the plates in this apparatus:

a) 10 minutes of artificial rain.

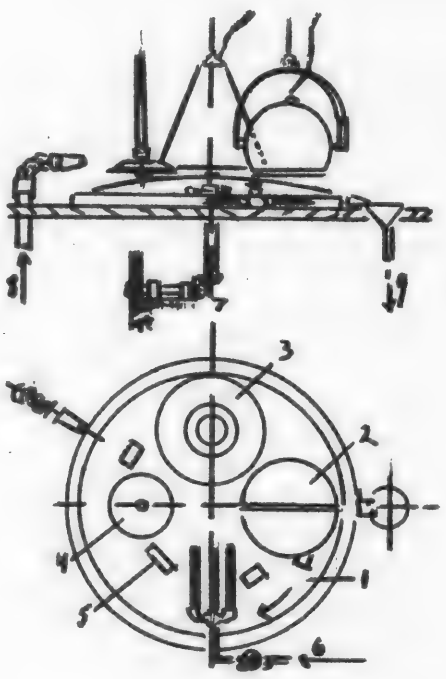

Accelerated Aging Apparatus

1-Wheel; 2-quartz lamp; 3-1000-watt electric bulb; 4-heating element (infrared rays); 5-sample under test; 6-water supply; 7-drive from electric motor; 8-outlet drain; 9-air supply from fan (artificial wind).

b) 20 minutes of infrared radiation, with the temperature raised from 40 to 60°, the heating element being 8 cm from the surface of the sheet.

c) 66 minutes of light radiation (from the electric bulb, the temperature being raised from 40 to 90°, the distance from the light source to the sheet being 15 cm.

d) 30 minutes of ultraviolet radiation, with a radiation temperature of 20 to 30°, the distance from the radiation source to the sheet being 12 cm.

The entire cycle (a complete revolution of the wheel) lasted 2 hours 6 minutes.

The entire test of the sheet comprised 200 cycles (or 420 hours). Longer tests were unnecessary, since this test was enough to make most of the coatings applied to the iron break down completely as the result of corrosion.

The spread of corrosion beneath the films during the testing of the samples is given in per cent in Table 6.

TABLE 6

Per Cent Corrosion of Samples Underneath Coatings When Tested in the LTI Weatherometer

Aging time, hours	Paint Vehicle				
	Linseed pentaerythritol ester	Cottonseed pentaerythritol ester	Tung oil	Linseed oil	Natural linseed oil
52.5	0	0	0	0	0
105	0	0	0	0	0
157.5	Specks	0	0	Specks	0
210	5	0	Specks	5	Specks
262.5	10	3 - 5	20, corroded in individual areas	15, corroded in individual areas	10, corroded in individual areas
315	20, corroded in tiny patches	10	Much yellowed, network of corroded spots, 50.	Much yellowed, corroded in tiny patches, 30	Much yellowed, 30, corroded in tiny patches
420	Film much yellowed, corroded in individual areas, 30-35	Film much yellowed, corroded in tiny patches, 15-20	Film turned brown, much peeling, corroded in continuous patches, 60-70	Film turned brown, partially peeling, corroded in patches, 40-50	Film turned brown, partially peeling, corroded in patches, 40-50

95-100% of the surface of the unprotected iron sheet was corroded after 52.4 hours.

It should be noted that the tung-oil paint vehicle proved to be one of the most resistant after 210 hours (100 cycles) of aging, whereas its position had changed markedly after 420 hours of aging. The film produced by a paint vehicle based on the "cottonseed" pentaerythritol ester gave the best results, the tung-oil vehicle yielding the worst results.

Table 6 indicates that films produced by pentaerythritol esters were found to resist corrosion better than films produced by vegetable oils.

LITERATURE CITED

[1] A.Ya.Drinberg, J. Appl. Chem. 19, 3, 258 (1946).

[2] A.G.Pamfilov and Shikher, J. Appl. Chem. 12, 1884 (1939); 13, 147 (1940); A.Ya. Drinberg, Trans. Paint and Lacquer Research Inst. 1, Theoretical Chemistry Press, (1934).

[3] Sweed and Salwater. Paint as Protection Against Corrosion. Theoretical Chemistry Press, (1936).

[4] A.V.Klebansky et al, Coll. Res. Reports, Inst. Appl. Chem., 38, 32 (1947).

[5] A.Ya.Drinberg and P.A.Antipova, Trans. Lensoviet Inst. Technol., Leningrad, 19, 66 (1947).

[6] A.Ya.Drinberg. The Technology of Film -Forming Substances. State Chemical Press (1948).

Received May 20, 1950

PROTECTING IRON AGAINST CORROSION BY COATINGS OF OIL AND CHANGES IN THE LATTER'S PHYSICAL PROPERTIES AS THE RESULT OF AGING*

A. Ya. Drinberg and M. G. Rokhlin

Lensoviet Institute of Technology, Leningrad

In our previous report [1] we discussed the anticorrosion protection of iron under atmospheric conditions by means of coatings based on oils and pentaerythritol esters. The aging conditions of the coatings have been kept constant to provide a basis for comparing the anticorrosion properties of these coatings with the changes in their mechanical properties during the aging process. These conditions were provided in an accelerated aging apparatus [2], in which such major factors in atmospheric aging as light, moist heat, the eolation of volatile substances, and the effect of oxygen (wherein it differs from the weatherometer [1]), were intensified. The effect of oxygen was produced by alternating oxygen under pressure and a vacuum to draw out the volatile substances.

The well-known difference between the results obtained in weatherometers of different types and those obtained under atmospheric conditions is apparently due to the fact that in the weatherometer the action of heat, light, and moisture is intensified, while the fundamental action of atmospheric oxygen is not.

Changes were made in the "accelerated aging apparatus" (Fig. 1)** to eliminate some of its deficiencies [2]. The apparatus was heated externally, by means of a coil of wire, which improved the temperature regulation; to increase the capacity of the apparatus, the 100-watt lamp was replaced by a considerably smaller one – a 40-watt 6-volt automobile headlight lamp.

A steel framework was used to suspend the samples, instead of a grid. The operating schedule of the apparatus was also changed somewhat. The first 4 hours of aging were scheduled as follows: 1 hour under pressure + 1 hour under vacuum, etc. In the ensuing period each cycle consisted of the following, owing to the decrease in the decomposition products evolved: 2 hours under pressure + 1 hour under vacuum. The temperature was maintained within the +80 to +90° range. The oxygen pressure was 3.0 to 4.5 atmospheres. The vacuum set up by a vacuum pump was 30 mm mercury column. One hour of exhaustion after each operating cycle was practically sufficient to remove the volatile decomposition products. For the tests [3] we prepared film samples: 1) on glass plates; and 2) on sheets of light sheet iron. Some of the samples were made up as so-called "free films". The glass plates, 1-1.5 mm thick, were 5 x 10 cm, 2.5 x 6 cm, and 2.5 x 10 cm in size.

The films deposited on them were tested for hardness (with the impact machine – All-Union Standard No. 10086·39), for solubility, and for loss of weight.

The iron sheets were made of light sheet iron: 1) 5 x 10 cm in size and 0.4

*Report X of a series on the polymerization and drying of oils and esters of the fatty acids.

**See plate p. 245.

mm thick for the subsequent test of the films for impact strength; and 2) 2.5 x 5 cm in size and 0.2 mm thick for the subsequent test of bending strength.

The so-called "free films" were tested: 1) for elasticity (reversible deformation); and 2) by determining the elementary composition of the films at various aging stages. Single-layer coatings, with a mean thickness of 25 ± 5μ, were applied to the glass plates and iron sheets. The "free films" were prepared as two-layer coatings on amalgamated tin-plate, 9 x 12 cm in size, the overall thickness of the film averaging 45 ± 5μ, the second coating being applied 5 days after the first one.

The film samples were tested in the accelerated aging apparatus for several cycles, until the typical outward signs of aging appeared. The degree of aging of the films was checked every two cycles as a rule (i.e., after every 8 hours of operation of the apparatus). In some cases, noted in Table 1, this procedure was varied.

Table 1 shows that the film produced by the "cottonseed" pentaerythritol ester was the best preserved after 48 hours of accelerated aging.

TABLE 1.

Changes in Films as a Result of Their Aging in the Accelerated Aging Apparatus

Aging time, hours	Paint vehicle			
	"linseed" pentaerythritol ester	"cottonseed" pentaerythritol ester	Tung oil	Linseed oil
4	Films almost colorless, with slightly yellowish tinge and slight luster			
8	Increased luster; films turned yellow			
16	No change in luster	No change in luster	Luster diminished	No change in luster
24	Iron begins to be exposed	Unbroken film	Unbroken film, crinkled in places	5% of the iron exposed, some pock marks
32	5% of the iron exposed	Unbroken film	5% of the iron exposed	5% of the iron exposed
48	Luster diminished Fine network 10% of the iron exposed	5% of the iron exposed	No luster, some pock marks, fine cracks; 10% of the iron exposed	Luster diminished, fine cracks; 20% of the iron exposed

The anticorrosion properties of the tested paint vehicles were determined by applying single-layer coatings of the latter to iron sheets and testing the latter in the accelerated-aging apparatus, using a somewhat different schedule. Twenty cm^3 of water was introduced into the accelerated-aging apparatus in the form of steam through a nozzle in the cover from a rubber tube connected to a steam boiler before every admission of oxygen.

The steam, which condensed on the surfaces of the sheets at a temperature of 80-90°, was introduced in order to provide a medium that promotes corrosion. No signs of corrosion appeared on the sheets when no steam was present, probably because the surface of the iron was passivated by the oxygen. This was confirmed by a test of such passivated sheets in the accelerated-aging apparatus, no corrosion being observed beneath the film after 32 hours of test with steam passed

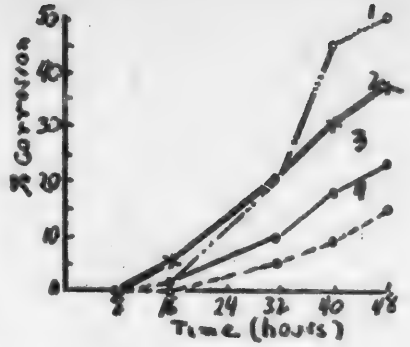

Fig. 2. Increase in corrosion underneath the film as aging progresses in the accelerated-aging apparatus.

Films: 1-Tung oil; 2-linseed oil; 3-"linseed" pentaerythritol ester; 4-"cottonseed" pentaerythritol ester.

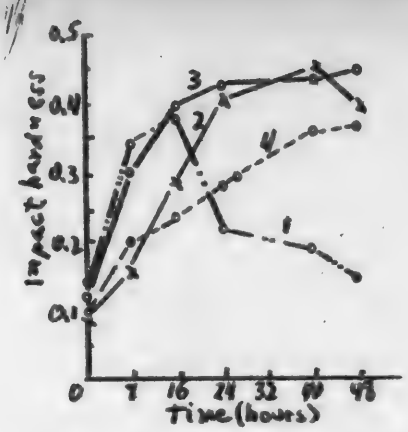

Fig. 3. Hardness of films as aging progresses in the accelerated-aging apparatus

Films: 1-Tung oil; 2-linseed oil; 3-"linseed" pentaerythritol ester; 4-"cottonseed" pentaerythritol ester.

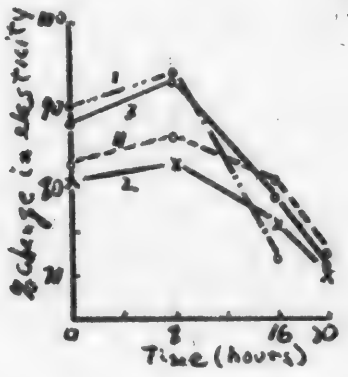

Fig. 4. Elasticity of the films, in per cent, as aging progresses in the accelerated-aging apparatus.

Films: 1-Tung oil; 2-linseed oil; 3-"linseed" pentaerythritol ester; 4-"cottonseed" pentaerythritol ester.

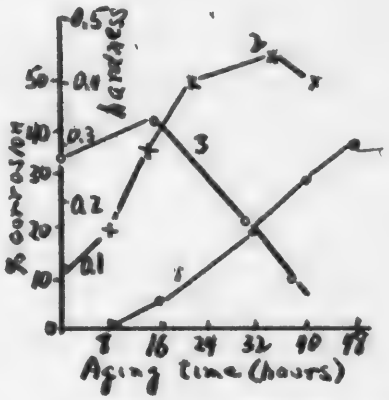

Fig. 5. Corrosion compared with changes in the mechanical properties of the film.

1-Corrosion; 2-hardness; 3-elasticity.

through the apparatus. Plates that had not been passivated, however, began to corrode after only 8 to 16 hours of aging in the apparatus. The method of determining the extent of corrosion by weighing the sheets after the films and the rust had been removed chemically did not yield perceptible results in these instances. Since the films were rather transparent, it was better to determine the corrosion planimetrically, i.e., by computing its spread over the surface of the metal in per cent. These results are plotted in Fig. 2. The film produced by the "cottonseed" pentaerythritol ester provided the best protection against corrosion. The film formed by the tung-oil vehicle proved to be least stable, even after only 40 hours of aging.

The hardness of the film on the glass was measured by the damping of a second-pendulum's oscillations. The curves in Fig. 3, plotted from the tabular data, indicate that during the aging process in the accelerated-aging apparatus the

hardness rises sharply at first for nearly all the films. Toward the end of the test, though, the hardness changes more slowly. The sole exception is the tung-oil vehicle, the hardness of which rose sharply at first, and then began to drop off, apparently because of the crinkling of the surface. In the film formed by the linseed-oil vehicle the intensive destruction of the three-dimensional polymer began to make itself felt during the final stage of aging; the surface began to be "crackled" with fissures.

The elasticity was tested with the "free films," strips 50 x 5 mm of which were cut off, not counting the extra length required for fastening in the clamps.

The test results are given in Fig. 4. The figure shows that after drying and before the beginning of the aging test, the films possessed lower reversible deformation strength; the films became more elastic than they were at the start after the first few hours of accelerated aging. This increase in elasticity was due to the fact that the polymerization of the film was probably complete after 8 hours of aging, which increased its ability to undergo reversible deformation. As aging progressed, the elasticity of the films dropped sharply, after which the films possessed no elongation at all, becoming brittle and breaking when the slightest force was applied to them.

As we see in Fig. 5, there is no linear relationship between corrosion and the change in the mechanical properties. The ultimate tensile strength rose during the initial aging period, but dropped off later.

The change in weight during the aging process was measured in the films applied to the glass plates. The initial weight of each of these films was taken as 100%.

The curves reproduced in Fig. 6 indicate that the tung-oil vehicle exhibited the greatest loss in weight after 48 hours of aging in the accelerated-aging apparatus. This was apparently due to its containing esters of the highly unsaturated eleostearic acid, as a result of which the reaction of oxidative decomposition, principally in the liquid phase, was intensified in it.

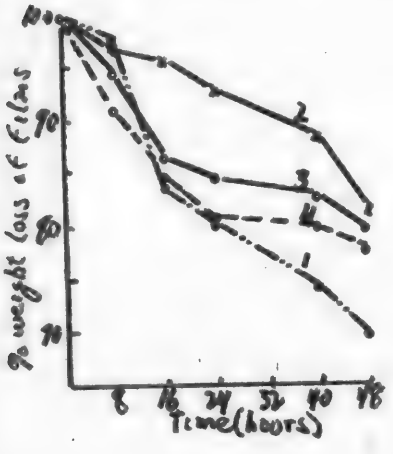

Fig. 6. Per cent decrease in weight of films as aging progresses in the accelerated-aging apparatus.

Films: 1-Tung oil; 2-linseed oil; 3-"linseed" pentaerythritol ester; 4-"cottonseed" pentaerythritol ester.

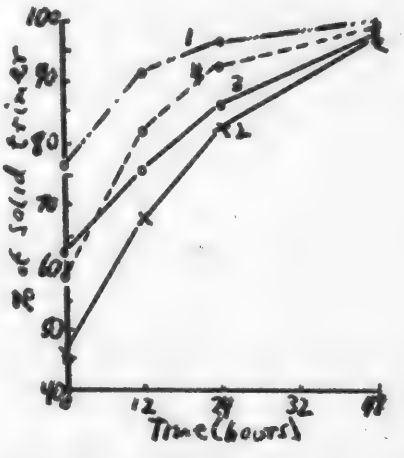

Fig. 7. Per cent increase of the solid three-dimensional polymer in the films as a function of aging time in the accelerated-aging apparatus.

Films: 1-Tung oil; 2-linseed oil; 3-"linseed" pentaerythritol ester; 4-"cottonseed" pentaerythritol ester.

The solubility of the films after drying and aging was determined by extracting the films applied to the glass plates in the usual manner in a Soxhlet apparatus. Benzene was used as the solvent. The films dried at 20° were extracted on the 15th day after their application. The films that had been tested for 12, 24, and 48 hours in the accelerated-aging apparatus, were extracted the very same day that their test in the apparatus was completed.

Each of these films was extracted for 6 hours at 80°. When the test was over, the films were dried to constant weight. The solubility of the films during various aging stages was determined from the difference in weight before and after extraction.

Fig. 7 shows that as aging progressed, all the films became less soluble, and that, therefore, the percentage of the three-dimensional polymer increased. The minimum solubility was exhibited by the film produced by the tung-oil vehicle.

For the sake of comparison we cite below data on the percentage of the three-dimensional polymer after 6 months of natural aging of films under atmospheric conditions and after 420 hours of accelerated aging of the same films in the weatherometer.

TABLE 2

Comparison of Film Aging Conditions as a Function of the Percentage of the Three-Dimensional Polymer

Aging conditions	Paint Vehicle			
	Linseed pentaerythritol ester	Cottonseed pentaerythritol ester	Tung oil	Linseed oil
After 6 months of natural aging	75.52	72.44	88.10	61.65
After 420 hours of accelerated aging (in the weatherometer)	93.41	90.90	97.85	95.05

As we see from a comparison of the data in Table 2 with the curve in Fig. 5, aging under natural conditions or in the weatherometer left more of the soluble phase in the films than did aging in the accelerated-aging apparatus.

The principal reason for these discrepancies is obviously the presence of a vacuum in the accelerated-aging apparatus, which promotes the evacuation of the decomposition products of the liquid phase in various films at different rates. Moreover, the action of oxygen under pressure increases with different rates of transition from this phase to the insoluble three-dimensional polymer.

We prepared oil paints to solve the problem of whether pigmented films exhibit the same behavior patterns as pure oil films during their accelerated aging. Red ocher was used as the pigment. The same paint vehicles were used as film bases as were used in all the previous tests.

The red ocher contained 93% of Fe_2O_3, in terms of the dry substance, 2.4% of moisture, and 0.9% of water-soluble salts. It did not contain any chlorides or sulfides. Its reaction was neutral. The oil paint was prepared from 76 parts of minium and 24 parts of the vehicle (covering power 35 g/cm^2; fineness 30-40). These figures meet the specifications of the All-Union Standards, People's Commissariat of Heavy Industry Nos. 7814/753 and 8163/1082.

Clean sheets of light sheet iron were covered with a single layer of red-ocher oil paint $45 \pm 5\mu$ thick. The other side of the sheet received a priming coat of

No. 137. Fifteen days after they were painted, the sheets were subjected to aging in the accelerated-aging apparatus, where they were kept for 48 hours according to the schedule set forth above.

Table 3 gives the anti-corrosion properties and the external changes in the pigmented films that were age-tested in the accelerated-aging apparatus.

TABLE 3

Changes in Pigmented Films Age-Tested in the Accelerated-Aging Apparatus

Aging time, hours	Pigmented films			
	Linseed pentaerythritol ester	Cottonseed pentaerythritol ester	Tung oil	Linseed oil
0	Brick brown color; matte luster			
16	Films turned dark; luster disappeared; no corrosion found			
32	All the films turned very dark; chalking set in			
48	2-3% corrosion	2-3% corrosion	10% corrosion	5% corrosion

Marked corrosion set in only toward the end of the test. The film was removed from the surface of the metal in order to compute the area affected by corrosion after 48 hours of aging. The film-forming material manifested the same effect upon the anti-corrosion properties of red-ocher coatings as when no pigment was used.

As is usually the case, pigmented films proved to be better anticorrosion coatings than the corresponding unpigmented films. The change in luster and color of the pigmented films set in somewhat earlier. The films consisting of pigmented pentaerythritol esters proved to be the best coatings.

LITERATURE CITED

[1] A.Ya.Drinberg and M.G.Rokhlin, J. Appl. Chem. 24, 2 (1951).*

[2] A.Ya.Drinberg and Reshentsev, J.Appl. Chem. 15, 346 (1942).

[3] All-Union Standard No. 10086-39.

*See previous article.

CHANGES IN THE ELEMENTARY COMPOSITION OF OIL FILMS DURING VARIOUS AGING PROCEDURES*

A. Ya. Drinberg and M. G. Rokhlin

Lensoviet Institute of Technology, Leningrad

An elementary analysis has been made of several oil films in order to provide a more complete characterization of the processes involved in the change of chemical composition of the films as the result of drying and aging. We selected for this purpose two types of films produced from linseed-oil esters and acids, viz.: linseed-oil films and films of esters of pentaerythritol and the fatty acids of linseed oil.

The elementary analysis employed the method of combustion with cupric oxide. The following materials were tested: a) the initial oil; b) free films after they had been dried and aged for 6 months under natural conditions; and c) free films after 24 hours of aging in the accelerated-aging apparatus.

Not all parts of the surface "aged" equally, owing to the varying thickness of the coating; we therefore reduced the experimental error by using average pulverized samples for the combustion test.

Moreover, in view of the fact that the tested films contained a siccative (ammounting to 0.17% of the oil by weight in terms of CoO), we corrected the weight of the initial samples accordingly. This correction (which was of the order of the fourth decimal place) allowed for the weight of the ash left in the boat after combustion. The data on combustion of the films are listed in Table 1.

The analysis data enable us to shed some light upon the changes that occur in oil films during their natural aging and their aging in the accelerated-aging apparatus. In comparison to the composition of the initial oils, the films analyzed after they had been aged under natural atmospheric conditions were considerably enriched with oxygen [1], whereas the films that had undergone an intensive aging in the accelerated-aging apparatus exhibited a considerable loss of oxygen.

This phenomenon is apparently due to the fact that aging under natural conditions results in the oxidation of the liquid phase in the main, much of the latter remaining in the film for a long time, with the exception of the low-molecular compounds that separate out from it [2]. When the film is aged in the accelerated-aging apparatus, however, much of the enriched oxygen in the liquid phase is exhausted from the film rapidly by the vacuum and the high temperature. The film is therefore less enriched with oxygen, and hence its carbon content, the three-dimensional polymer, is relatively higher. This is clearly borne out by the fact that films lose considerable weight during aging in the accelerated-aging apparatus and contain a lower percentage of soluble products, as a result of the losses in the liquid phase, thus becoming brittle and highly crumbly.

---

*Report XI of a series on the polymerization and drying of oils and esters of the fatty acids.

TABLE 1

Elementary Analysis of Oil Films After Aging Under Natural Conditions and in an Accelerated-Aging Apparatus

Description of sample	Weight of film before combustion, g	Weight of volatile products after combustion, g		Elementary composition, %		
		CO_2	H_2O	C	H	O
Analysis of Linseed-Oil Films						
Composition of the crude linseed oil ...	0.1710	0.4668	0.1640	74.5	10.65	14.85
	0.1918	0.5250	0.1872	74.7	10.85	14.45
Films after 6 months of natural aging ...	0.1612	0.3838	0.1314	64.95	9.05	26.0
	0.1902	0.4272	0.1474	64.7	8.9	26.4
Films after 24 hours of aging in the accelerated-aging apparatus.....	0.1874	0.5562	0.1358	80.95	8.05	11.00
	0.1750	0.5174	0.1308	80.65	8.3	11.05
Analysis of Linseed Pentaerythritol-Ester Films						
Composition of the ester after synthesis	0.1820	0.4924	0.1688	73.8	10.3	15.9
	0.1696	0.4602	0.1610	74.0	10.55	15.45
Films after 6 months of natural aging ...	0.1666	0.4058	0.1460	66.45	9.75	23.8
	0.1582	0.3838	0.1326	66.2	9.45	24.35
Films after 24 hours of aging in the accelerated-aging apparatus	0.1490	0.4338	0.1166	79.4	8.7	11.9
	0.1722	0.5028	0.1300	79.65	8.4	11.95

The data listed in Table 1 indicate, moreover, that the oxygen enrichment of films formed by natural paint vehicles during the process of natural aging is higher than that of films of the "pentaerythritol ester", which also age more slowly.

It is also worthy of note that after films made of a pentaerythritol ester had been aged in the accelerated-aging apparatus, they retained somewhat more oxygen that films made of the linseed-oil vehicle. It is hard to say, however, whether this was due to the higher oxygen content of the initial pentaerythritol ester or to the fact that films made of the pentaerythritol esters aged more slowly in the accelerated-aging apparatus, as our experiments have shown, than films made of the linseed-oil vehicle.

The aging of oil films when various accelerating factors are allowed to act upon them, principally light, heat, and catalysts, must be regarded as the result of the chemical action of oxygen, exactly as in the drying process [1].

No matter what the methods or conditions that bring about the aging process, various irreversible physicochemical changes take place in the film as aging progresses.

The percentage of the liquid, plasticizing phase diminishes, and the percentage

of the solid phase rises. The elasticity and solubility of the films diminish. The anti-corrosion properties of the films are impaired, and their disintegration is accelerated.

The behavior patterns of changes in the nature of the films' anticorrosion properties and in the rate of their disintegration observed during the aging process were largely dependent upon the method of aging employed.

Whereas corrosion spread underneath each film at different rates at the beginning and end of the tests during aging under atmospheric conditions, as a natural result of the inconstancy of meteorological conditions, corrosion was more uniform during artificial aging.

Table 2 gives a summary of our data on the anticorrosion properties of oil films, as tested after: a) 6 months of aging under atmospheric conditions; b) 420 hours of testing in the weatherometer; and c) 48 hours of aging in the accelerated-aging apparatus.

TABLE 2

Data on the Anticorrosion Properties of Oil Films

Paint vehicle and tested film	Spread of corrosion due to aging of the films, in % of surface.		
	Under atmospheric conditions	In the weatherometer	In the accelerated-aging apparatus
Linseed pentaerythritol ester	30	30-35	20-25
Cottonseed pentaerythritol ester	10	15-20	15
Tung oil	60	60-70	50
Linseed oil	40-50	40-50	35-40

Table 2 shows that the final changes in the anticorrosion properties were different, depending upon the method used in the aging test. The overall pattern of the changes remained the same, however, irrespective of the method employed: all three methods indicated that the films made of the "cottonseed" pentaerythritol ester had the highest anticorrosion properties, while the tung-oil film had the lowest [3]. Similarly, the anticorrosion properties of the film made of the "linseed" pentaerythritol ester proved to be better than those of the natural linseed oil.

As for the chemical changes occurring in the films when different test methods are used, they also differed, at least during the initial aging stage, depending upon the intensity of the oxidation and polymerization processes, as well as upon the rate at which the products of oxidative decomposition were removed from the films. Since the rate of removal of the volatile oxidation products from the liquid phase was not high during aging under atmospheric conditions or in the weatherometer, the films would have to be enriched with oxygen. On the other hand, the films that were tested in the accelerated-aging apparatus were highly "impoverished" as far as oxygen was concerned, as the elementary-analysis data indicated, owing to the evacuation of the liquid-phase products that were enriched with oxygen.

SUMMARY

1. Reports IX, X, and XI deal with an investigation of the aging of iron coatings based on vegetable oils and the pentaerythritol esters of the former's acids.

2. Coatings based on the pentaerythritol esters of the acids in semidrying oils provide the longest anticorrosion protection, while tung-oil coatings provide the shortest. This relative order is maintained even when pigmented films are tested.

3. It has been shown that there is no direct connection between the anticorrosion properties of these coatings and the mechanical properties of the films.

In comparing the changes of various properties stress should be laid upon the anti-corrosion properties.

4. A comparison of the aging of oil coatings under atmospheric conditions, in the Leningrad Institute of Technology weatherometer, and in the accelerated-aging apparatus has shown that the results of accelerated tests differ from those made under atmospheric conditions, though the order of the various vegetable-oil materials remains the same as far as the aging rate of their coatings is concerned.

LITERATURE CITED

[1] A.Ya.Drinberg and Yushin, J. Gen.Chem. 16, 23-24, 2066 (1946).

[2] Orlov. Researches on the Kinetics of Chemical Reactions and Catalysis. (1906).

[3] A.Ya.Drinberg, Trans. Lensoviet Institute Technology, Leningrad, 14, 7 (1947).

Received May 20, 1950

LETTERS TO THE EDITOR

Dear Sir:

The Journal of Applied Chemistry has published an article by A.I.Zhilin, An Investigation of Raw Materials for the Manufacture of Mineral Wool, * in which the author criticizes our paper, Technological Investigation of Raw Materials for the Manufacture of Mineral Wool, published in 1948, ** in the pages of your journal.

According to A.I.Zhilin, we "made uncritical use of the data of American authors and ignored several investigations by Soviet research workers," thus arriving at a number of false conclusions in our paper. Furthermore, A.I.Zhilin systematically accuses us of "overestimating" and "uncritically" approaching the work of McCaffrey, of employing "obsolete" methods for determining the flowability of melts, etc., etc.

Inasmuch as A.I.Zhilin's article is a striking example of unfair criticism, we feel we must bring the following facts to your attention.

Our paper **, published in the Journal of Applied Chemistry, was a description of our experimental research on raw materials for the manufacture of mineral wool.

The experimental section, which constituted the bulk of the paper, was preceded by a survey of the literature. In this review, we cited the research of Academician Pavlov, Academician Levinson-Lessing, Selivanov, Dilaktorsky, N.N. Kurnakov, Kaufman, Khrapkovsky, Chernyak and Aslanova, Perkal and Epstein, and others. We also cited some foreign sources (chiefly the patent literature), including the McCaffrey diagram of slag viscositites.

To prove his assertion that we paid no attention to Soviet researchers, A. I.Zhilin cites the following example. Speaking of the percentage of MgO in a melt and criticizing our opinion on this subject, he cites a paper by I.P.Semik, published in the magazine Steel. *** I.P.Semik's paper is no doubt valuable and interesting, but we could hardly "ignore" it, since our paper was published a a whole year earlier.

All of A.I.Zhilin's "criticism" of our paper boils down to the "uncritical use of the data of American authors," namely, of the paper by McCaffrey referred to above.

In our paper, following the work of Academician Pavlov, we cite some experimental data from McCaffrey's paper.

In Academician Pavlov's paper, he criticizes McCaffrey's research, and we begin by mentioning and citing this paper by Academician Pavlov.

A.I.Zhilin does not proceed in this fashion. In his book, Slag Wool, **** he

---

*J. Appl. Chem. 23,11,1157 (1950).

**J. Appl. Chem. 21,3,195 (1948).

***Steel 1 (1949).

****A. I. Zhilin and E. K. Garilov, Construction Press (1946).

writes: "...The first of our observations showed that the slag had to be sufficiently mobile at 1300-1400° to ensure good fiber formation.... Frailing, who made use of the well-known (our italics) work of McCaffrey on the viscosity of slags, came to the same conclusion...'

Thus, in his own book, A.I.Zhilin calls McCaffrey's work well-known, stressing that Frailing came to the same conclusion as A.I.Zhilin, i.e., he extols McCaffrey's and Frailing's researches, without a word of criticism.

In the book mentioned above, A.I.Zhilin cites scores of quotations from American sources, without a word of criticism, attributing to foreign authors the wholly unmerited honor of discovery and priority in production of mineral wool, praising this production abroad and characterizing Soviet production as "primitive" (Ibid., p 6).

A.I.Zhilin criticizes the work of the well-known Russian scientist B.P.Selivanov, asserting that B.P.Selivanov's "flowability expression" and the "filament method" he had developed for determining the fluidity of slags were obsolete. A.I.Zhilin states: "In the initial stages of slag research, the method of determining fluidity proposed by B.P.Selivanov was still acceptable, but today viscosity is everywhere measured in poises." Disparaging the merits of the exceptionally simple and reliable method proposed by a Russian scientist, A.I.Zhilin makes an assertion that is untrue. Indeed, had A.I.Zhilin followed the domestic literature attentively, he could have convinced himself that the method of Prof. B.P. Selivanov, which he had consigned to the archives, the "filament" method, is being used by our research workers. Academician I.I.Chernov has presented a paper by N.N.Kurnakov and others,* in which extensive use is made of the B.P. Selivanov method, the authors concluding that "hence, the viscosity in the molten state does not indicate the flowability of melts, determination of the latter requiring other methods and devices than those employed in viscosity research.' A.I. Zhilin gives our scientific workers unsound advice on problems of method.

Censuring us as people who approach the works of American authors without the needed analysis, A.I.Zhilin casts doubt upon some of the conclusions in our paper. Here is a sample of A.I.Zhilin's "criticism."

On page 1064, A.I.Zhilin writes that we fail to bear in mind the fact that an increase in the percentage of MgO diminishes the viscosity. In our paper, the following is to be read on P. 197 in this connection:

"...the introduction of up to 5% MgO into the melt diminishes the latter's viscosity appreciably. Any further increase in the MgO percentage makes the melts even more fluid, so that at 15-20% MgO the viscosity of the slags is 6 to 8 times less than that of slags containing no MgO..."

Further, we point out in our paper (P. 201) that the viscosity of the melt, to which A.I.Zhilin refers, may be decreased by "raising the MgO content," but that this is undesirable, since this is disadvantageous in the given case — with a low percentage of Fe_2O_3 — and "would result in raising the melting point."

These quotations suffice to demonstrate that what A.I.Zhilin lacks is self-criticism of his own work, and that his "criticism" is not objective.

Respectfully yours,

V. Zhuravlev and M.Sychev.

*Dokl. USSR Acad. Sci. II, 3, (1946).

A Photocolorimetric Method of Determining Small Quantities of Milk Sugar p.: 193

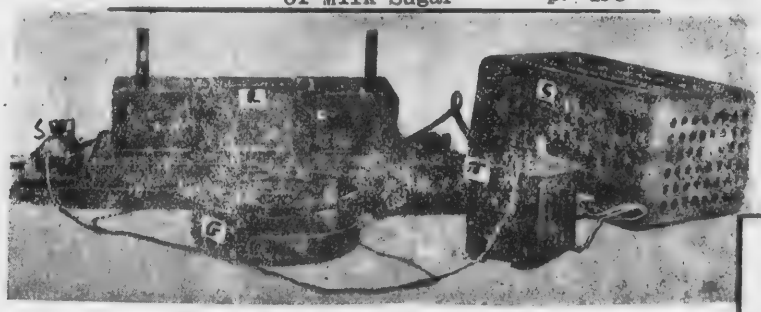

Fig. 4 Test-tube photocolorimeter

L-light source; S-current Stabilizer; 5-transformer; G-galvanometer; Sw-Switch; D-diaphragm

A Compound Helix as a Catalyst Carrier p.: 223

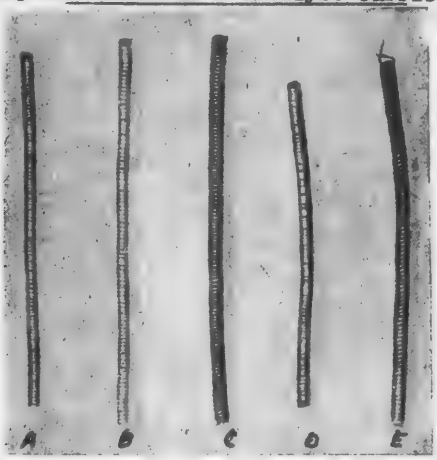

Fig. 1 Simple helixes-catalyst carriers

a-copper; b-aluminum; c-iron; d-nichrome; e-nickeline

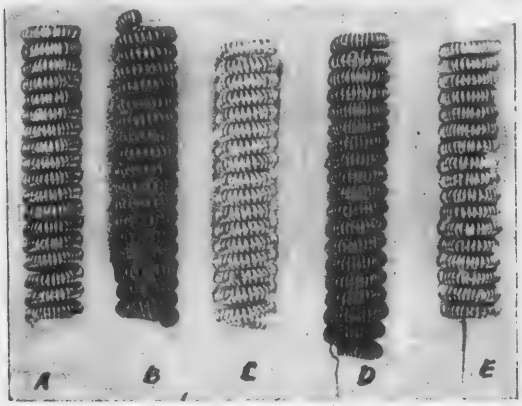

Fig. 2 Compound helixes-catalyst carriers

a-copper; b-iron; c-aluminum; d-nickeline; e-nichrome

P rotecting Iron Against Corrosion p.: 233

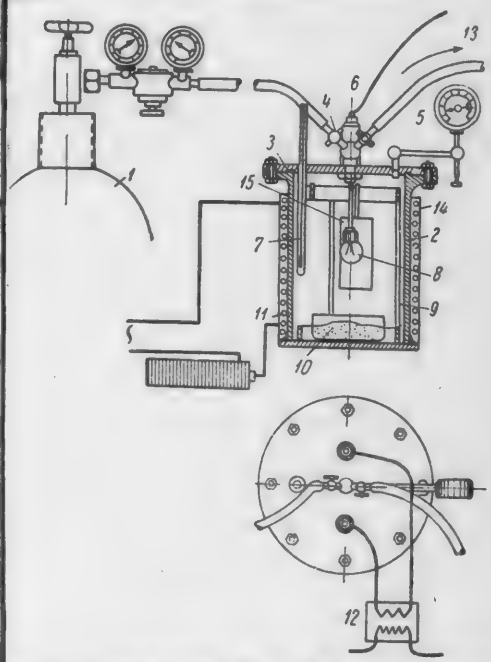

Fig. 1. Cross-section of the high speed apparatus

1-oxygen tank; 2-housing of the high-speed apparatus; 3-cover; 4-valve; 5-manometer; 6-spark plugs; 5-thermometer; 8-electric bulb (40 watt, 60 volt); 9-sample frame; 10-cup with silica gel; 11-electric heating coil; 12-transformer; 13-tube leading to vacuum pump; 14-asbestos insulation; 15-sheet with coating to be tested.

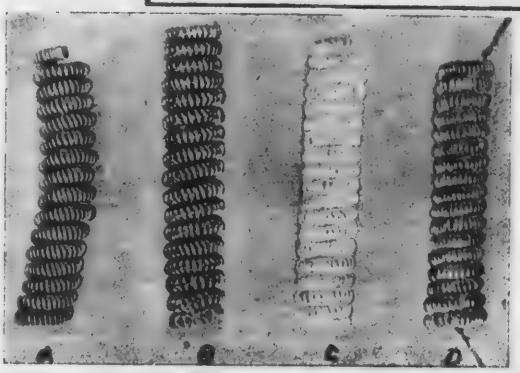

Fig. 3 Compound helixes coated with catalysts

a-aluminum coated chemically with alumina; b-nichrome, coated thermally with platinum; c-nichrome, coated with alumina; d-nichrome, coated with clay.